Use of ultrasound in enhancing productivity of biotechnological processes

A thesis presented in partial fulfilment of the requirements for the degree of
Doctor of Philosophy in Biochemical Engineering
at Massey University, Palmerston North, New Zealand

AHMAD ZIAD BIN SULAIMAN

2011

Abstract

This study focused on identifying optimum sonication regimens (e.g. intensity, duty cycles) that may intensify bioprocesses without damaging the biocatalyst. Possible mechanisms of productivity enhancement in various biotechnology processing scenarios were investigated. Three model processes were used: 1) production of bioethanol from lactose by fermentation with the yeast *Kluyveromyces marxianus*; 2) β-galactosidase catalyzed hydrolysis of lactose in a homogeneous cell-free system; and 3) hydrolysis of soluble and insoluble particulate cellulose of various sizes, catalyzed by soluble cellulase. The above processes involved: 1) conversion of a soluble substrate by a live catalyst in the presence of gas-liquid mass transfer; 2) a cell-free homogeneous bioreaction system; and 3) a heterogeneous reaction system involving substantial solid-liquid mass transfer limitations depending on the size of the substrate (i.e. soluble and insoluble particulate cellulose).

Low intensity ultrasound (11.8 W cm^{-2} sonication power at the sonotrode tip), enhanced the ethanol productivity of the batch fermentation process. At the specified sonication intensity a duty cycle of 20% was found to be optimal. A duty cycle of 40% adversely affected the fermentation. With the best duty cycle of 20%, the final ethanol concentration was 5.2±0.68 g L^{-1}, or nearly 3.5-fold that of the control fermentation. The productivity enhancing effect of sonication was attributed to a possible improved desorption of carbon dioxide from the fermentation broth. Ultrasound may also have facilitated transport of lactose into the cell by affecting cell permeability. While ultrasound apparently enhanced desorption of carbon dioxide, it also damaged yeast enzymes such as β-galactosidase and this may explain why a 40% duty cycle had an adverse impact on the fermentation. Although at the highest duty cycle of 40% sonication reduced cell growth, cell viability remained high at ≥70% during most of the fermentation. In continuous fermentations, sonication always enhanced the steady-state biomass concentration and ethanol concentration at all dilution rates tested relative to the corresponding controls.

Ultrasound effectively influenced enzyme-substrate binding/unbinding for β-galactosidase mediated hydrolysis of lactose in a cell-free system. A short irradiation pulse (i.e. 10% duty cycle), applied at the highest irradiation power (11.8 W cm^{-2}),

improved the initial hydrolysis rate, by nearly 1.4-fold relative to control. This effect of ultrasound was possibly due to its accelerative effect on collision frequency of the enzyme and substrate molecules as a consequence of the microturbulence caused by sonication.

The cellulase-mediated hydrolysis of soluble cellulose as well as particulate cellulose was enhanced by sonication at a 10% duty cycle and power intensity of 11.8 W cm^{-2}, but prolonged sonication adversely impacted the enzyme stability at a constant temperature of 50 °C relative to control.

Acknowledgements

In the name of Allah, most benevolent, ever merciful

I would like to express my sincere appreciation and thanks to my principal supervisor Professor Yusuf Chisti for his constant encouragement, guidance, precious advice, criticisms, friendship and continuous support throughout this study. It was a pleasure to work with him.

I am specially grateful for the financial support provided by Ministry of Higher Education, Malaysia, under a SLAI scholarship and a study leave provided by Universiti Malaysia Pahang.

Other individuals that deserve my thanks are:
Professor Clive Davis and Associate Professor Pak Lam Yu for their support and for being special friends;
Associate Professor Dr Mazzuca-Sobczuk for useful discussions and for being a special friend;
The Microsuite manager, Anne-Marie Jackson for providing me with the research materials and some memorable fun-times;
The lab technicians, Judy Collins, John Sykes, John Edwards and Clive Bardell for help and technical advice;

My research colleagues, Pat, Farhan, Ta, Sadia, Tawan, Haider, Naila, Shazla, Khaizura, Syaifuddin and Xue Mei for sharing many thoughts during my work in the Micro-Suite laboratories;
The other postgraduate students that have come and gone over the past four years and the present students; and
My Malaysian friends for motivation and for being special friends.

Lastly, I wish to express my unlimited appreciation to my beloved wife Azilah Ajit, my daughter Aqilah Batrisyia and my family for their irreplaceable encouragement, undying love and prayers. To my mum for her infinite patience, sacrifice and understanding during the years of this study.

Above all, I thank God the almighty for his grace, mercy and guidance which enabled the successful completion of this study.

Table of Contents

List of Figures

List of Tables

Abbreviations

A	Cross-sectional area (m^2)
a_L	Interfacial area per unit liquid volume (m^{-1})
C^*	Dissolved oxygen saturation concentration (mol L^{-1})
C_0	Dissolved oxygen concentration in bulk liquid phase (% sat or mol L^{-1})
C_L	Actual instantaneous concentration of dissolved oxygen in the broth (mol L^{-1})
CMC	Carboxymethyl cellulose
C_p	Dissolved oxygen concentration measured by probe (mol L^{-1} or % of air saturation)
D	Dilution rate (h^{-1})
E_o	Initial enzyme concentration (g L^{-1})
E_{max}	Maximum ethanol concentration (g L^{-1})
f	Frequency (s^{-1})
H	Henry's law constant
I	Sonication intensity (W cm^{-2})
k_L	Mass transfer coefficient (m s^{-1})
k_La_L	Volumetric mass transfer coefficient (s^{-1})
K_m	Michaelis constant (g L^{-1})
k_p	Response coefficient of oxygen probe (s^{-1})
K_s	Saturation constant for substrate (g L^{-1})
P	Power input (W)
P_E	Ethanol productivity (g L^{-1} h^{-1})
P_{ir}	Irradiation power of ultrasound (W)
P_x	Biomass productivity (g L^{-1} h^{-1})
q_p	Average biomass specific ethanol production rate (g g^{-1} h^{-1})
q_s	Average biomass specific lactose uptake rate (g g^{-1} h^{-1})
S	Substrate concentration (g L^{-1})
S_e	Substrate concentration in the reactor at steady state (g L^{-1})
S_o	Initial substrate concentration (g L^{-1})
t	Time (s)

t_m	Mass transfer time (s)
V_i	Initial reaction rate (M s^{-1})
V_L	Liquid volume in the reactor (m^3)
V_{max}	Maximum reaction rate (M s^{-1})
X_{max}	Biomass concentration (g L^{-1})
$Y_{p/s}$	Ethanol yield on substrate (g g^{-1})
$Y_{x/s}$	Biomass yield on substrate (g g^{-1})
τ_p	Probe response time (s)
μ	Liquid viscosity (mNs/m^2)
μ	Specific growth rate (h^{-1})
μ_{max}	Maximum specific growth rate (h^{-1})
ρ	Density (kg/m^3)

CHAPTER 1

INTRODUCTION

Ultrasound, or sound of frequency >20 kHz, is inaudible to humans but many species rely on it for ranging, navigation and communication (Chisti, 2003a). Ultrasound has numerous applications in medical imaging, sonochemical processing, nondestructive testing and welding (Gogate and Kabadi, 2009; Mason and Lorimer, 1988; Mason and Lorimer, 2002). Ultrasound can destroy microbial and other cells and this well-known effect has perhaps discouraged research on possible beneficial effects of ultrasound on biocatalysis. Potentially, finely tuned ultrasound can enhance diffusive transport both within and outside a cell to influence rates of reactions and yields of metabolites (Bar, 1988; Chisti, 2003b; Chu *et al.*, 2000; Chuanyun *et al.*, 2003; Gogate and Kabadi, 2009; Kilby and Hunter, 1990; Rokhina *et al.*, 2009; Zabaneh and Bar, 1991). Ultrasound influences enzyme-catalyzed reactions in other ways, including possible effects on formation and dissociation of the enzyme–substrate complex (Chisti, 2003b; Lin *et al.*, 2010; Yachmenev *et al.*, 2002; Yachmenev *et al.*, 2004). Substrate and product inhibition characteristics of an enzyme appear to be influenced by ultrasound (Aliyu and Hepher, 2000; Basedow and Ebert, 1977; Imai *et al.*, 2004; Jian *et al.*, 2008). Ultrasound can induce live cells to take-up genetic material from the environment (Gogate and Kabadi, 2009; Rokhina *et al.*, 2009).

This research investigated the use of ultrasound to enhance the productivity of biotechnological processes. Three distinct types of processes were examined: (1) conversion of lactose to bioethanol involving a live yeast; (2) hydrolysis of lactose (a small molecule) to glucose and galactose involving the enzyme β-galactosidase in the absence of any live cells; (3) hydrolysis of soluble cellulose (a macromolecule) and particulate cellulose (a solid substrate) with the enzyme cellulase in the absence of live material. The aim was to identify the sonication regimens that might be suitable for enhancing the productivity of a diverse range of bioprocesses and attempt to elucidate the possible mechanisms involved in any productivity enhancement.

Much work exists on using ultrasound to damage or break microbial cells (Chisti and Moo-Young, 1986), but few studies have attempted to use ultrasound to enhance productivity of microbial and enzymatic processes. Nearly all the work on ultrasonically enhancing productivity of biocatalytic processes has been reviewed by Chisti (2003b) and Rokhina *et al.* (2009).

CHAPTER 2

LITERATURE REVIEW

2.1 Ultrasound

Sound of frequency >20 kHz is generally regarded as ultrasound and is inaudible to humans. The upper limit of ultrasound frequency is not precisely defined but is commonly taken to be 5 MHz in gases and 500 MHz in liquids and solids (Leighton, 2007; Mason and Lorimer, 1988; Mason and Lorimer, 2002). The ultrasound may be divided broadly into "low power" or "high frequency ultrasound" and "power ultrasound". Low power ultrasound (2-10 MHz generally) is used in medical scanning and chemical analyses. High energy (low frequency) or "power ultrasound" of between 20 and 100 kHz frequency range is used for cleaning, plastic welding and enhancing the rates of chemical reactions. Power ultrasound of ~ 20 kHz is the focus of this study.

Ultrasonic waves are generated by mechanical vibrations of an object at the same frequency as the frequency of ultrasound. Propagation of ultrasound in liquid media produces alternating compression and rarefaction cycles. During a rarefaction cycle, the rapid reduction in pressure leads to formation of gas and vapour bubbles in the liquid. These bubbles grow in the rarefaction phase and in the next compression phase, the bubbles implode violently (Suslick, 1988). During implosion, very high temperatures (approximately 5000 K) and pressures (estimated at 50000 kPa) can occur inside these bubbles (Gogate and Kabadi, 2009; Rokhina *et al.*, 2009). This formation, expansion and implosion of bubble is known as cavitation. Cavitation creates a shockwave that propagates in the liquid.

2.2 Effects of ultrasound

High-intensity ultrasound produces various effects as it propagates through a medium. Several mechanisms have been invoked in explaining the effects of ultrasound, but not all mechanisms involved are known or well understood. Most of the reported effects have been attributed to one or more of the following factors:

2.2.1 Cavitation

Cavitation in liquids generally: causes rapid and complete degassing; may initiate various reactions by generating free chemical radicals; accelerates chemical reactions by facilitating the micromixing of reactants; breaks covalent and other bonds; disperses aggregates; increases emulsification rates; improves diffusion rates; micronizes dispersed solids and liquids; assists the extraction of substances from animal and plant tissue and microbial biomass; erodes and breaksdown susceptible particles, including microorganisms (Gogate and Kabadi, 2009).

2.2.2 Compression and rarefaction

A high-intensity acoustic wave propagating through a solid medium produces a rapid succession of compression and rarefaction events which subject the material to repeated contraction and expansion cycles. This phenomenon, known as “rectified diffusion” of sound is important in acoustically enhanced drying and dewatering processes that involve noticeable migration of water (Suslick *et al.*, 1999). In dense materials that are practically incompressible, the alternating acoustic stress facilitates dewatering by either maintaining open the existing channels for water migration or creating new ones (Ensminger, 1988; Muralidhara *et al.*, 1985; Suslick, 1990). Dense materials usually “fracture” under acoustic stress (Lockner, 1993). Microscopic channels are created in directions normal to wave propagation during rarefaction, or parallel to wave propagation during compression (Floros and Liang, 1994).

2.2.3 Turbulance

High-intensity ultrasound in low-viscosity liquids and gases produces violent agitation, which can be used to disperse particles (Lin *et al.*, 2010) and enhance mixing. At liquid/solid or gas/solid interfaces, acoustic waves cause extreme turbulence known as "acoustic streaming" or "micro streaming" (Nyborg, 1982). This thins the diffusion boundary layer, increases the convective mass transfer, and accelerates diffusion in systems where ordinary mixing is not possible (Mason and Lorimer, 2002; Suslick and Nyborg, 1990).

2.3 Use of ultrasound in biotechnological processes

Ultrasound is widely used in laboratory protocols for breaking cell walls to release intracellular products (Chisti and Moo-Young, 1986; Iida *et al.*, 2008). Enzymes and other fragile macromolecules are known to be susceptible to damage by ultrasound (Potapovich *et al.*, 2005). Nevertheless, suitably applied ultrasound has the potential for enhancing the productivity of bioprocesses involving live cells and bioactive enzymes (Bar, 1988; Chisti, 2003b; Chu *et al.*, 2000; Chuanyun *et al.*, 2003; Chuanyun *et al.*, 2004; Gogate and Kabadi, 2009; Kilby and Hunter, 1990; Rokhina *et al.*, 2009; Shewale and Pandit, 2009; Zabaneh and Bar, 1991).

Potential benefits of using ultrasound in nonmicrobial processing of food (Kardos and Luche, 2001; Knorr *et al.*, 2004; Mason *et al.*, 1996; Patist and Bates, 2008) and biological treatment of waste (Liu *et al.*, 2007; Schläfer *et al.*, 2000; Xie *et al.*, 2009) have been discussed in the literature, but are of little direct relevance here.

Many of the effects of ultrasound in biotechnology processes have been ascribed to the factors mentioned in Section 2.2. For example, ultrasound induced cavitation has found various applications in biotechnological processes (Gogate and Kabadi, 2009). Ultrasonic enhancement of bioprocesses has been attributed to: improved interphase mass transfer as a consequence of microstreaming and turbulence induced in a fluid by sonication (Chisti, 2003b; Gogate and Kabadi, 2009; Khanal *et al.*, 2007; Nyborg, 1982; Sinisterra, 1992; Thompson and Doraiswamy, 1999); the extremely high local pressures and temperatures generated under high intensity sonication (Suslick, 1988; Suslick, 1989; Suslick and Price, 1999); permeability enhancement of microbial cell walls (Chu *et al.*, 2000; Chuanyun *et al.*, 2004; Kilby and Hunter, 1990; Lanchun *et al.*, 2003a; Lanchun *et*

al., 2003b; Runyan *et al.*, 2006); transmission of sonomechanical forces into the cell to influence biochemical processes (Chisti, 2003b; Radel *et al.*, 2000); enhanced intramolecular motion in macromolecules such as enzymes to improve enzyme–substrate interactions (Chisti, 2003b); and changes in microbial morphology that may facilitate certain phenomena (Herran *et al.*, 2008; Sainz Herrán *et al.*, 2010). There are also examples of fermentation processes in which ultrasound has produced clearly observable effects on microbial morphology without damaging the microorganisms, but has failed to achieve any enhancement of metabolite production (Herrán *et al.*, 2008; Sainz Herrán *et al.*, 2010).

2.4 Effect of ultrasound on microbial fermentation

Suitably applied ultrasound is known to enhance the productivity of at least some microbial fermentations (Chisti, 2003b; Neis, 2007), but the causes of such enhancements are not entirely clear. Productivity enhancements by ultrasound may be brought about by some or all of the following factors:

1. Improved mass transfer to/from cells by ultrasound induced microturbulence in the broth.
2. Improved mass transfer to/from cells by disruption of clumps and flocs of cells without damage to individual cells.
3. Enhancement of gas-liquid, liquid-liquid and solid-liquid mass transfer by sonication in fermentations in which a limiting substrate is provided as a gas, solid or water immiscible liquid.
4. Ultrasound induced enhanced secretion of hydrolytic and other enzymes.
5. Possible induction of productivity-enhancing intracellular motions by ultrasound.
6. Ultrasound induced movement within and outside a cell to cause enhanced enzyme-substrate interactions.

Use of ultrasound has been widely discussed for inactivation and disruption of microorganisms (Chisti and Moo-Young, 1986; Chisti and Moo-Young, 2002), but not so much for enhancing their production performance. Effects of sonication for productivity enhancement have been previously reported for certain bacteria (Bar, 1988; Chu *et al.*, 2000; Joyce *et al.*, 2003; Runyan *et al.*, 2006; Sakakibara *et al.*, 1994; Wang and Sakakibara, 1997; Wood *et al.*, 1997; Wu *et al.*, 2000; Zabaneh and Bar, 1991),

filamentous fungi (Chuanyun *et al.*, 2003; Chuanyun *et al.*, 2004) and plant cells (Böhm *et al.*, 2000). Bakers' yeast (*Saccharomyces cerevisiae*) appears to have been the only yeast that has been assessed to some level in ultrasound irradiated fermentations (Anderson, 1953; Jomdecha and Prateepasen, 2006; Lanchun *et al.*, 2003b; Matsuura *et al.*, 1994).

Sonication of course has an associated heating effect that is quite substantial. A rise in temperature will enhance rate of nutrient/metabolite transport and rate of biochemical reactions. Unfortunately, elevated temperatures also damage enzymes and cells. Therefore, temperature must be carefully controlled during sonication, for example by using a thermostated reaction vessel. All of the above listed enhancement mechanisms are quite independent of temperature and could occur under conditions of precisely controlled temperature. The studies reported here were conducted under controlled temperature so that any observed effects could be ascribed to ultrasound directly.

Prior work on sonicated fermentations for producing bioethanol is pertinent to this study and is therefore reviewed here briefly. Nearly all such work focused on the yeast *S. cerevisiae*. Ultrasound intensity that is otherwise nonlethal to *S. cerevisiae*, appears to affect the integrity of the cell vacuole and rearrange the intracellular contents (Radel *et al.*, 2000). Relatively low power diagnostic ultrasound of the frequency range 1–10 MHz is generally considered less damaging to cells than the power ultrasound (frequency range of 20–100 kHz); nevertheless, 2.2 MHz ultrasound applied continuously at an electrical power input of 14 W to a broth volume of 64 mL killed 25% of *S. cerevisiae* cells exposed for 60 min (Radel *et al.*, 2000). Continuous sonication at 1 MHz and 10.5 W cm^{-2} has inhibited *S. cerevisiae* fermentation, but intermittent sonication at the same intensity was less damaging (Anderson, 1953).

In production of wine, beer and sake from soluble sugars using immobilized cells of *S. cerevisiae*, extremely low intensity sonication at 0.3 mW cm^{-2} and 43 kHz stimulated the fermentation to reduce the fermentation time to 50–64% (Matsuura *et al.*, 1994). Ultrasound (20 kHz) used at intensities of 0.2, 0.4 and 0.8 W cm^{-2} was claimed to accelerate the growth of *S. cerevisiae* in a medium that contained only dissolved nutrients (Jomdecha and Prateepasen, 2006), but the data did not clearly support this claim. Marginal improvements to *S. cerevisiae* growth were observed on controlled exposure to power ultrasound by Lanchun *et al.* (2003b).

Some bioethanol fermentations require pretreatment of the substrate. In pretreatment of starch, sonication in the absence of enzymes and microorganisms has been repeatedly shown to enhance the yield of fermentable sugars (Nitayavardhana *et al.*, 2010) and thereby increase the ethanol yield in a subsequent nonsonicated fermentation. This effect is of course a purely physical consequence of the sonication-induced rupture of the starch granules and does not involve any biological activity. Similar phenomena have been observed in bacterial fermentations for producing ethanol. For example, a 20% enhancement in ethanol yield was reported by intermittent sonication of a paper pulp slurry being enzymatically hydrolyzed and fermented in a combined saccharification-fermentation process that used the bacterium *Klebsiella oxytoca* (Wood *et al.*, 1997). Productivity enhancements have been claimed by sonication in some other *S. cerevisiae* fermentations (Schläfer *et al.*, 2000). Power ultrasound has been claimed to enhance the permeability of *S. cerevisiae* cells to proteases (Lanchun *et al.*, 2003a) and Ca^{2+} (Lanchun *et al.*, 2003b).

This study is not concerned with ultrasonic pretreatment processes that do not involve biological action, but exclusively with processes involving sonication during microbial catalysis and enzyme catalysis.

2.5 Ethanol production from lactose by *Kluyveromyces marxianus*

One of the model processes investigated in this study is the production of ethanol from lactose by fermentation with live cells of *Kluyveromyces marxianus* (Belem and Lee, 1998). This process is well known, but how it might respond to ultrasound is mostly unknown. Both the substrate (i.e., lactose) and the product (i.e., ethanol) of this process are water-soluble small molecules. This process is not expected to be subject to any mass transfer limitation at cell-liquid interface. No evidence exists for limitations due to transport of lactose to cells, or transport of ethanol from the cells to the bulk fluid, in this well known fermentation.

Lactose ($C_{12}H_{22}O_{11}$) is a disaccharide that consists of β-D-galactose and β-D-glucose molecules linked through a β-1-4 glycosidic linkage. Lactose is a relatively small molecule with a molar mass of 342.3 g mol^{-1}. Hydrolysis of lactose produces glucose and galactose (Ladero *et al.*, 2000; Novalin *et al.*, 2005). At concentration used typically in fermentations (20-100 g L^{-1}) lactose is fully soluble in water at 30 ºC.

Kluyveromyces marxianus is a well-known yeast that grows on lactose and converts it to ethanol. *K. marxianus* has been formerly referred to as *Kluyveromyces fragilis* (Belem and Lee, 1998; Guimarães *et al.*, 2010; Lukondeh *et al.*, 2005). *K. marxianus* has been widely used to produce ethanol from lactose-containing media (Barberis and Segovia, 1997; Bojorge *et al.*, 1999; Grba *et al.*, 2002; Guimarães *et al.*, 2010; Krzystek and Ledakowicz, 2000; Lukondeh *et al.*, 2005; Marison and von Stockar, 1987; Mehaia and Cheryan, 1984; Ozilgen *et al.*, 1988; Zafar *et al.*, 2005), but in conventional nonsonicated fermentations. The yeast *K. marxianus* and its biotechnological potential have been reviewed elsewhere (Fonseca *et al.*, 2008; Lane and Morrissey, 2010). A typical batch fermentation of lactose by *K. marxianus* is shown in Figure 2.1 (Lukondeh *et al.*, 2005).

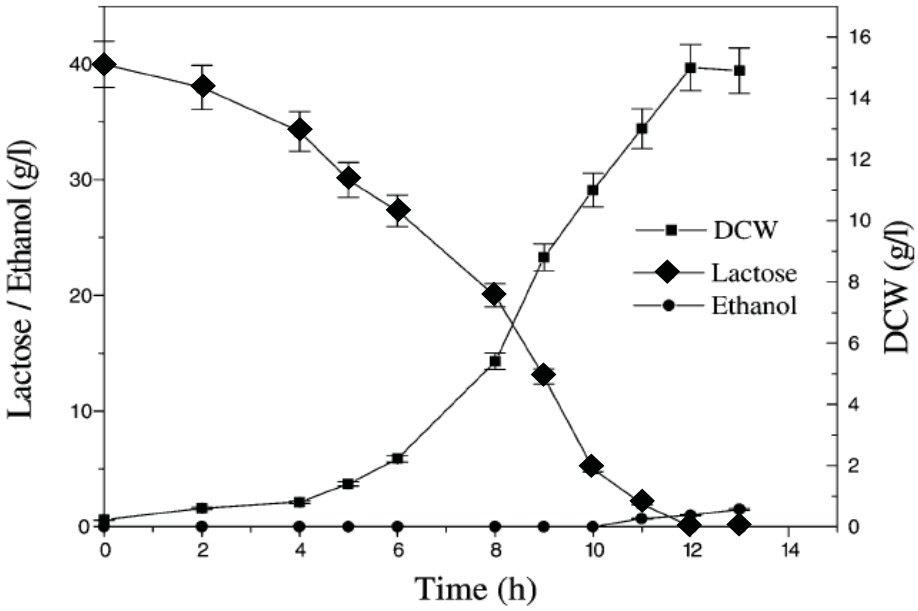

Figure 2.1 Batch lactose fermentation by *K. marxianus* at an initial lactose concentration of 40 g L^{-1}, 30 °C and pH 5.0 (Lukondeh *et al.*, 2005). (DCW is dry cell weight.)

A batch fermentation of ethanol is typically characterized in terms of the parameters noted in Table 2.1. Calculation of these is basic information and is fully explained by Doran (1995) and other textbooks. These parameters are used in this study to quantitatively compare the control and the variously sonicated batch fermentations.

Table 2.2 summarizes the published kinetic parameters for batch fermentation of lactose by *K. marxianus*.

Table 2.1 Some of the parameters used to characterize a fermentation (Doran, 1995)

Parameter	Symbol	Units	Definition
Specific biomass growth rate	μ	h^{-1}	Biomass growth rate per unit biomass concentration during exponential growth
Average specific lactose uptake rate	q_s	$g\ g^{-1}\ h^{-1}$	Average lactose consumption rate per unit biomass produced
Biomass yield on substrate	$Y_{x/s}$	$g\ g^{-1}$	Mass of biomass produced per unit substrate consumed
Biomass concentration	X_{max}	$g\ L^{-1}$	Maximum concentration of biomass in fermentation
Biomass productivity	P_x	$g\ L^{-1}\ h^{-1}$	Biomass production rate per unit volume per unit time
Maximum ethanol concentration	E_{max}	$g\ L^{-1}$	Maximum concentration of ethanol in broth
Ethanol productivity	P_E	$g\ L^{-1}\ h^{-1}$	Mass of ethanol produced per unit volume per unit time
Ethanol yield on substrate	$Y_{p/s}$	$g\ g^{-1}$	Mass of ethanol formed per unit mass of biomass formed
Average specific ethanol production rate	q_p	$g\ g^{-1}\ h^{-1}$	(Ethanol yield on biomass) × average growth rate

Table 2.2 Published kinetic parameters for batch fermentation of lactose by *K. marxianus*

Microorganism	Initial lactose concentration ($g\ L^{-1}$)	μ (h^{-1})	$Y_{x/s}$ ($g\ g^{-1}$)	$Y_{p/s}$ ($g\ g^{-1}$)	Reference
K. marxianus FII510700	40	0.35	0.41	-	(Lukondeh *et al.*, 2005)
K. marxianus (MTCC 1288)	50	0.401	0.219	0.127	(Zafar *et al.*, 2005)
K. marxianus (VST44)	10.5	0.1096	0.69	0.49	(Grba *et al.*, 2002)
K. marxianus (ZIM75)	10.5	0.0996	0.6	0.49	(Grba *et al.*, 2002)
K. marxianus (ATCC 8554)	43.5	0.4	0.3	0.2	(Bojorge *et al.*, 1999)
K. fragilis (UCD #55-61)	20	0.00698	0.5	-	(Ozilgen *et al.*, 1988)
K. fragilis NRRL-Y-1109	42.66	-	0.462	-	(Barberis and Segovia, 1997)
K. fragilis	50	0.4896	0.0886	-	(Krzystek and Ledakowicz, 2000)
K. fragilis (NRRL-Y-2415)	50	0.0682	0.04	0.404	(Mehaia and Cheryan, 1984)

Fermentations are typically carried out as batches, therefore, a study of the effect of ultrasound on a model batch fermentation may have some direct practical value. Unfortunately, the environment (e.g. concentration of nutrients, products and biomass) in a batch fermentation is continuously changing and therefore, steady state continuous fermentations are better suited to a study of how ultrasound might affect a fermentation process.

No previous studies appear to have been performed on how sonication might affect a fermentation at steady state. In view of the possible insights that may be gained from continuous steady state operation and the utility of batch fermentations, both continuous and batch fermentation processes were investigated in this work.

A continuous fermentation at steady-state is commonly characterized in terms of the dilution rate D; the maximum biomass concentration (X_{max}); the residual substrate concentration (S); the biomass yield coefficient on substrate ($Y_{x/s}$); the biomass productivity (P_x); maximum concentration of the product (E_{max}); productivity of the product (P_E); and the product yield on substrate ($Y_{p/s}$). The dilution rate cannot exceed the maximum specific growth rate for the microorganisms, or the cells will be washed out. In

a continuous fermentation at steady-state the dilution rate equals the specific growth rate (Guimarães *et al.*, 2010; Kim *et al.*, 1998; Moresi *et al.*, 1990; Teixeira *et al.*, 1990).

In a well-mixed continuous fermentation the cells are removed at a rate equal to their growth rate, and the growth rate of cells is equal to the dilution rate (i.e. $\mu = D$). Cell growth commonly depends on the concentration of the limiting substrate S in accordance with Monod kinetics:

$$\mu = D = \frac{\mu_{max} S}{K_s + S} \tag{2.1}$$

where μ is the specific growth rate at substrate concentration S and μ_{max} is the maximum possible specific growth rate on the substrate. K_s is the substrate concentration at which μ is half of the maximum value μ_{max}. K_s and μ_{max} are constants.

2.6 Factors affecting the fermentation

Factors which influence a fermentation process include temperature, pH, types and concentrations of nutrients, aeration (oxygen) and inoculum size. By optimizing these variables, a fermentation may be improved significantly. Fermentation of lactose by *K. marxianus* is a relatively well studied process, although no systematic studies exist of the effects of sonication on this process. The effects of temperature, pH and inoculum size have been investigated (Brady *et al.*, 1995; Furlan *et al.*, 2001; Guimarães *et al.*, 2010; Tomaska *et al.*, 1995). Generally, the optimal ranges of temperature, pH and inoculum size are 30-40 °C, 5-7 and 1%-10% (v/v), respectively. The role of dissolved oxygen in *Kluyveromyces* fermentations has been discussed by Marison and von Stockar (1987), Barberis and Segovia (1997), Nor *et al.* (2001), Lukondeh *et al.* (2005) and Huang *et al.* (2006). A low oxygen microaerophilic environment tends to maximize the yield of ethanol on lactose whereas a highly aerobic environment favors production of biomass. In this work, the aim was neither to maximise ethanol yield nor to achieve a high biomass yield, but simply to study the effects of sonication in comparison with control fermentations. Relatively aerobic conditions were therefore used.

Most of the studies of the effects of ultrasound on fermentations involving live cells are summarized in Table 2.3. Most of the earlier work has focused on *Saccharomyces cerevisiae*. Invariably, fermentations were conducted batch-wise and

effects of both continuous and intermittent sonication were evaluated. In most cases, continuous sonication damaged cells and lowered the ethanol yield. Intermittent sonication was generally less damaging and in some cases was actually beneficial. Activities of enzymes in extracellular broth were often enhanced by sonication because of enhanced enzyme leakage from cells, or outright cell damage (Sakakibara *et al.*, 1994). In general, standing wave ultrasound did not damage cells but standing wave ultrasound is not generally linked with improving a fermentation (Chisti, 2003b). (A standing wave is generated when a wave travelling in one direction meets a wave of the same frequency travelling in the opposite direction (Chisti, 2003b).) Standing wave ultrasound is used in clumping cells for improved separation and is not the focus of this work as it has not been shown to significantly enhance either chemical reactions or fermentations. Clearly, systematic studies involving both batch and continuous culture and a broad range (intermittent, continuous, various intensities) of sonication on fermentation are non existent. Also, no work appears to have been done on sonicated *K. marxianus* fermentation.

Table 2.3 Prior sonication studies of fermentation processes

Sound frequency	Power/ intensity	Stimulation time	Fermentation	Micro-organism	Transducer construction	Findings	Reference(s)
24 kHz	2W	1 s / every 15 s and 30 min treatment time	Shake flask (working volume = 300 mL) - batch	*Saccharomyces cerevisiae*	Immersed the ultrasound probe in the culture medium	- enhanced the proteinase activity - low-intensity ultrasound changed the flocculation behaviour of *S. cerevisiae* - improved behaviour of the cells' metabolism - low ultrasound intensity changed the osmotic properties of membrane, improved transfer of substrate, drove up enzyme synthesis and enzyme activity	(Lanchun *et al.*, 2003a)
25 kHz	150 W	Not reported	2 × 5 L bioreactor - continuous flow	*Saccharomyces cerevisiae*	Transducer was attached at the bottom of the bioreactor	- increasing the energy input (0.3 to 12) W/L did not increase the biological activity - at low frequency, the ethanol concentration increased up to 67 % (this was obtained at intermittent application of ultrasound – on and off) - discontinuous ultrasonic treatments were more beneficial for activating fermentation than the continuous exposure - ethanol production and cell growth were accelerated by the ultrasound treatment	(Schläfer *et al.*, 2000)
43 kHz	30 mW/cm^2	Continuously	Jar fermenter	*Saccharomyces cerevisiae*	Transducer was placed under the fermenter	- at intensity 454 mW/L broth foaming and CO_2 evolution were observed immediately - dissolved CO_2 in the broth decreased rapidly - continuous irradiation did not have an effect on ethanol production	(Matsuura *et al.*, 1994)

22 MHz	14 W	Not reported	Using separation system and modified separation system	*Saccharomyces cerevisiae*	Transducer was attached at the glass wall of the system	- no loss in cell viability for cells treated with standing wave up to period of 2 h - based on scanning electron micrographs (SEM) morphological changes occurred with the application of ultrasound compared with a control - ultrasound altered the internal components of the cells	(Radel *et al.*, 2000)
200 kHz	17.2 kW/m^2	Continuously and pulsation	Volume = 500 mL	*Lactobacillus* strains	Transducers attached below the bottom of the fermenter	- continuous sonication decreased cell viability - the intracellular contents was released to the fermentation medium by sonication - the maximum release of β-galactosidase during sonicated fermentation was in the exponential phase of culture - lactose hydrolysis was effectively enhanced with the presence of β-galactosidase in the culture medium due to sonication	(Wang and Sakakibara, 1997)
1 MHz	25 W	Continuously and pulsation	Volume = 2.5 mL	*Saccharomyces cerevisiae*	The transducer was immersed directly in the culture medium	- both continuous and pulsed radiation caused a marked reduction in the rate of anaerobic fermentation. - no conclusions were made about the effects of irradiation on total growth - ultrasound prolonged the lag phase of culture	(Anderson, 1953)

Low frequency = 20 kHz, High frequency = 512 kHz and 850 kHz	At low frequency = 0.18 and 0.24 W/m^2 At high frequency = 0.071 and 0.064 W/m^2	Continuously	2 L flask	*Bacillus subtillis*	The transducer was immersed directly in the culture medium	- using high power ultrasound in low volumes of culture suspension resulted in a continuous reduction in cell number - using high power ultrasound in larger volumes resulted in effective declumping of the cells - low intensity ultrasound resulted in raising the cell numbers as a result of declumping. The kill rate was low.	(Joyce *et al.*, 2003)
Not reported	Tested with three different energy levels 1. low (957 W m^{-3}) 2. medium (2870 W m^{-3}) 3. high (4783 W m^{-3})	20%, 60% and 100% duty cycles	Slurry bubble column reactor (25 L total volume) and (23 L working volume)	*Aspergillus terreus*	The sonotrode was inserted in the reactor column at the headplate	- sonication at any power level tested, did not affect biomass growth profiles - medium and high intensity sonication greatly reduced production of lovastatin and substantially altered the growth morphology - medium and high intensity ultrasound disrupted fungal pellets and caused biomass to grow mainly as dispersed hyphae - sonication affected broth rheology because rheology depended on the morphology of the suspended biomass	(Herran *et al.*, 2008)
Low frequency ultrasound 20 kHz	0.2, 0.4 and 0.8 W cm^{-2}	10% duty cycle and the duration of simulation of 10 min	Erlenmeyer flask with 200 mL working volume	*Saccharomyces cerevisiae*	Sonotrode was immersed 2 cm into the culture inside the flask	- at any power level tested, ultrasound enhanced the yeast growth - ultrasound increased productivity and decreased the fermentation time	(Jomdecha and Prateepasen, 2006)
18, 20, 24, 28, 30 kHz	Not reported	50% duty cycle, stimulated once every 12 h, treatment time of 30 min	Erlenmeyer flask 250 mL	*Ecemothecium ashbyii*	The sonotrode was inserted in the flask	- fermentation time was shortened by 36 h and production rate of riboflavin was increased	(Chuanyun *et al.*, 2003)

Furthermore, in most previous sonication studies (Table 2.3) the sound transducers was placed directly in the fermentation broth in the bioreactor, or attached to the bioreactor vessel. Ultrasound does not penetrate too deeply in a broth and most of the earlier studies used arrangements of sonication which exposed a poorly defined volume of the broth to ultrasound. A better arrangement for controlled sonication is to place the sound transducer (sonotrode) in a recycle loop with a small, cooled chamber of a defined volume that can be relatively uniformly sonicated. Sonic energy is mostly dissipated at the tip of a sonotrode. The recycle rate through the sonication chamber can be used to further control the exposure of the broth to ultrasound. A recycle loop also allows for better control of temperature.

2.7 Effect of ultrasound on β-galactosidase

The intracellular enzyme β-galactosidase is responsible for the hydrolysis of lactose to glucose and galactose in microorganisms such as *K. marxianus*. The hydrolysis products are then consumed in various metabolic pathways. A study of the effects of ultrasound on β-galactosidase-catalysed hydrolysis of lactose in a cell-free system can provide direct evidence whether in a fermentation involving *K. marxianus* the lactose hydrolysis step is somehow being influenced by ultrasound, or some other metabolic steps are being affected. Therefore, a study of lactose hydrolysis in a cell-free system is relevant to what might be happening in a fermentation. In addition, such a study can inform about the possible modes of action of ultrasound on an enzymatic reaction which, unlike a fermentation, does not involve gas-liquid mass transfer issues or solid-liquid mass transfer issues. β-Galactosidase mediated hydrolysis of lactose is also used in dairy processing (Husain, 2010; Gekas and Lopez-Leiva, 1985; Nguyen *et al.*, 2009; Santos *et al.*, 1998, Pessela *et al.*, 2003), but is of no direct relevance here.

β-Galactosidase catalyzed hydrolysis of lactose follows Michaelis-Menten type of kinetics (Bakken *et al.*, 1992; Carrara and Rubiolo, 1996; Gekas and Lopez-Leiva, 1985). Thus,

$$V = \frac{V_{max}\, S}{K_m + S} \qquad (2.2)$$

where V is the rate of reaction at a given temperature and pH; V_{max}, a constant, is the maximum possible reaction rate at a given concentration of the enzyme; S is the concentration of the substrate, lactose; and K_m is Michaelis-Menten constant. Numerically, K_m is the concentration of the substrate at which the reaction rate is half of its maximum value, V_{max}. The rate of reaction can be measured by measuring the concentration of glucose produced by the reaction. The reaction must be carried out at a carefully controlled temperature as V, V_{max} and K_m can be highly temperature-dependent. This is specially important in experiments involving sonication, as the ultrasound energy imparted to a fluid results in a rise in temperature. The methods for determining the reaction kinetic parameters V_{max} and K_m from measured values of the initial rate V at various substrate concentrations S, are available in the literature. (Cavaille and Combes, 1995; Yang and Okos, 1989).

A few studies of the effects of sonication on enzymes in cell-free systems have been reported (Kardos and Luche, 2001; Sakakibara *et al.*, 1994; Wang *et al.*, 1996; Wang and Sakakibara, 1997). Both positive and negative effects have been observed. Enzyme activity has been enhanced under mild ultrasound irradiation (Özbek and Ülgen, 2000; Sakakibara *et al.*, 1996), but intense sonication damages enzymes (Gogate and Kabadi, 2009; Potapovich *et al.*, 2005). The activity of β-galactosidase appears to be influenced by the acoustic power and duty cycle of sonication (Özbek and Ülgen, 2000).

2.8 Effects of ultrasound on gas-liquid mass transfer

Extensive existing literature demonstrates that ultrasound as used in chemical reactors and other non-biological process enhances gas-liquid, liquid-liquid and solid-liquid mass transfer (Chisti, 1999). Similar effects may occur in fermenters or bioreactors, even though only low intensity sonication is expected to be used in them. In *K. marxianus* fermentation cell-liquid and gas-liquid mass transfer are involved and may be affected by ultrasound (Kumar *et al.*, 2004). Gas-liquid mass transfer, i.e., transfer of oxygen from the gas phase to the liquid and desorption of carbon dioxide from the liquid to the gas phase, are especially relevant. Gas-liquid mass transfer is briefly reviewed here.

The productivity of aerobic fermentations is often limited by the availability of oxygen in the fermentation broth. In *K. marxianus* fermentations, biomass production is enhanced by increased oxygen supply but ethanol production is suppressed. Oxygen

supply can be enhanced by increasing the rate of oxygen transfer into the liquid from the gas. The volumetric oxygen transfer rate is given as follows:

$$\text{Volumetric oxygen transfer rate} = k_L a_L (C^* - C_L) \quad (2.3)$$

where C_L is the concentration of dissolved oxygen in the liquid, C^* is the saturation concentration of dissolved oxygen in the absence of consumption and $k_L a_L$ is the overall volumetric mass transfer coefficient that is used to characterize the mass transfer rate in the bioreactor. In $k_L a_L$, k_L is the liquid-film mass transfer coefficient and a_L is the interfacial area per unit liquid volume. $k_L a_L$ is generally increased by increasing a_L. Because the surface area of spheres is proportional to the diameter squared, while the volume is proportional to the diameter cubed, a_L is inversely proportional to the bubble diameter. $k_L a_L$ itself depends on the operating conditions (i.e. aeration rate, the rheological properties of the fluid, broth density, surface tension, the system geometry, the intensity of agitation) (Cruz *et al.*, 1999).

In a fermentation broth, the solubility of oxygen is controlled by the partial pressure of oxygen in the gas phase, the temperature and the presence of other solutes. The solubility of a sparingly soluble gas such as oxygen is often modeled by Henry's law:

$$C^* = \frac{P_G}{H} \quad (2.4)$$

where C^* is liquid phase saturation concentration of oxygen, P_G is the partial pressure of oxygen in the gas in contact with the liquid, and H is Henry's law constant.

Many methods are available to determine $k_L a_L$ in bioreactors (Chisti, 1999; Chisti and Moo-Young, 2002). These have been reviewed by Gogate and Pandit (1999). A common method that is used in bioreactors is the dynamic gassing-in method. This method is typically used in a model fluid (e.g. water, fermentation medium) in which there is no consumption of oxygen. A calibrated dissolved oxygen probe is installed in the bioreactor filled with the model fluid at the normal fermentation temperature and mixing state (controlled by the agitation speed). The fluid is first sparged with nitrogen to desorb the dissolved oxygen. Once a low oxygen concentration has been reached, the flow of nitrogen is stopped. Air is now used to sparge the fluid at some preset flow rate. Oxygen

transfers from the air and dissolves in the fluid. Increase in oxygen concentration with time is monitored. Oxygen concentration increases with time as follows:

$$\frac{dC_L}{dt} = k_L a_L (C^* - C_L) \tag{2.5}$$

Integration of the above equation between the limit of $t = 0$, $C_L = C_o$ and $t = t$, $C_L = C_L$, gives:

$$\ln\left(\frac{C^* - C_L}{C^* - C_o}\right) = -k_L a_L t \tag{2.6}$$

where C_o is the dissolved oxygen concentration at time zero. The left-hand-side of the above equation can be calculated at any time t using the measured values of C^*, C_L and C_o. A semilog plot of Equation (2.6) provides $k_L a_L$ as the slope. In the event of an oxygen consuming reaction occurring in the bioreactor, Equation (2.6) needs to be modified as discussed by Lamping *et al.* (2003).

Dissolved oxygen (DO) probes are widely used to monitor the concentration of dissolved oxygen in bioreactors. Polarographic type of DO probe is the most common (Philichi and Stenstrom, 1989). Equation (2.6) assumes that the oxygen concentration measured is instantaneous. In practice this is not so and a dissolved oxygen probe with a rapid response time is required for measurement of C_L or the dynamic method will not give an accurate value of $k_L a_L$. Probe response time can be measured by instantly transferring the probe from an oxygen free medium to an oxygen saturated medium (Badino *et al.*, 2000; Boodhoo *et al.*, 2008; Carbajal and Tecante, 2004; Fadavi and Chisti, 2005; Kumar *et al.*, 2004; Lamping *et al.*, 2003; Leeuwen, 1979; Linek *et al.*, 1987; Mueller *et al.*, 1967; Nakanoh and Yoshida, 1980; Philichi and Stenstrom, 1989; Tribe *et al.*, 1995) and measuring the time required to attain 63.7% of the final equilibrium oxygen concentration (Dunn and Einsele, 1975; Fadavi and Chisti, 2005; Ruchti *et al.*, 1981; Van't Riet, 1979).

The time constant of the probe is the time required to attain 63.7% of the final steady state dissolved oxygen concentration. If the time constant is less than 10 s, ($1/ k_L a_L$ is < 0.1 s^{-1}), Equation (2.6) can be used to determine the value of $k_L a_L$. However, if the $k_L a_L$ is larger than 0.1 s^{-1}, or the probe response time is longer than 10 s, the following

equation needs to be used in calculating the k_La_L from the measured dynamic response curves (Nakanoh and Yoshida, 1980; Van't Riet, 1979):

$$C_p = \frac{1}{t_m - \tau_p}\left[t_m \exp\left(\frac{-t}{t_m}\right) - \tau_p \exp\left(\frac{-t}{\tau_p}\right)\right] \quad (2.7)$$

where C_p is the DO concentration measured by the probe at time t, t_m is $1/ k_La_L$ and τ_p is the response time of the DO probe.

Equation (2.7) can be solved for k_La_L using Microsoft Excel (Badino *et al.*, 2000; Boodhoo *et al.*, 2008; Lamping *et al.*, 2003) using previously determined τ_p. The methodology is as follows: at any time t, a C_p value is computed so that it exactly matches the experimentally measured C_p value at that instance. t_m is varied to achieve the match for a fixed experimentally measured τ_p. The various t_m values are then averaged to obtain a single value of t_m that best describes the measured oxygen concentration profile. This best-fit value of t_m is then used to calculate the k_La_L, or $1/t_m$.

Intense ultrasound can enhance gas-liquid mass transfer coefficient by 50-110% relative to control (Kumar *et al.*, 2004). Sonication decreases bubble size, increases gas hold-up and enhances interfacial turbulence. No literature exists on k_La_L intensification in bioreactors involving live cultures. A study of the effect of ultrasound on k_La_L may help in understanding possible reasons for any observed effects of ultrasound in a fermentation.

2.9 Effect of ultrasound on enzymatic hydrolysis of cellulose

Cellulose is a polymer of glucose. It is one of the most widely available carbohydrates in nature. As the major constituent of plant matter, billions of tons of it are created each year through photosynthesis. Photosynthesis produces 1.8 trillion tons of biodegradable substances annually and about 40% of this is cellulose (Fan *et al.*, 1987). In view of its low cost, abundance and renewability, cellulose is an important resource that can potentially provide huge quantities of glucose for manufacture of bioethanol and many other chemicals by fermentation. The interest in cellulose in this work is for a different reason: cellulose is a macromolecule that, depending on the number of monomer units in its structure, may be fully soluble in water, or may occur as insoluble particles. Enzyme mediated hydrolysis of cellulose with and without ultrasound, offers an opportunity to

investigate the effect of substrate molecule size and solid-liquid mass transfer effects in a bioreactor. Cellulose molecules with relatively few monomer units, i.e. low molecular weight cellulose, are water soluble. In contrast, high molecular weight cellulose occurs as insoluble particles and its hydrolysis involves solid-liquid mass transfer effects as the soluble enzyme must interact with an undissolved particulate substrate. The enzyme involved in hydrolysis of cellulose is cellulase (EC 3.2.1.4). Enzymatic hydrolysis of cellulose has been extensively investigated (Chandel *et al.*, 2007), but mostly without ultrasound. Cellulase is an enzyme complex which breaks down cellulose to glucose. It is produced mainly by bacteria found in the ruminating chambers of herbivores and by various wood-rotting fungi. Three general types of enzymes make up the cellulase complex (Fan *et al.*, 1987). Endocellulase breaks internal bonds in cellulose to disrupt the crystalline structure of cellulose and expose individual cellulose polysaccharide chains to further enzymatic action. Exocellulase cleaves 2-4 units from the ends of the exposed chains (Fan *et al.*, 1987). Cellobiase, or beta-glucosidase, then hydrolyses the products of exocellulase to individual monosaccharides.

The cellulase enzyme complex selected for this study was the commercial preparation *Accellerase*^{TM} *1000* produced by Genencor International B.V., the Netherlands. This enzyme preparation is produced using a genetically engineered strain of *Tricoderma reesei*, and contains all necessary enzyme activities (i.e. endocellulase, exocellulase and cellobiase) to hydrolyze cellulose to glucose. *Tricoderma reesei* cellulase enzyme complex has been thoroughly studied (Ahamed and Vermette, 2010; Beldman *et al.*, 1987). This complex converts crystalline, amorphous and chemically derived celluloses quantitatively to glucose (Al-Zuhair, 2008).

The enzymatic hydrolysis of cellulose has a low efficiency due to factors relating to the substrate as well as the enzyme. Mass transfer limitation – diffusion of enzyme and the substrate to allow adsorption (Fan *et al.*, 1987; Lee *et al.*, 1982; Lin *et al.*, 2010; van Wyk, 1997; Várnai *et al.*, 2010; Xiao *et al.*, 2005; Xiao *et al.*, 2010), is one factor. Mass transfer limitations can be severe as both the substrate and the enzyme are macromolecules. This limitation worsens as the size of the cellulose substrate increases. Mass transfer resistances include the bulk phase resistance, the resistance due to the liquid film around cellulose particles and resistance through the capillary pores of cellulose particles (Baldascini *et al.*, 2001; Bisset and Sternberg, 1978). Mass transfer can be potentially enhanced by turbulence enhancing effect of ultrasound. A physical contact between the enzyme and the substrate is necessary for cellulase to function.

Enzymatic hydrolysis of cellulose has been commonly interpreted in terms of earlier mentioned Michaelis-Menten kinetics (Bailey and Ollis, 1986; Counotte and Prins, 1979; Fan *et al.*, 1987; Lineweaver and Burk, 1934; Shuler and Kargi, 2002). Kinetic parameters of the enzymatic hydrolysis for various cellulosic substrates have been reported (Imai *et al.*, 2004), but mostly in nonsonicated conditions. Li and co-workers (2004) determined the Michaelis constant K_m of cellulose hydrolysis using a variety of pulps. The K_m value was found to increase under continuous ultrasonication. Hydrolysis of cellulose is generally followed by measuring the production of reducing sugars (Mandels *et al.*, 2004; Ortega and Busto, 2001) and reduction of viscosity of the medium (Sreenath, 1993). Viscosity declines as cellulose molecules reduce in size.

Ultrasound has been applied to enzymatic hydrolysis of cellulose (Aliyu and Hepher, 2000; Imai *et al.*, 2004; Filson and Dawson-Andoh, 2009; Li *et al.*, 2004; Rolz, 1986; Yachmenev *et al.*, 2002; Yachmenev *et al.*, 2004) as well as to its acid hydrolysis (Choi and Kim, 1994; Kristol *et al.*, 1984; Lii *et al.*, 1999; Mecozzi *et al.*, 2002; Schuchardt *et al.*, 1987; Tuulmets and Raik, 1999). In both cases the rate of hydrolysis appears to be enhanced by sonication as a consequence of intense microscale turbulence produced (Basedow and Ebert, 1977; Chisti, 2003; Czechowska-Biskup *et al.*, 2005). Unlike in acid hydrolysis, prolonged or intense ultrasonication can damage cellulase and therefore selection of a suitable sonication regimen is important in an enzymatic hydrolysis process. Ultrasound intensity and irradiation dose are easily controlled. In general, ultrasound at low intensity (Mason and Lorimer, 2002) can enhance the productivity of the enzymatic hydrolysis without damaging the enzyme (Chisti, 2003; Rokhina *et al.*, 2009).

2.10 Objectives of study

This work focused on examining the effects of ultrasound on various model bioprocesses. Sonication regimens which could influence a process relative to control were identified. Attempts were made to understand the possible causes of ultrasound-induced enhancement in diverse model reaction situations. The model processes investigated included: 1) a fermentation involving cells and gas-liquid mass transfer effects; 2) a cell-free enzyme catalysed hydrolysis of a small molecule that was not likely to encounter any major mass transfer limitations; 3) enzyme-mediated hydrolysis of a macromolecular

substrate in which the size of the substrate entity could be varied substantially and solid-liquid mass transfer limitations occurred.

2.11 Contributions of the study

This work identifies methods for implementing sonication for enhancing the productivity and economics of various types of biotechnology based production processes. The specific processes involved included a process involving a live microbial cell and two processes involving cell-free enzyme catalysed reactions. In the latter category, examples are studied of processes involving small molecules, dissolved macromolecules and an undissolved solid substrate. An improved understanding is gained of possible mechanisms of ultrasound-induced enhancements in several distinct types of bioreaction scenarios.

CHAPTER 3

MATERIALS AND METHODS

The study focused on the use of ultrasound to enhance the productivity of biotechnological processes. The following three model bioprocesses were used:

1. Production of bioethanol from lactose using live cells of the yeast *Kluyveromyces marxianus*;
2. Hydrolysis of lactose in a cell-free medium using β-galactosidase of *Kluyveromyces lactis*; and
3. Hydrolysis of dissolved and particulate cellulose to glucose using the enzyme cellulase.

The above processes involved three distinct types of biocatalysis: (1) a live cell using intracellular machinery to convert a small soluble substrate (lactose) to ethanol in a heterogeneous bioreaction system; (2) a cell-free enzyme hydrolyzing a dissolved small molecule (lactose) to monosaccharides in a homogeneous reaction system; and (3) a soluble enzyme hydrolyzing a soluble macromolecule, i.e., dissolved cellulose, and the same substrate in an undissolved particulate form. The reaction system 3 involved both homogeneous catalysis and heterogeneous catalysis. The experimental systems and methods involved in the study of the above identified bioreaction systems are described in separate sections in this chapter.

3.1 Effects of ultrasound on conversion of lactose to ethanol by live cells

3.1.1 Introduction

A well-known model fermentation system was used to assess the effects of sonication. The fermentation process involved the conversion of lactose to ethanol by the yeast *Kluyveromyces marxianus* ATCC 46537. Both batch and continuous fermentations were conducted with and without sonication. Fermentations were aerated to achieve both cell growth and ethanol production. Aeration conditions were not selected to specifically favor either biomass production or ethanol production.

3.1.2 Culture medium

Based on the extensive literature on *K. marxianus* fermentation (Barberis and Segovia, 1997; Guimarães *et al.*, 2010; Hewitt and Wassink, 1984; Krzystek and Ledakowicz, 2000; Lukondeh *et al.*, 2005; Marison and Stockar, 1987; Mehaia and Cheryan, 1984; Nor *et al.*, 2001; Ozilgen *et al.*, 1988; Vallet *et al.*, 1998; Zafar *et al.*, 2005), the medium shown in Table 3.1 was selected for the fermentation (Lukondeh *et al.*, 2005).

Table 3.1 Composition of the culture medium for batch and continuous fermentations

Component	Concentration (g L^{-1})	Source
Lactose	50	Ajax Finechem Pty Ltd (www.ajaxfinechem.com), catalog no. B/No. 0707294
Yeast extract	2	Merck-Schuchardt (www.merck.de), catalog no. 2013/08/31
$(NH_4)_2SO_4$	6.25	BDH-Analar Chemicals Ltd, catalog no. A223201
$MgSO_4.7H_2O$	2	BIOLAB (www.thermofisher.com.au), catalog no. BSPML241-500
KH_2PO_4	4	BIOLAB (www.thermofisher.com.au), catalog no. BSPPL951.500

The medium was prepared by dissolving the above components in distilled water.

3.1.3 Microorganism, maintenance and preparation

Kluyveromyces marxianus ATCC 46537 was obtained from the American Type Culture Collection, USA (www.atcc.org). The yeast was supplied as a freeze-dried powder in a glass vial. The cells were rehydrated in sterile YM broth, incubated at 30 °C for 24-h and then inoculated on agar slants. After a further incubation period (30 °C, 24 h), the slants were stored at 4 °C. The maintenance agar medium was made using deionized water and had the composition shown in Table 3.1. The medium also contained 15 g L^{-1} agar (catalog no. 9002-18-0, Merck-Schuchardt, Darmstadt, Germany, www.merck.de). The medium was sterilized by autoclaving (121 °C, 15-min for volumes of < 10 L; 121 °C, 25 min for volumes of ≥ 10 L). The slants were kept at 4 °C and subcultured every 2-months. This stock culture was used for inoculum preparation throughout this study.

Agar plates were prepared from slants in the usual way. Seed cultures were prepared by inoculating a single colony from an agar plate into 80 mL of a sterile medium

contained in a 250 mL shake flask. The medium was as described (Table 3.1) and had been sterilized as mentioned above. The culture was incubated (30 °C) in an orbital shaking incubator (180 rpm; Multitron II Incubator Shaker, Laurel, MD, USA, www.atrbiotech.com) for 24 h. This culture (50 mL) was used to inoculate 150 mL of the earlier specified sterile liquid medium contained in a 1000 mL shake flask. The flask was incubated as specified above. After the specified incubation period, the inoculum had a spectrophotometric absorbance of 0.7 at 620 nm (Ultraspec 2000, model 80-2106-00 spectrophotometer; Pharmacia Biotech Inc., Piscataway, NJ, USA) and contained ~4×10^7 cells mL^{-1}. All subsequent fermentations were inoculated using the above inoculum at a level of 5% by volume.

3.1.4 Batch bioreactor fermentations

A 7.5-L stirred bioreactor (BIOFLO 110 New Brunswick Scientific, East Brunswick, NJ, USA, www.nbsc.com) was used (Figure 3.1). The working volume was 3-L. The internal diameter of the jacketed glass bioreactor vessel was 0.18 m. The vessel was fully baffled with 4 vertical baffles spaced equidistance around the periphery. The baffle width was 19 mm. A central shaft supported two 6-bladed Rushton disc turbine agitators. The agitators were identical with a diameter of 59.6 mm and were spaced 0.15 m apart on the shaft. The lower agitator was located 59.6 mm above the bottom of the vessel. A single hole sparger was used for aeration. The sparger hole diameter was 4.3 mm and it was located directly below the lower agitator, about 30 mm above the base of the vessel.

All fermentations were run as aseptic aerobic batch cultures. The air inlet and exhaust ports on the bioreactor were installed with sterile hydrophobic membrane filters (0.2 μm; either Sartorious, Gottingen, Germany, or Millipore, Bedford, MA, USA). The assembled bioreactor filled with the earlier specified liquid medium was autoclaved (121 °C, 20 min) with the pH and the dissolved oxygen electrodes installed. The pH electrode (Ingold gel-filled electrode, model no. 465-35-SC-P-K9/270/9848; Mettler-Toledo, www.mt.com) had been calibrated using pH 7.0 and pH 4.0 buffers prior to autoclaving.

The concentration of dissolved oxygen (DO) in the broth was measured online using a polarographic electrode (model In Pro 6800 sensor 12/25 mm; Mettler-Toledo, www.mt.com). The DO electrode had been calibrated at 30 °C in the sterilized culture medium. For the calibration, the liquid medium was first bubbled with nitrogen (New

Zealand Industrial Gases Ltd., Palmerston North, New Zealand) until the dissolved oxygen reading failed to decline further. The DO readout was then adjusted to read 0%. Nitrogen flow was then replaced with a preset air flow of 2.67 vvm, with the impeller rotating at 500 rpm. Once the measured concentration of dissolved oxygen had stabilized, it was adjusted to an air saturation value of 100% (Chisti, 1989; Chisti, 2010; Fadavi and Chisti, 2005).

A 20 kHz, 600 W maximum power, Misonix Sonicator® 3000 (Misonix, Inc., Farmingdale, NY, USA, www.misonix.com) ultrasound generator was used in combination with a standard tapped sonic horn (Misonix, Inc., part no. 200 with 12.7 mm tip diameter, 127 mm length), or sonotrode, installed in an external 800B Misonix Flocell® with a 3.175 mm diameter inlet orifice (Figure 3.2). The horn had a replaceable flat tip made of titanium alloy (Misonix, Inc., part no. 406). The flow cell, with the sonic horn in place, was autoclaved (121 °C, 20 min), cooled to room temperature, and connected to the bioreactor aseptically using sterile silicone tubing (Figure 3.1). The broth from the bioreactor was recirculated continuously through the sonic chamber using a peristaltic pump (Masterflex model no. 7554-60; Cole Parmer Instrument Co., Chicago, IL, USA, www.masterflex.com). The recirculation flow rate was fixed at 0.2 L min^{-1}. The recirculation commenced after the fermenter had been inoculated and briefly mixed. All fermentations were carried out with recirculation of the broth through the sonic chamber, but ultrasound was not applied to the control fermentations. For fermentations that were sonicated, sonication commenced at specified conditions only after 9.5 h of inoculation of the bioreactor.

The sterile bioreactor was inoculated with 150 mL (5% by vol) of the earlier specified inoculum. The final volume of the broth in the fermenter after inoculation was 3,150 mL. The fermentation temperature was controlled at 30.0±0.2 °C. The agitation speed and aeration rate were maintained at 500 rpm and 2.67 vvm, respectively. The pH and the dissolved oxygen concentration were monitored, but not controlled. Sterile (121 °C, 15 min) antifoam emulsion (catalog no. A 6426-100G, 10 g/100 mL of water; Sigma-Aldrich, St. Louis, MO, USA) was added to the fermenter in response to a foam sensor to automatically suppress severe foaming. Each batch fermentation was run for 24 hours. Samples were taken periodically. The optical density and the cell viability were measured immediately after sampling, as specified in Section 3.1.7.1 and 3.1.7.4. For the other measurements, the samples were centrifuged at 2000 × g for 10-min (model 0008931

centrifuge; Eppendorf AG, Germany, www.eppendorf.com) immediately after collection and the supernatant was stored at 4 °C for further analysis (Section 3.1.7.2, 3.1.7.3 and 3.1.7.5). The storage period did not exceed 3 days.

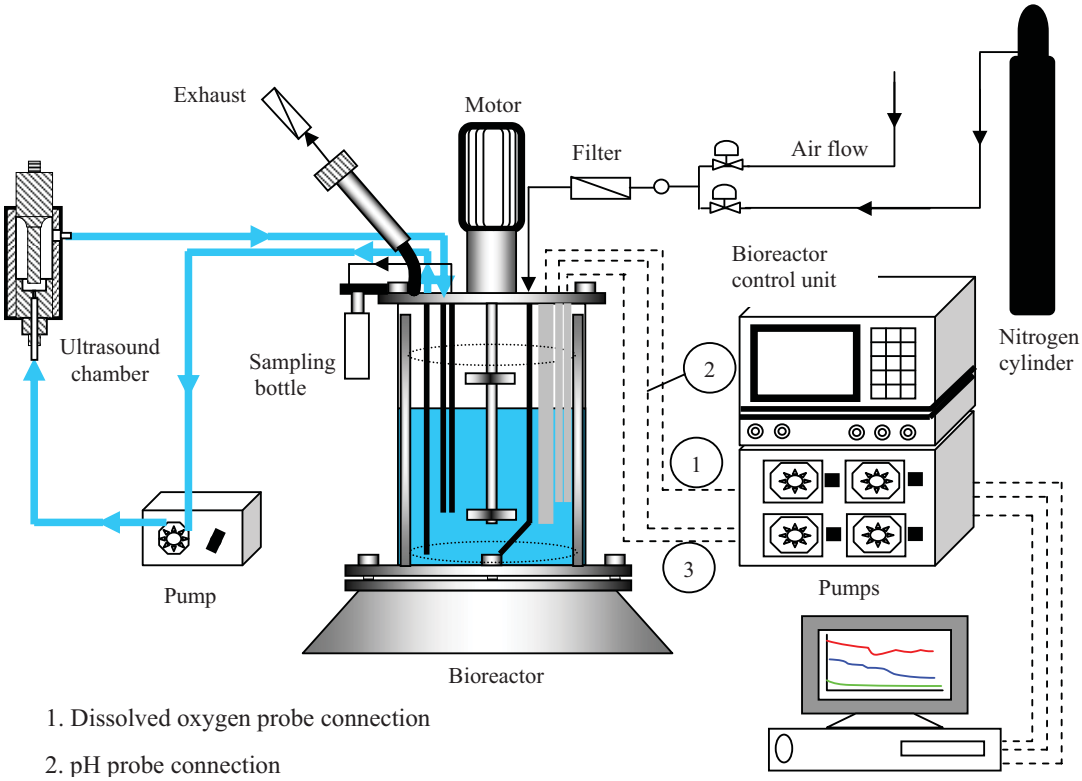

Figure 3.1 Schematic diagram of the batch ultrasound assisted fermentation system.

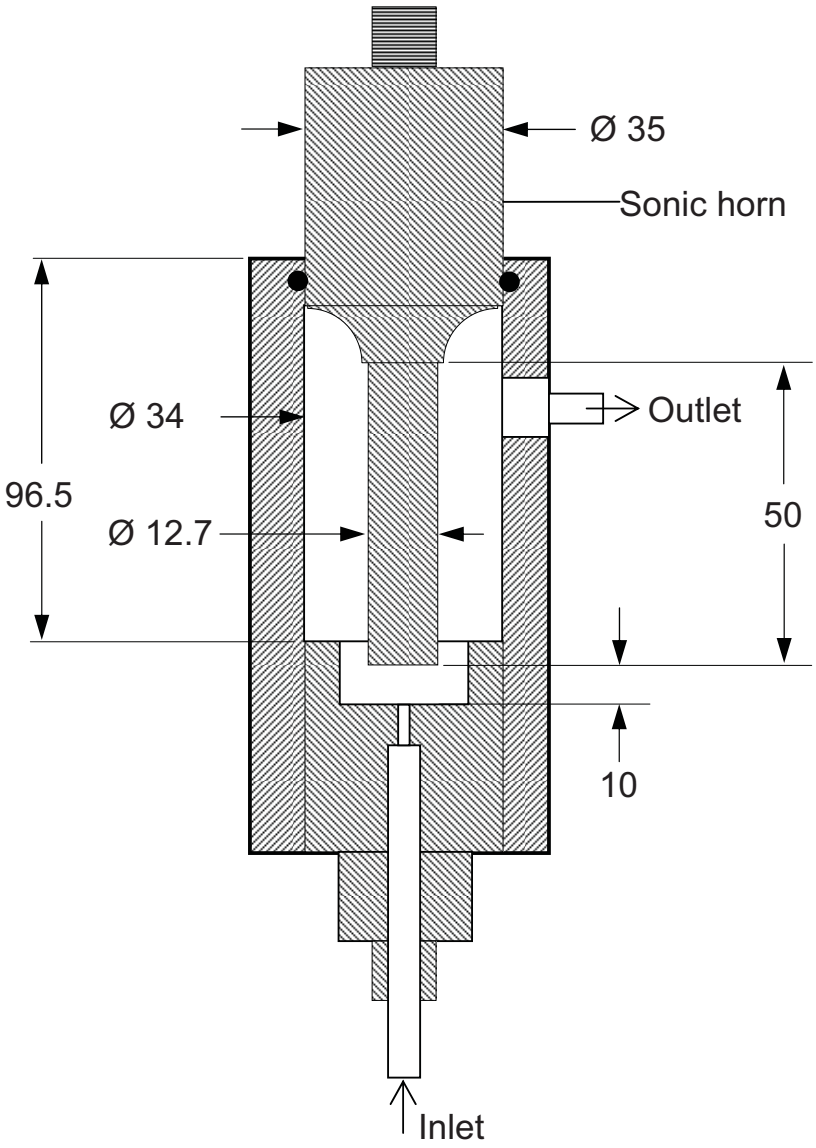

Figure 3.2 Ultrasonic flow cell dimensions (mm).

3.1.5 Sonobioreactor fermentations

For ultrasound-assisted fermentations, the ultrasound power level was varied by adjusting the amplitude setting of the sonotrode and the cumulative average-ultrasound dose could be varied by adjusting the duty cycle. The amplitude was set at position 2 to correspond to a power input P of 15 W, or a sonication intensity I of 11.8 W cm^{-2}. The power input (P) was read directly from the display panel of the ultrasound generator (Figure 3.3).The sonication intensity was calculated using the following equation (Chisti, 2003b):

$$I = \frac{P}{A} \tag{3.1}$$

where A (cm^2) was the area of the sonotrode tip. The A value was 1.27 cm^2. The cumulative sonic energy imparted to the fluid depended on the duty cycle of sonication (Table 3.2). The duty cycle determined the proportion of the time that the sonication was "on". A pulse ratio (Table 3.2) of 1:9 for example meant that the sonication occurred for one 'unit' of time followed by a nine 'units' period of no sonication. Duty cycle of 10% was equivalent to sonication for 1 s followed by a rest period (no sonication) of 10 s. A sonication duty cycle of 100% meant uninterrupted sonication. The time units of seconds were used in setting the duty cycle. Duty cycles of 10%, 20% (1 s sonication, 5 s rest period) and 40% (2 s sonication, 5 s rest period) were used (Table 3.2)

Figure 3.3 Ultrasound generator (Misonix Sonicator 3000).

Table 3.2 Sonication regimens used at a fixed sound intensity of 11.8 W cm^{-2}

Duty cycle (%)	Pulse ratio
10	Sonication for 1 s followed by a rest period (no sonication) of 10 s
20	Sonication for 1 s, rest period of 5 s
40	Sonication for 2 s, rest period of 5 s

3.1.6 Continuous bioreactor fermentations

All continuous fermentations commenced in a batch mode, as outlined in Section 3.1.4, and were later switched to continuous feeding of substrate. Continuous operation began after a batch fermentation period for 15 h. The sterile feed composition was as shown in Table 3.1. Antifoam was added automatically as described in Section 3.1.4. pH and dissolved oxygen were continually measured but not controlled (Figure 3.4).

Precalibrated peristaltic pump was used for feeding (Figure 3.5). The harvest pump was always run faster than the feed pump such that the volume in the bioreactor did not change (Scragg, 1991). Samples (45 mL) were removed after each residence time, and more frequently after three residence times, to establish that a steady state condition had been attained. Dilution rates of 0.05 h^{-1}, 0.075 h^{-1}, 0.1 h^{-1}, 0.15 h^{-1} and 0.20 h^{-1} were used. Dilution rate was calculated as the steady state feed flow rate divided by the constant volume of the broth in the bioreactor. A steady state condition was normally assumed to exist after three residence times if the biomass dry weight, ethanol and lactose concentrations remained constant (±10%). The broth from the bioreactor was continuously re-circulated through the externally mounted ultrasonic chamber as described in Section 3.1.4.

Optimal sonication conditions identified in batch fermentations were used in continuous fermentations. Thus, the sonication duty cycle and intensity were 20% and 11.8 W cm^{-2}, respectively. At various steady-states attained in control culture (no ultrasound), sonication was started at preset conditions to see the effect on steady state values of biomass concentration, ethanol concentration and lactose concentration. Sound was then switched off to see that the original control steady-state was regained. Samples were withdrawn periodically from the bioreactor aseptically for measurements of lactose concentration, biomass concentration and ethanol concentration. Figure 3.4 shows a schematic diagram of the continuous fermentation process.

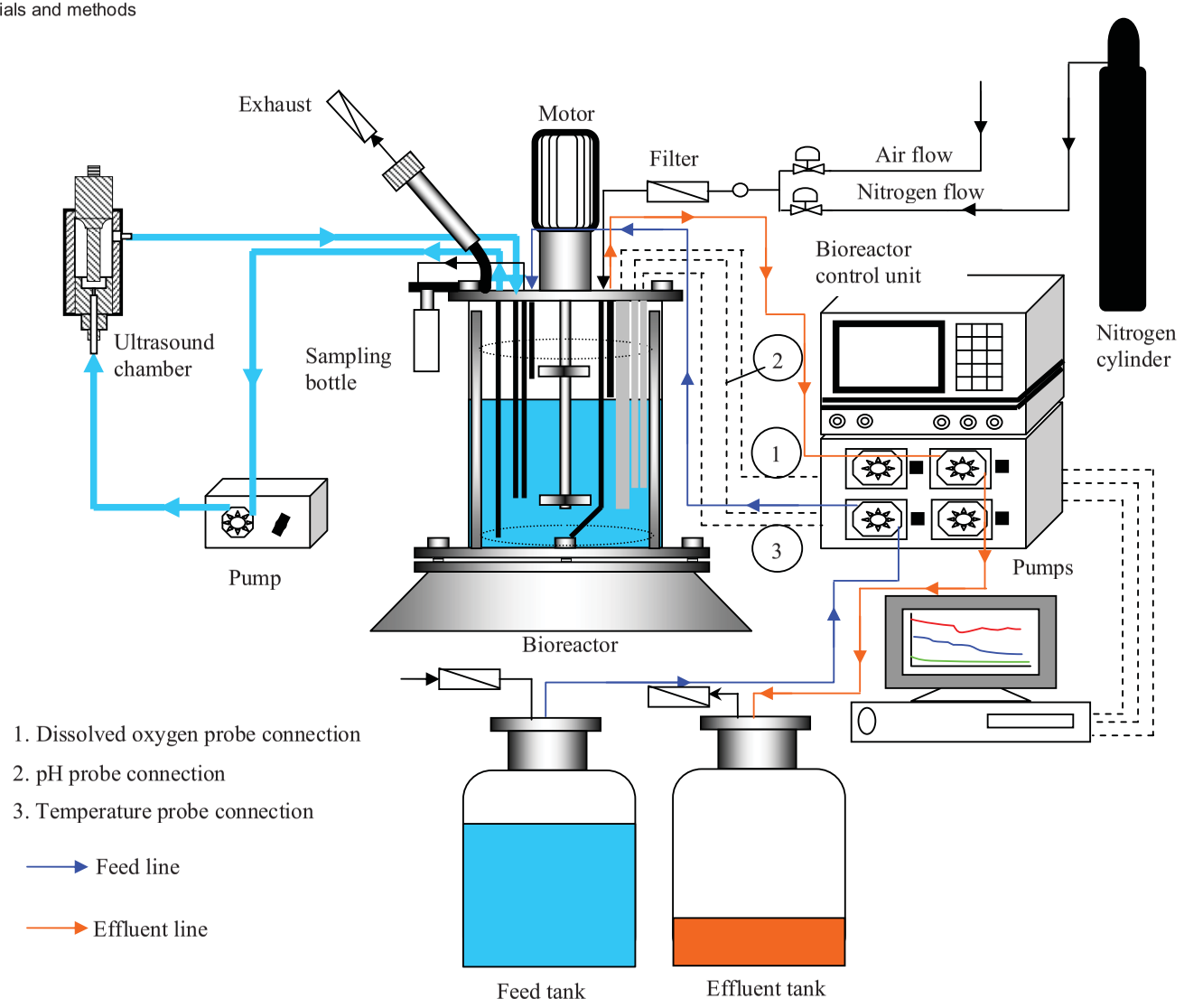

Figure 3.4 Setup for continuous fermentation.

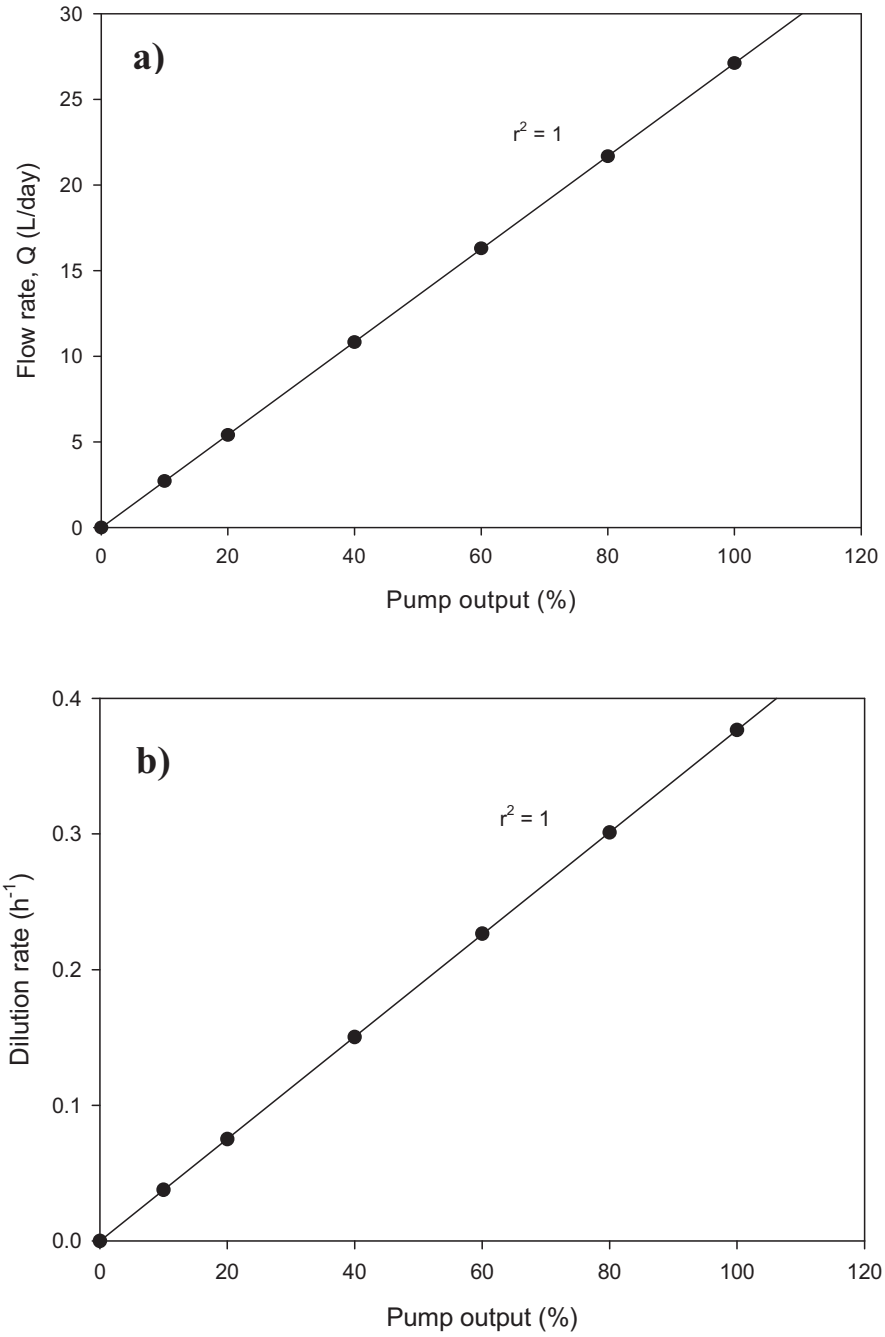

Figure 3.5 (a) Fermenter feed pump calibration plot and (b) the corresponding dilution rate.

3.1.7 Analytical methods

3.1.7.1 Biomass concentration

Biomass concentration was measured by using spectrophotometry that had been calibrated by gravimetry. Absorbance was measured at 620 nm using a UV/Visible spectrophotometer (Ultraspec 2000, Pharmacia Biotech, Model 80-2106-00) that had been zeroed using a blank of the sterile medium. Typically, a 1 mL sample of the fermentation broth was diluted with 24 mL of the sterile medium prior to measurement. This way the spectrophotometric absorbance was always ≤ 0.7.

For biomass dry weight measurement by gravimetry, a known volume (35 mL) of the fermentation broth sample was centrifuged at 2415 × *g* for 10 min. The supernatant was discarded and the cells were washed twice by re-suspending in deionised water (2 × 35 mL) and centrifuging as previously described. The washed suspension was filtered through a pre-weighed cellulose acetate membrane filter (47 mm in diameter, 0.45 μm in pore size) under suction (Doran, 1995; Shuler and Kargi, 1992; Wang, 2007). The membrane with the wet biomass was dried in an oven (Contherm Digital Series Five Incubator, Lower Hutt, New Zealand, Cat. No: 245M) at 105 °C for overnight. After drying, the membrane was cooled to room temperature in a dessiccator and weighed. The measured dry weight of biomass and the original volume of the sample (35 mL) were used to calculate a dry weight concentration. A second identical sample of the fermentation broth was diluted (1:25 dilution by volume) with the sterilized medium (Table 3.1) and the absorbance was measured by spectrophotometry as described above. A calibration curve for absorbance of diluted sample at (1:25 dilution) versus dry weight (undiluted sample) is shown in Figure 3.6 and was linear up to about an absorbance of 0.7. Linear regression was used to establish the following calibration equation:

$$\text{Dry biomass concentration (g/L)} = \frac{A_{620}}{6.95 \times 10^{-2}} \qquad (3.2)$$

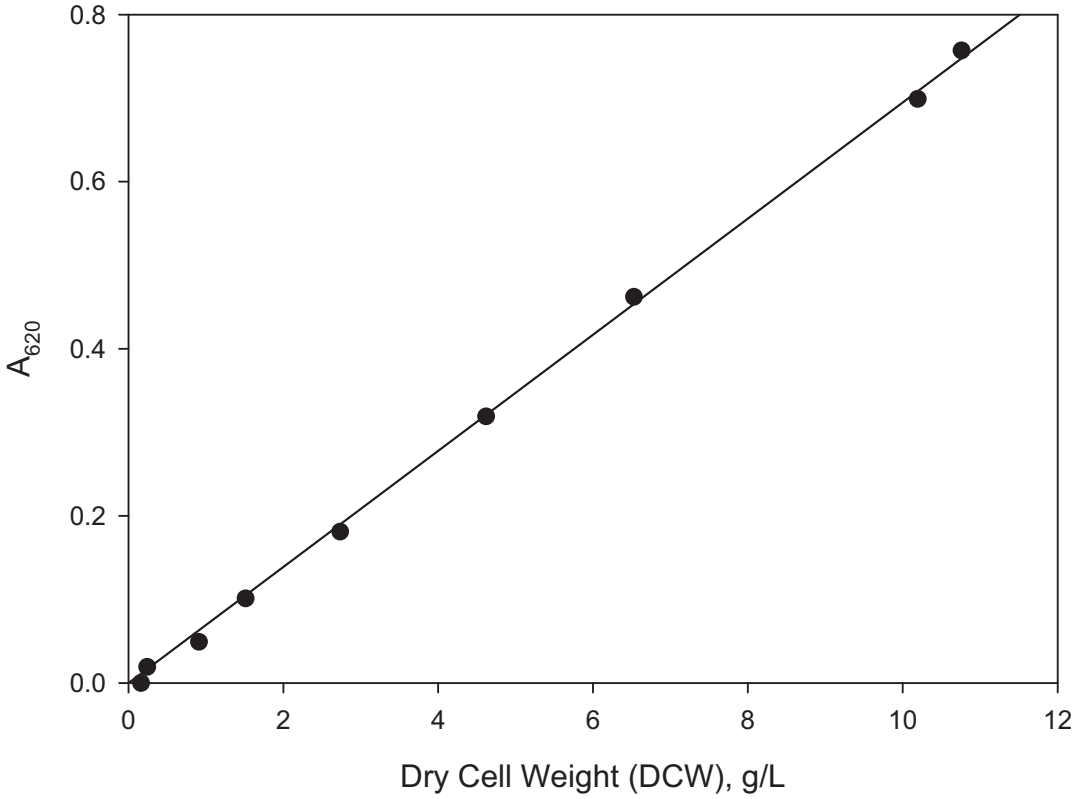

Figure 3.6 Calibration curve for A_{620} at 1:25 dilution versus actual dry biomass concentration.

3.1.7.2 Lactose concentration

Lactose concentration was determined using a modified dinitrosalicylic acid (DNS) method based on Miller (1959). Thus, a 1% (w/v) solution of DNS reagent was prepared by dissolving 10 g DNS and 2 g of phenol in 1000 mL of a solution of sodium hydroxide (10 g L^{-1}) and sodium sulfite (0.5 g L^{-1}). The broth sample was centrifuged (Section 3.1.7.1) and a portion of the supernatant containing lactose was appropriately diluted with deionized water. The diluted sample (3 mL) was mixed with 3 mL of DNS reagent and heated for 15 min on a boiling water bath. One milliliter of Rochelle salt solution (potassium-sodium tartrate, 400 g L^{-1}) was added and the resulting mixture was cooled to ambient temperature in a cold water bath. The absorbance of the cooled solution was measured at 575 nm (Ultraspec 2000, model 80-2106-00 spectrophotometer; Pharmacia Biotech Inc., Piscataway, NJ, USA) against a blank that had been prepared using deionized water instead of the sample. The absorbance was converted to lactose concentration using a standard curve (Figure 3.7). The standard curve had been prepared using lactose solutions of known concentrations. The equation of the standard curve was the following:

$$\text{Lactose concentration } (\mu\text{g/mL}) = \frac{A_{575}}{5.2 \times 10^{-3}} \qquad (3.3)$$

where A_{575} was the spectrophotometric absorbance at 575 nm. The above equation applied to an absorbance range of 0 to 0.7. Linear regression of Equation (3.3) allowed calculation of lactose concentration from absorbance measurements.

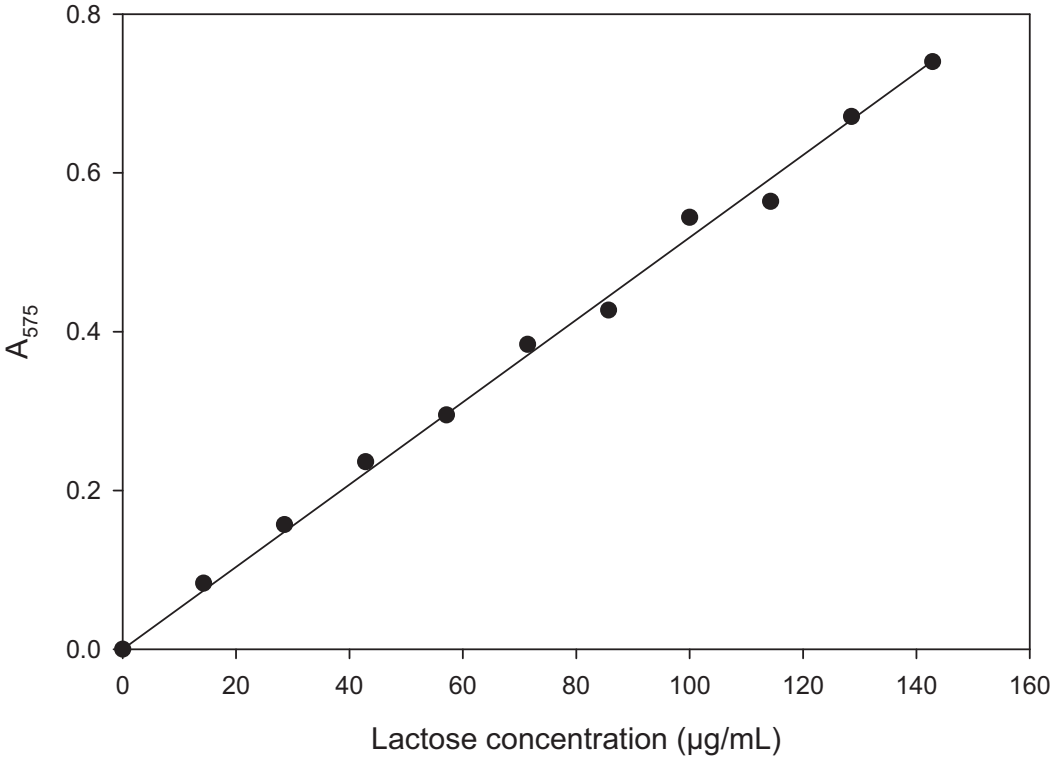

Figure 3.7 Calibration curve for lactose concentration.

3.1.7.3 Ethanol concentration

Ethanol concentration in the broth supernatant was determined using a gas chromatograph (model GC 6000 Vega Series 2; Carlo Erba Instruments, Milan, Italy) fitted with a flame ionization detector and chromato-integrator (model D-2500; Hitachi, Tokyo, Japan). The carrier gas was nitrogen at a flow rate of 40 mL min^{-1}. The column temperature was 200 °C. Standard ethanol solutions were prepared in the concentration range of 2 to 8 g L^{-1} by diluting absolute ethanol with deionized water. The sample volume injected was 2 µL. The sample had been prefiltered through a 0.45 µm membrane filter. The ethanol concentration of the culture supernatant sample was

calculated by measuring the relative area under the ethanol peak and comparing it with the standard curve prepared using the standard solutions.

3.1.7.4 Cell viability

Cell viability was measured by plate counts (Wang and Sakakibara, 1997) and methylene blue staining methods (Boyd *et al.*, 2003; Sami *et al.*, 1994; Trevors *et al.*, 1983), to validate the methylene blue method against the more time consuming but accurate plate count. For plate count, appropriate serial dilution of the broth was prepared in the culture media specified in Section 3.1.3. An identically diluted sample of the broth (known volume) was plated on an agar plate that was incubated at 30 °C for 48 h. Numbers of colonies produced were counted using a Colony Counter (Suntex Instruments. Co Ltd, Taipei Taiwan, Model 560. www.suntex.com.tw). Percent viability was calculated as:

$$\text{Viability (\%)} = \frac{\text{Number of colonies produced by a given volume of broth}}{\text{Total cell count in the same volume}} \times 100\%$$

For determining cell viability by the methylene blue staining method (Hansen, 2000; Painting and Kirsop, 1990), a 10 µL aliquot of serially diluted freshly sampled yeast broth was mixed with 10 µL of a methylene blue solution and incubated for 5 min (Hansen, 2000; Painting and Kirsop, 1990). The cell suspension was then counted on a hemacytometer at 400 × magnification. The viability was calculated as the ratio of the unstained cell count (viable cells) and the total count:

$$\text{Viability (\%)} = \frac{\text{Number of live cells}}{\text{Number of live cells} + \text{Number of dead cells}} \times 100\%$$

3.1.7.5 Activity of β-galactosidase

Activity of the extracellular β-galactosidase was measured in the cell-free culture supernatant (Section 3.1.7.2) as specified in the Sigma enzymatic assay for β-galactosidase (Sigma, 1994). The activity was determined using the synthetic substrate o-nitrophenyl-β-D-galactopyranoside, ONPG (catalog no. N1127-25G; Sigma-Aldrich, St. Louis, MO, USA). One unit of β-galactosidase activity was defined as the amount of the enzyme that liberated 1.0 μmol of o-nitrophenol from 5 mM ONPG per minute at pH 3.5 and 25 °C.

The intracellular β-galactosidase activity was measured according to the method described by Wang and Sakakibara (1997). A 35 mL sample of the broth was centrifuged (3300 × g, 10-min) to recover the cells. The cells were washed (2×35 mL) with 0.1 M phosphate buffer, pH 6.5. The washed cells were resuspended in 35 mL of deionized water using a vortex mixer. The suspension was cooled in an ice-water bath at 4 °C and sonicated at 550 W, 20 kHz, for 30 s (Misonix Sonicator® 3000, Misonix, Inc., Farmingdale, NY, USA). The optimum sonication time (30 s) for the cell breakage was established in preliminary experiments by using different sonication periods and measuring the released enzyme activity (Figure 3.8). Sonication for 30 s released all the entire releasable enzyme. The sonicated suspensions was centrifuged (12000 × g, 30-min; Hitachi CR-22GII refrigerated centrifuge, Hitachi Koki Co., Ltd., Tokyo, Japan) at 4 °C. The supernatant was collected and analyzed in accordance with the procedure given above for the determination of the extracellular β-galactosidase activity.

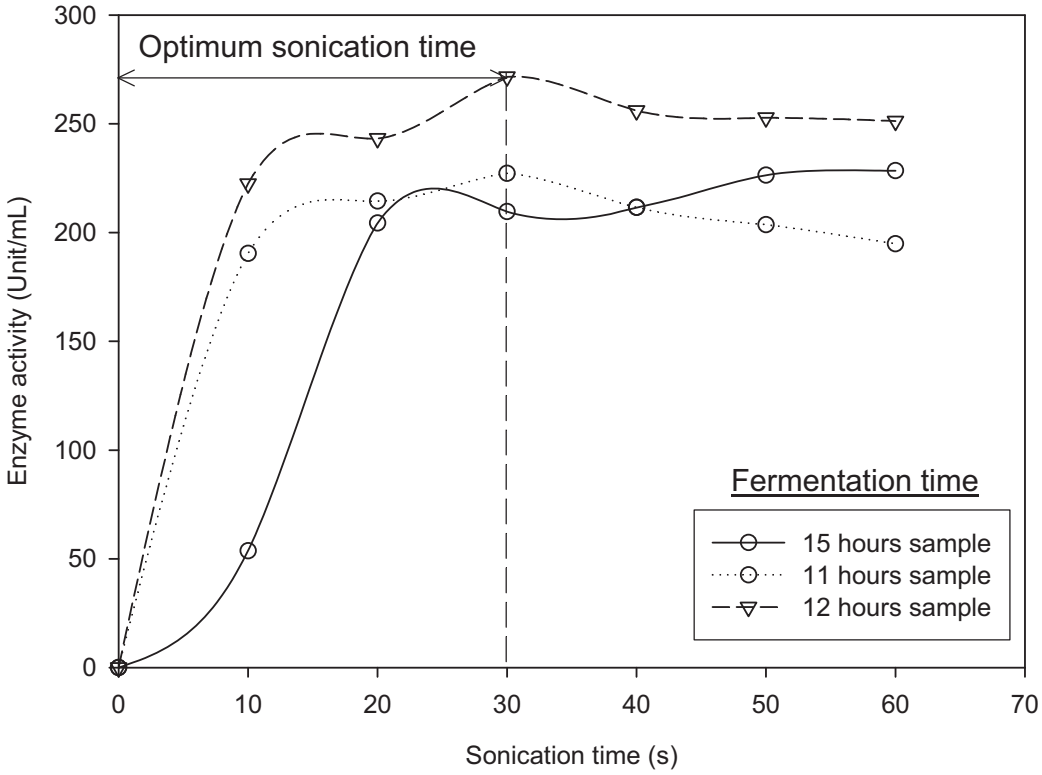

Figure 3.8 Release of intracellular β-galactosidase activity after various periods of sonication. Samples were sonicated continuously for the specified period at 550 W and 20 kHz.

3.1.8 Gas-liquid mass transfer measurements

3.1.8.1 Response time of the dissolved oxygen electrode

The response time of the dissolved oxygen electrode was measured in water and the uninoculated lactose medium. Measurements were made at a constant temperature of 30 °C, as used in the fermentation. The calibrated electrode was placed in a beaker of the appropriate medium (800 mL in 1-L beaker) bubbled with nitrogen. Once the reading had stabilized to zero, the probe was instantaneously transferred to a second identical beaker bubbled with air at a flow rate of 8 L min^{-1} at ambient atmospheric pressure. The liquid in the second beaker was saturated with oxygen as it had been sparging with air for at least 2 minutes prior to the transfer of the electrode. From the instance of transfer, or time zero, the response of the DO electrode was recorded at 1-2 s intervals until the

saturation concentration was reached. The time required to attain 63.7% of the full response was read from the graph (Figure 3.9 and Figure 3.10) as the response time of the electrode (Chisti, 1989; Chisti, 2010; Fadavi and Chisti, 2005).

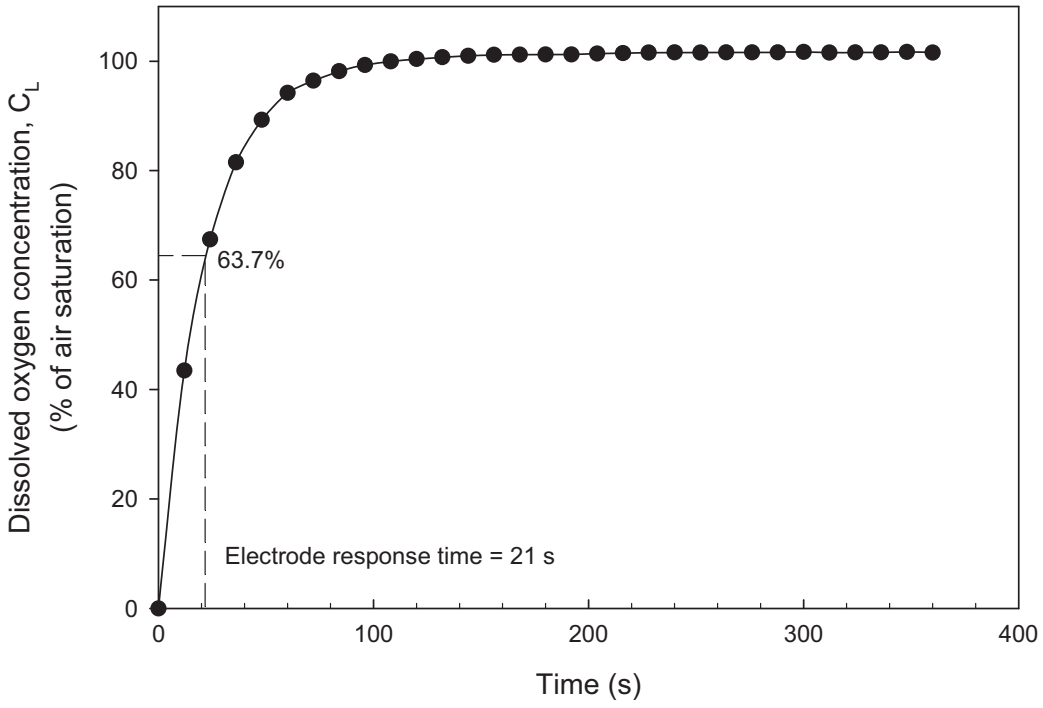

Figure 3.9 Dissolved oxygen electrode response versus time from the instance of transfer to oxygen-saturated water.

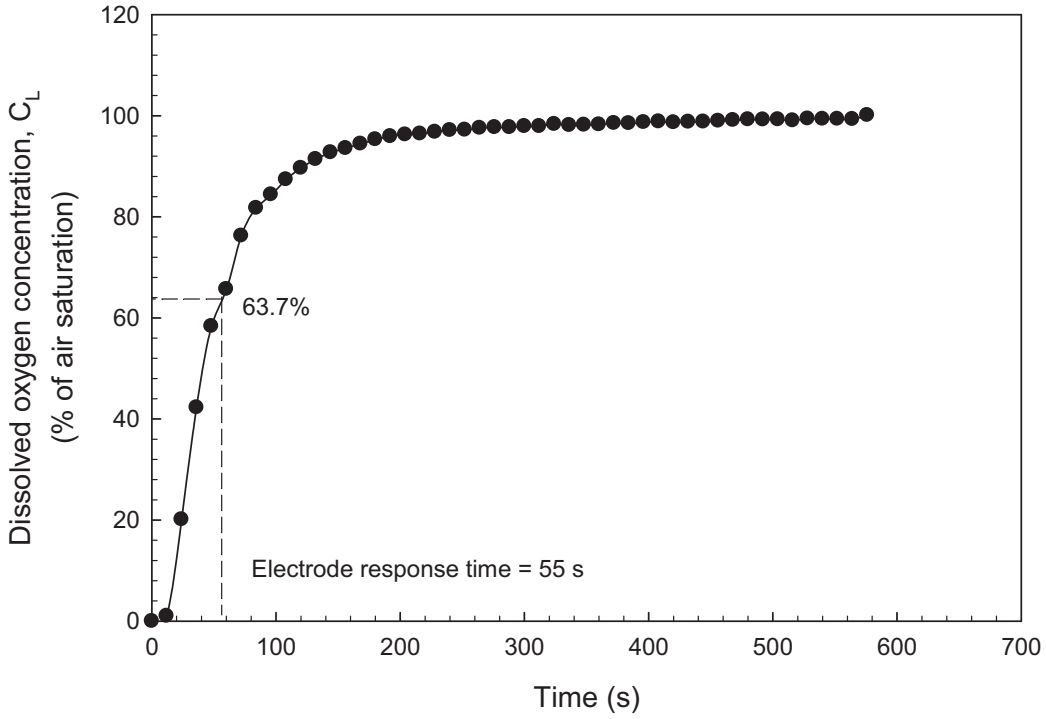

Figure 3.10 Dissolved oxygen electrode response versus time from the instance of transfer to oxygen-saturated lactose medium.

3.1.8.2 Overall volumetric gas-liquid mass transfer coefficient, $k_L a_L$

The overall volumetric oxygen mass transfer coefficient $k_L a_L$ was measured in de-ionised water and the lactose based-medium in the 7.5-L bioreactor (3 L of working volume) with and without ultrasound. The liquid was continuously recirculated between the bioreactor and the sonication chamber at a flow rate of 0.2 L min^{-1} (Figure 3.1). This circulation occurred also in nonsonicated experiments. In sonicated measurements, the ultrasound intensity was either 11.8 W cm^{-2} (low-intensity sonication) or 50.3 W cm^{-2} (high-intensity sonication). In both cases, the duty cycle was set at 100%. Control experiments did not use sonication. Various impeller agitation speeds (200-800 rpm) and aeration rates (0-3 vvm) were used in different experiments. All measurements were made at 30 °C.

The static gassing in method was employed to obtain the dissolved oxygen concentration profile as a function of time from which k_La_L was calculated (Bandyopadhyay *et al.*, 1967). After calibration of the DO electrode, the liquid medium was first sparged with nitrogen until the oxygen concentration reduced to zero. Air was then sparged at a preset rate in the range of 0 – 3 vvm with the selected impeller rotation rate of between 200 – 800 rpm.

As the average measured response time, τ_p, of the DO probe used in this study was 21 s (air-water system) and 55 s (air-uninoculated lactose medium) at 30°C, therefore k_p (where $k_p = 1/\tau_p$) was 0.0476 s^{-1} and 0.0182 s^{-1}, respectively. In view of the relatively slow response of the probe, the average k_La_L for each experiment was obtained by using Equation (2.7). The Goal Seek function in Microsoft Excel was used to match the value of C_p measured by the probe to the value calculated from Equation (2.7), using t_m (i.e. 1/ k_La_L) as the fitting parameter (Boodhoo *et al.*, 2008; Lamping *et al.*, 2003). See Appendix 4.

3.2 Effects of ultrasound on β-galactosidase-mediated hydrolysis of lactose

3.2.1 Introduction

Hydrolysis of lactose to glucose and galactose via the action of the enzyme β-galactosidase was used as a reaction system. The reaction was carried out in a 7.5 liter (3 L working volume) stirred bioreactor (as described in Section 3.1.4).

3.2.2 Enzyme and substrate

The β-galactosidase (EC 3.2.1.23) enzyme used in this study was purchased from Sigma (catalog no. G3665/12/21/10/2; Sigma-Aldrich, St. Louis, MO, USA) under the commercial name of Lactozyme. The enzyme was in a liquid form and had been produced by *Kluyveromyces lactis*. It was stored at 4°C in a refrigerator. The activity of the enzyme was 3000 Unit mL^{-1}. Lactose was purchased from Ajax Finechem Pty Ltd. The hydrolysis reaction was carried out in 25 mM phosphate buffer solution, pH 6.5, at 37 °C.

3.2.3 Experimental setup and operation

The batch bioreactor used was exactly as described in Section 3.1.4 (Figure 3.1). The pH and dissolved oxygen sensors were installed, but not used. Aeration was not used. The working volume of the bioreactor was 3 L. The temperature was controlled at 37 °C. The agitation speed was maintained at 300 rpm. In all experiments, including the nonsonicated controls, the lactose medium was circulated through the sonication chamber (Section 3.1.4, Figure 3.1) at a flow rate of 0.2 L min^{-1}. In different sonicated experiments, the irradiation power (P_{ir}) of ultrasound was 3 W, 6 W and 15 W, corresponding to a sonication intensity of 2.4, 4.7 and 11.8 W cm^{-2}, respectively. Sonication duty cycles of 10%, 20% and 40% were used (Table 3.2).

To allow the calculation of certain kinetic parameters, experiments were carried out at initial lactose concentrations of 5, 10, 20, 30, 40, 50, 60 g L^{-1}. The enzyme concentration was always 1.0 mL L^{-1}. The substrate was dissolved in 25 mM phosphate buffer solution, pH 6.5, at 37 °C. Enzyme was added to start the reaction. The experiments were carried out in duplicate and the reproducibility was at least within the range of ±5%. Samples were taken from the reaction solution at specified time intervals, the hydrolysis reaction was stopped by immediate boiling (100 °C, 10-min) and the glucose concentration was measured immediately after cooling to room temperature.

3.2.4 Glucose analysis

Glucose concentration was measured using a YSI fixed enzyme sugar analyzer (Model 2700/230V, Yellow Springs Instruments Co. USA). A 2.50 g L^{-1} solution of glucose was used as a calibration standard. The sample volume injected was 25 μL.

3.2.5 Enzyme stability

To investigate if sonication affected the β-galactosidase stability, the experiments were carried out at 37 °C in the 7.5-L bioreactor (3 L of working volume). In all experiments, including the nonsonicated controls, the enzyme solution was circulated through the sonication chamber (as described in Section 3.1.4, Figure 3.1) at a flow rate of 0.2 L

min^{-1}. Enzyme solution of 1.0 mL L^{-1} was mixed with 25 mM phosphate buffer, pH 6.5. Lactose was not added. Control experiment did not use ultrasound. For sonicated experiments, the power intensity was always 11.8 W cm^{-2}. Duty cycle values of 10%, 20% and 40% were tested in separate experiments. Samples (45 mL) were withdrawn periodically and the enzyme activity was measured as explained in Section 3.2.6.

3.2.6 β-Galactosidase activity

A sample (100 μL) taken from the reaction solution was mixed with 2 mL of ortho-nitrophenyl-β-galactoside (ONPG) solution (prepared by dissolving 300 mg ONPG in 100 mL of 100 mM phosphate buffer solution, pH 7.3). The mixture was incubated at 28 °C for 5 min. The reaction was then stopped by adding 1 M Na_2CO_3 solution (1 mL) to the mixture. A blank was prepared by mixing 2 mL ONPG and 1 mL Na_2CO_3 solution in phosphate buffer. The absorbance value of the sample was read against the blank at 420 nm (Demirhan and Ozbek, 2009; Sakakibara *et al.*, 1994; Wang *et al.*, 1996; Wang and Sakakibara, 1997).

3.3 Effects of ultrasound on enzymatic hydrolysis of cellulose

3.3.1 Introduction

The effect of low intensity ultrasound on enzymatic hydrolysis of cellulose was investigated using both soluble cellulose and suspended particulate cellulose.

3.3.2 Enzyme and substrates

A commercial cellulase (EC 3.2.1.4) enzyme *Accellerase 1000* was used. The enzyme was purchased in a soluble form from Genencor, Rochester, NY, USA (www.genencor.com). It had been produced by a genetically modified strain of the fungus *Trichoderma reesei.* The activity of the enzyme as specified by the supplier was 2500 Unit CMC g^{-1}. The optimal temperature and pH for the enzyme as specified by the supplier were 50 °C and 4.8, respectively. The enzyme solution was stored at 4°C.

The soluble substrate was carboxymethyl cellulose (low viscosity, sodium carboxymethylcellulose, CMC, Sigma, catalog no. CAS 9004-32-4). It was in the form of a soluble powder. The insoluble particulate cellulose substrate was Solka-Floc. It had been purchased from International Fiber Corporation, USA (AlphaCel powdered cellulose, CAS # : 9004-34-6). Three grades of Solka-Floc were used. These were BH 300, BH 40 and CH 10. They differed only in the average size of the particles. The particle sizes were 30 μm, 60 μm and 290 μm for the grades BH 300, BH 40 and CH 10, respectively.

3.3.3 Substrate preparation

Clear solutions of CMC at various initial concentrations (0.5 – 4% w/v; g/100 mL) were prepared by dissolving the powder in 500 mL of 0.05 M acetate buffer, pH 4.8 (Aliyu and Hepher, 2000; Melo and Kennedy, 1993; Sreenath, 1993) at 80-85 °C and making up to the required concentrations by adding the same cold buffer at 6 to 10° C (Sreenath, 1993). Slurries of insoluble Solka-Floc were prepared by suspending the particles of a given size in 0.05 mM acetate buffer, pH 4.8, at various initial concentrations (0.5 – 4% w/v; g/100 mL) (Howell and Stuck, 1975; Yeh *et al.*, 2010). Irrespective of the type of substrate and its concentration, the initial enzyme concentration, was always at 0.1 g L^{-1}. The hydrolysis was carried out in a well-mixed reactor (Section 3.3.4). The reaction was started by adding the enzyme to a well-mixed substrate mixture that was at a controlled temperature of 50 °C.

3.3.4 Cellulose hydrolysis

Hydrolysis of cellulose was carried out in a stirred beaker of 2-L. The initial working volume was 1-L. The internal diameter of the glass reactor vessel was 0.14 m. The vessel was fully baffled with 4-vertical baffles spaced equidistance around the periphery. The baffle width was 14 mm. A central shaft supported one 6-bladed Rushton disc turbine agitator. The agitator was identical with a diameter of 46 mm. The agitator was located 46 mm above the bottom of the vessel. The agitation speed was always 500 rpm. A 20 kHz, 600 W maximum power, Misonix Sonicator® 3000 (Misonix, Inc., Farmingdale,

NY, USA. www.misonix.com) ultrasound generator was used in combination with a standard tapped sonic horn (Misonix, Inc., part no. 200 with 12.7 mm tip diameter, 127 mm length), or sonotrode. The sonic horn shown in Figure 3.2 was used without the outer chamber shown in the figure. The horn had a replaceable flat tip made of titanium alloy (Misonix, Inc., part no. 406). The sonic horn was mounted in the 2-L beaker such that its flat tip was 41.7 mm above the bottom of the beaker and was on the left-hand-side of the beaker at a distance of 58.4 mm from the turbine central shaft (Figure 3.11).

The control experiments did not use sonication although the sonotrode was installed in the reactor. For ultrasound-assisted hydrolysis, the sonication amplitude in different experiments were set at positions 0.6, 1.2 and 2 to correspond to a power input P of 3, 6 and 15 W, or a sonication intensity I of 2.4, 4.7 and 11.8 W cm^{-2}, respectively. For every power level tested, sonication duty cycles of 10%, 20% and 40% were used for experiments involving soluble cellulose, CMC. Power and duty cycle combinations that proved optimal for CMC hydrolysis were used in enzymatic hydrolysis of the particulate substrate.

Once the reactor had attained the required temperature, ultrasonic irradiation was started and 2-min later the enzyme was added to commence the reaction. Measurements were made for 20-min. During this time, the solids-free liquid samples were withdrawn periodically and analyzed for the concentration of glucose. The enzyme in the sample was heat inactivated by boiling (100 °C) for 5 min. The sample was then centrifuged at 2415 × g for 10-min to remove any residual solids. The glucose concentration was measured in the supernatant as described in Section 3.2.4.

3.3.5 Cellulase stability

The stability of the enzyme under various sonication regimens, including control (no sonication) was investigated by sonicating the enzyme solution without the substrate being added. The experiments were carried out in a stirred beaker of 2-L. The initial working volume was 1-L (as described in Section 3.3.4, Figure 3.11). Enzyme solutions were prepared by mixing the enzyme with 0.05 M acetate buffer, pH 4.8, to obtain a final enzyme concentration of 0.1 g L^{-1}. The enzyme stability was measured at 50° C for 60 min. Separate experiments used sonication power intensities of 2.4 W cm^{-2}, 4.7 W

cm^{-2} and 11.8 W cm^{-2}. At each power intensity, duty cycles of 10%, 20% and 40% were tested. Samples (15 mL) were withdrawn periodically, diluted appropriately with 0.05 M acetate buffer, and measured for the activity of cellulase as explained in Section 3.3.6.

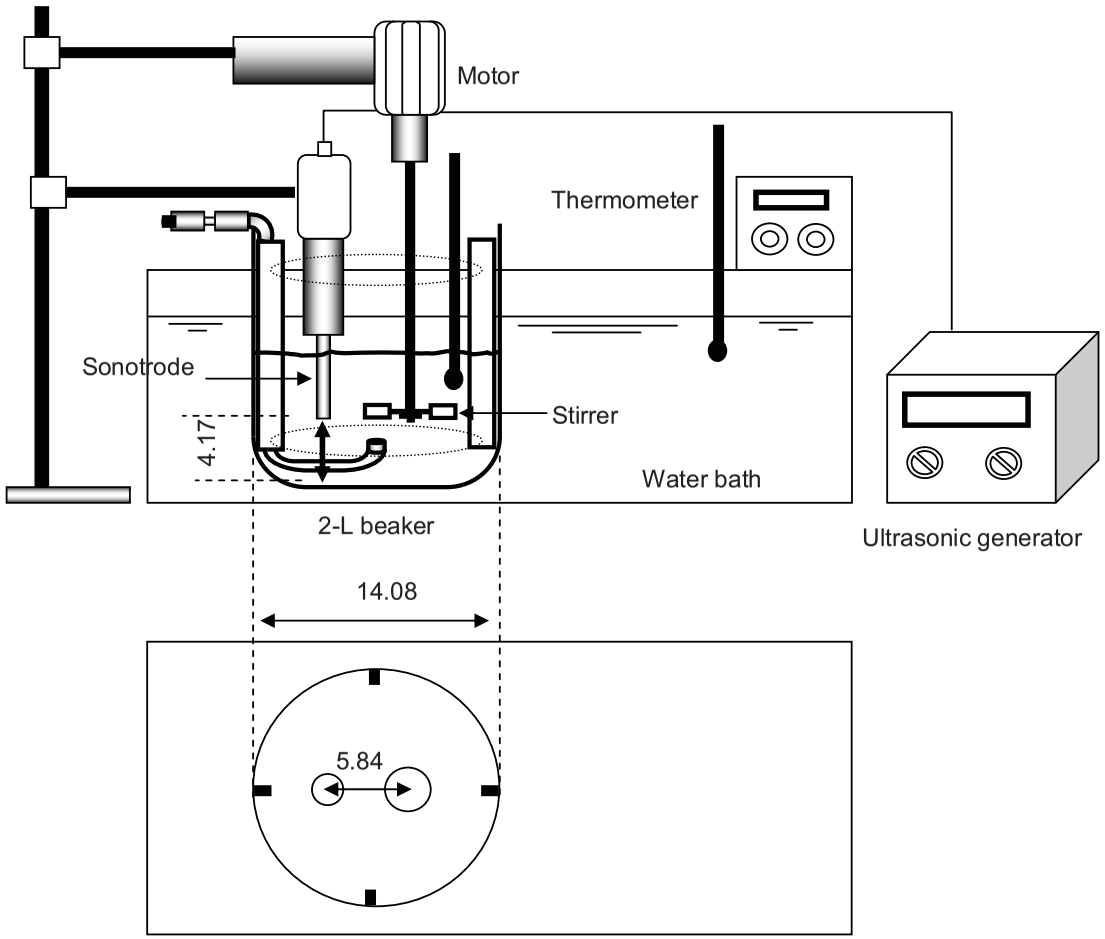

Figure 3.11 Schematic diagram of the 2-L stirred beaker system used for enzymatic hydrolysis of cellulose (dimension in cm)

3.3.6 Cellulase activity assay

For determining the residual cellulase activity a 1 mL sample of the enzyme solution (Section 3.3.5) was mixed with 1 mL of a 1% (w/v) solution of low viscosity sodium carboxymethyl cellulose (SIGMA, catalog no: CAS 9004-32-4). The CMC solution had been prepared in 0.05 M acetate buffer, pH 4.8. The mixture was incubated at 50 °C, pH 4.8, for 1 h (Mandels *et al.*, 2004; Ortega and Busto, 2001; Sreenath, 1993). The reducing sugars produced were then determined following Miller method (Miller, 1959). The rate of release of reducing sugars was proportional to the enzyme activity (Mandels *et al.*, 2004). One unit of cellulase was the quantity that liberated 1.0 μmol of reducing sugars (expressed as glucose equivalents) from cellulose in one hour at pH 4.8 and 50 °C.

CHAPTER 4

RESULTS AND DISCUSSION

The various sections of this chapter separately discuss the effects of sonication on the fermentation involving live cells (Section 4.1), the cell-free lactose hydrolysis by β-galactosidase (Section 4.2) and cellulose hydrolysis by cellulase (Section 4.3). Section 4.4 then attempts to establish a unified picture of the effects of sonication on bioreaction systems, based on the findings of Section 4.1-4.3.

4.1 Bioethanol fermentation using *K. marxianus*

4.1.1 Baseline determination (nonsonicated batch fermentation)

For evaluating the effects of sonication on *K. marxianus* fermentations, baseline data were first obtained using nonsonicated, or control fermentation. The results of duplicate nonsonicated batch fermentations are shown in Figure 4.1. The fermentation was essentially complete by 24 h (Figure 4.1). The biomass growth, the ethanol production and lactose consumption profiles were consistent with expectations for an aerated fermentation. The error bars in Figure 4.1 demonstrated a good reproducibility of the fermentations. In the first 6 h of fermentation (Zone 1, Figure 4.1), there was little growth, lactose consumption was slow and no significant ethanol production occurred. During this period, the yeast cells were adapting to the aerated and nutrient rich environment of the bioreactor. Once the cells had adjusted to the new environment, growth become rapid (Zone 2, Figure 4.1), the rate of lactose consumption increased and the ethanol concentration increased. Under the aerobic conditions used (2.67 vvm constant aeration rate), the maximum biomass concentration and the final ethanol concentration were 9.71 ± 0.08 g L^{-1} and 1.48 ± 0.36 g L^{-1}, respectively. By around 16 h the fermentation began to slow (Zone 3) because of a depletion of lactose. The results in Figure 4.1 were consistent with trends reported by Lukondeh *et al.* (2005) and Marquez *et al.* (2005) for this fermentation. The final ethanol concentration was relatively low

compared to what is possible for this fermentation, but this was because the aerobic conditions used favoured production of biomass rather than ethanol. The data in Figure 4.1 were used to compute the various fermentation kinetic parameters, as discussed later (Section 4.1.2), for comparison with sonicated fermentations.

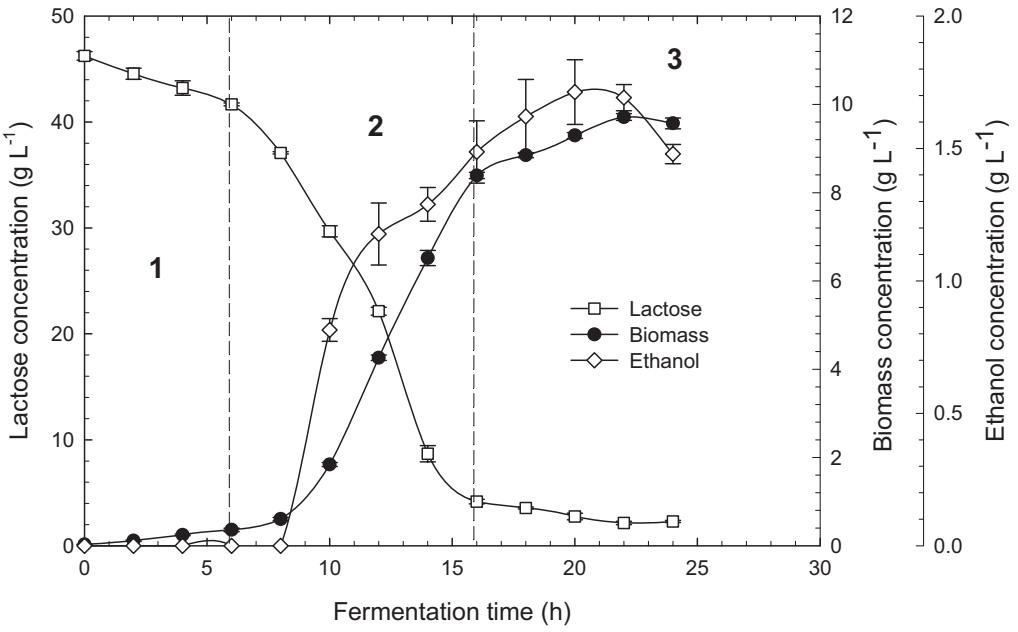

Figure 4.1 A typical control fermentation profile of *K. marxianus* at initial lactose concentration of 50 g L^{-1}, 30 °C, pH 5.0 and inoculum size of 5% by volume.

4.1.2 Sonicated batch fermentations

All sonicated batch fermentations were carried out under exactly the same conditions as the control fermentations (Section 4.1.1) with the exception that ultrasound was applied at the specified power intensity and duty cycles (Section 3.1.5). Sonication duty cycles of 10%, 20% and 40%, at a constant power intensity of 11.8 W cm^{-2}, were used in separate batch experiments. The control fermentation was not subjected to ultrasound irradiation. Sonication at 11.8 W cm^{-2} and the specified duty cycle commenced 9.5 h after inoculation of a batch fermentation.

The profiles of biomass growth, lactose consumption and the dissolved oxygen concentration are shown in Figure 4.2 in comparison to controls. All the profiles were

comparable prior to the beginning of sonication. Sonication at duty cycles of 10% and 20% substantially improved the final growth concentration relative to control, but increasing the duty cycle to 40% adversely affected the growth rate and the final biomass concentration (Figure 4.2a). The reduced biomass growth rate and final concentration at the highest duty cycle were clearly reflected in a slower rate of lactose consumption and a higher concentration of the residual lactose for this fermentation (Figure 4.2b). Lactose consumption of the fermentations conducted at duty cycles of 10 and 20% was comparable to that of the control (Figure 4.2b).

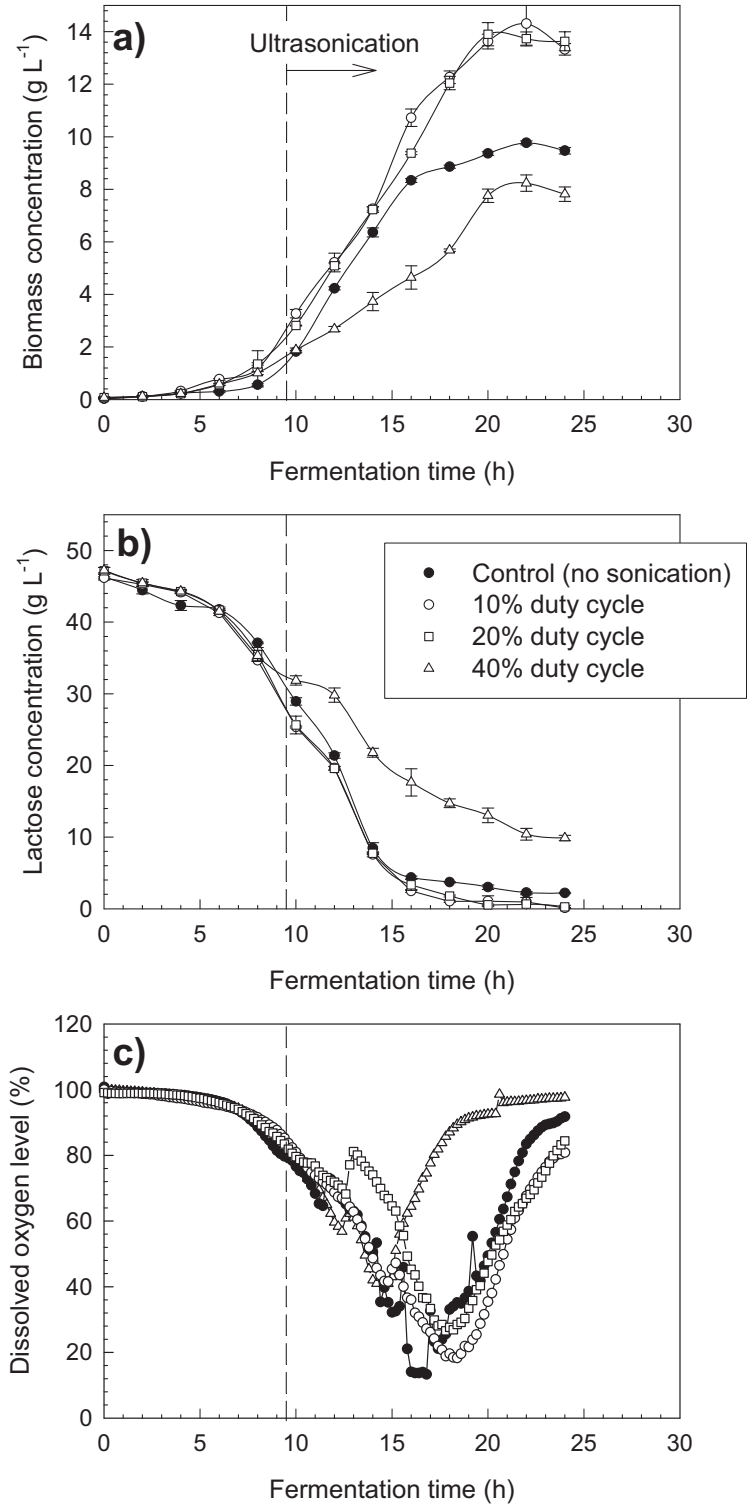

Figure 4.2 Effects of sonication on: (a) biomass concentration; (b) lactose concentration; and (c) dissolved oxygen concentration. Except for the nonsonicated control, the sonication intensity was 11.8 W cm^{-2}. Each of the profiles shown in (a) and (b) is an average of three independent fermentations.

The adverse effect of sonication at 40% duty cycle was reflected also in the dissolved oxygen concentration profiles (Figure 4.2c). Thus, at the 40% duty cycle, because of a reduced rate of consumption of lactose, the decline in the dissolved oxygen concentration during exponential growth was less than for the other fermentations and the oxygen concentration recovered earlier (Figure 4.2c) suggesting an earlier end to exponential growth even though plenty of lactose remained in the broth. Clearly, even at a relatively high intensity of 11.8 W cm^{-2}, ultrasound stimulated growth of *K. marxianus* on a soluble substrate so long as the duty cycle was appropriately selected. Each sonication event had to be followed by a recovery period of no sonication to prevent adverse impact on the yeast. No other work has been reported on sonication of *K. marxianus*, but continuous sonication of *S. cerevisiae* with diagnostic ultrasound (1 MHz) at a lower intensity (10.5 W cm^{-2}) than used here, has proved to be inhibitory (Anderson, 1953) while intermittent sonication was less damaging. For any fixed set of conditions, the data in Figure 4.2 are for two completely independently conducted fermentations and demonstrate excellent reproducibility.

For the fermentations profiled in Figure 4.2, the ethanol production data are shown in Figure 4.3 in comparison to the control fermentation. All duty cycles tested improved ethanol production relative to control, but the duty cycles of 10% and 20% were clearly the most effective. With the best duty cycle of 20%, the final ethanol concentration of 5.2±0.68 g L^{-1} was nearly 3.5-fold that of the control fermentation. For this sonication regimen, the ethanol yield on lactose was 0.109 g g^{-1} compared to a yield of 0.034 g g^{-1} for the control culture. The ethanol productivity of the culture sonicated at a duty cycle of 20% was 3.5-fold greater than for the control.

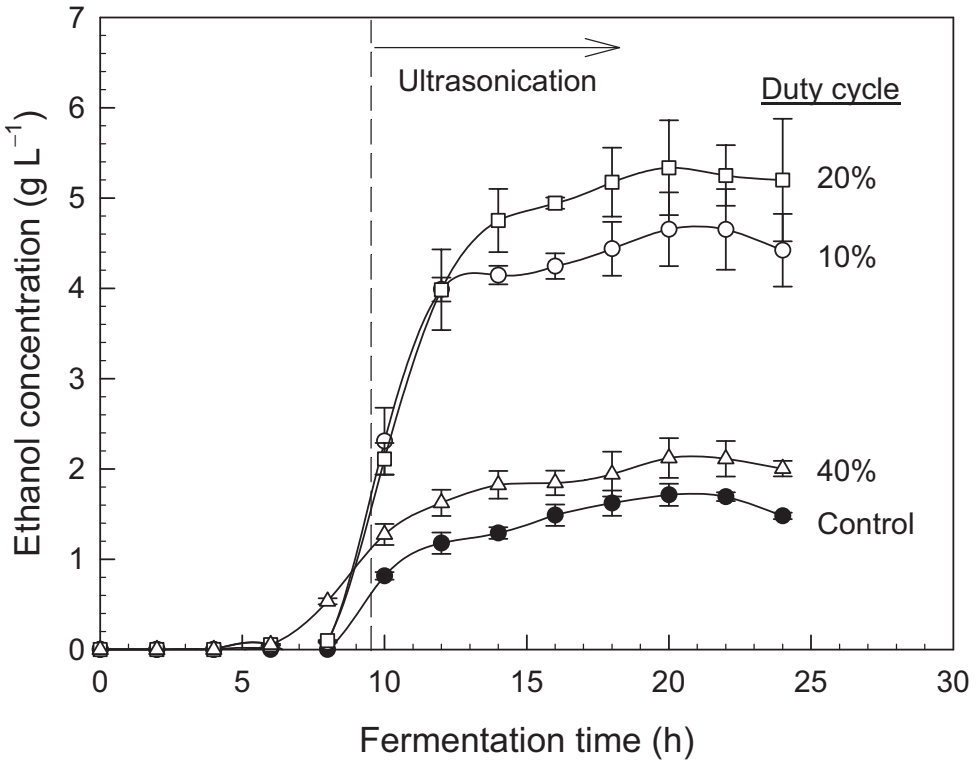

Figure 4.3 Ethanol concentration profiles. The sonication intensity was 11.8 W cm^{-2} except for the nonsonicated control culture. Each of the profiles shown is an average of three independent fermentations.

Ultrasonication is known to improve interfacial mass transfer. Mass transfer enhancements have been attained at power intensities as low as 2.2 W cm^{-2} (Bar, 1988). Therefore, a plausible improved gas-liquid mass transfer of oxygen as a consequence of sonication (Ashokkumar *et al.*, 2007) may potentially explain the observed increase in the concentration of the biomass (Figure 4.2a) relative to control; however, it does not explain the increased concentration of ethanol (Figure 4.3) that is normally produced optimally under conditions of a low dissolved oxygen concentration (Guimarães *et al.*, 2010). In the present study, the dissolved oxygen concentration did not drop to much less than 20% of air saturation as shown in Figure 4.2c.

Improved production of ethanol (Figure 4.3) must therefore have a different explanation. One of the products of the fermentation is carbon dioxide. Elevated concentrations of dissolved carbon dioxide are known to inhibit *S. cerevisiae* (Jones and Greenfield, 1982; Norton and Krauss, 1972) and have a similar effect on *K. marxianus*

(Guimarães *et al.*, 2010). In aerobic growth of bakers' yeast, an increase in the partial pressure of carbon dioxide to > 0.4 atm reduces both respiratory activity and the biomass yield on substrate (Jones and Greenfield, 1982). A CO_2 partial pressure of 0.4 atm at 30 °C (Henry law constant of 28.57 mM CO_2/atm; Jones and Greenfield, 1982) translates to a dissolved carbon dioxide (undissociated) concentration of 11.4 mM. In a highly aerobic fermentation, the dissolved oxygen concentration is not likely to rise to the level of 11.4 mM; nevertheless, improved gas-liquid mass transfer may have contributed to improved removal of the highly soluble carbon dioxide from the broth to enhance the ethanol productivity relative to control. Rapid desorption of carbon dioxide from a fermentation broth commonly produces foaming, as it does in a glass of beer. The fermentation broth was indeed observed to foam within minutes of commencing sonication as shown Figure 4.4. At the recycle rate used, nearly 63% of the broth in the bioreactor had passed through the sonication chamber at least once by 10-min when the picture (Figure 4.4b) was taken. Foaming may also be attributed to release of intracellular proteins, but up to a sonication duty cycle of 20% biomass growth was in fact better than in the control culture (Figure 4.4a), suggesting little or no cell lysis. The pH profiles for the fermentations shown in Figure 4.2 and Figure 4.3 have previously been published (see Figure 7 of Sulaiman *et al.*, 2011; Appendix 7). No distinct pH changes attributable to a possible change in the concentration of dissolved carbon dioxide could be observed and the pH values for the different sonicated regimens were generally within ± 0.2 pH units of the measured value (Sulaiman *et al.*, 2011).

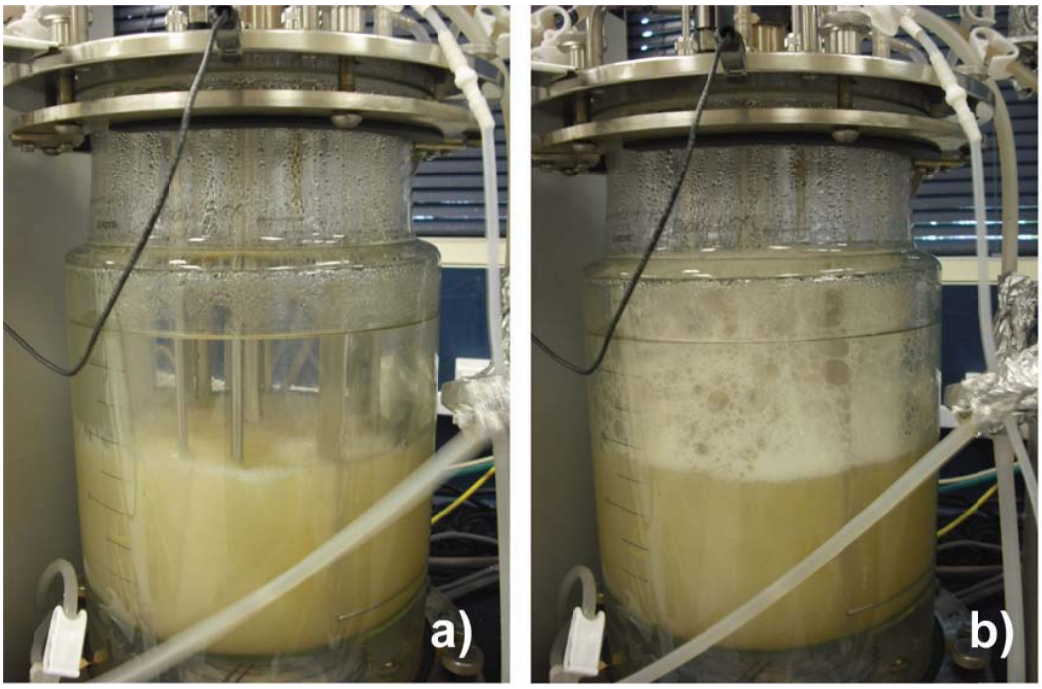

Figure 4.4 Foaming behavior of the fermentation: (a) just before sonication commenced 9.5 h after inoculation; (b) the same fermentation 10 min after sonication commenced at a power intensity of 11.8 W cm^{-2} and a duty cycle of 20%.

The kinetic parameters for the various fermentations (Figure 4.2, Figure 4.3) are compared in Table 4.1. Under the best sonication regimen of a 20% duty cycle, the sonicated fermentation was substantially superior to the control culture (Table 4.1). For example, compared to control, the biomass yield on lactose was 33% greater for the sonicated culture; the maximum biomass concentration was 42% greater; the maximum biomass productivity was 57% greater; the final ethanol yield on lactose was 3-fold greater; the final ethanol concentration was 3.5-fold greater; and the final ethanol productivity was 3.5-fold greater (Table 4.1). The specific equations used in calculating the parameters in Table 4.1 are noted in Appendix 1.

Table 4.1 Comparison of fermentation kinetics

Kinetic parameter	Sonication regimens (duty cycle)[a]			
	Control (no sonication)	10%	20%	40%
Maximum specific growth rate, μ (h^{-1})	0.203±0.011	0.206±0.027	0.217±0.007	0.179±0.017
Average specific lactose uptake rate, q_s (g g^{-1} h^{-1})	0.206±0.003	0.151±0.010	0.172±0.006	0.208±0.009
Maximum biomass yield on lactose, $Y_{x/s}$ (g g^{-1})	0.220±0.003	0.300±0.020	0.292±0.010	0.218±0.010
Maximum biomass concentration, X_{max} (g L^{-1})	9.712±0.076	13.755±0.850	13.813±0.443	8.388±0.315
Maximum biomass productivity, P_x (g L^{-1} h^{-1})	0.441±0.003	0.625±0.039	0.693±0.022	0.381±0.014
Final ethanol yield on substrate, $Y_{p/s}$ (g g^{-1})	0.034±0.001	0.096±0.009	0.109±0.014	0.052±0.002
Final ethanol concentration (g L^{-1})	1.479±0.036	4.421±0.042	5.199±0.677	2.003±0.086
Final ethanol productivity, P_E (g L^{-1} h^{-1})	0.062±0.002	0.184±0.017	0.217±0.028	0.083±0.004
Average biomass specific ethanol production rate, q_p (g g^{-1} h^{-1})	$(6.35\pm0.16)\times10^{-3}$	$(13.39\pm1.47)\times10^{-3}$	$(15.68\pm2.10)\times10^{-3}$	$(9.95\pm0.57)\times10^{-3}$

[a] Except for the control culture, the sonication power intensity was always 11.8 W cm^{-2}. All data are based on three replicate fermentations for each set of conditions.

For the experimental system used in batch and continuous fermentations, the bioreactor could always be considered to be well mixed. This could be readily demonstrated by comparing the mixing time in the bioreactor with the residence time of the recycle flow in the reactor. Thus, the residence time t_R of the recycle stream was calculated as follows:

$$t_R = \frac{V_L}{Q_L} \tag{4.1}$$

where V_L is the working volume (3 L) in the bioreactor and Q_L is the previously specified recycle flow rate. The residence time was always 15 min. The mixing time in the bioreactor was calculated using the following equation (Fasano and Penney, 1991):

$$t_\theta = \frac{\ln(1-\theta)}{1.06N(D/T)^{2.17}(T/H)^{0.5}} \tag{4.2}$$

where t_θ is the time required to attain a fractional homogeneity of θ (e.g. a θ-value of 0.99 is equivalent to 99% of the fully mixed state), N is the rotational speed of the impeller, D is the diameter of the impeller, T is the diameter of the mixing vessel and H is the depth of fluid in the tank. For the earlier specified bioreactor geometry and $H = T$, the mixing time for attaining a 99% homogeneity was found to be 0.096 min. Thus, the residence time in the bioreactor was nearly 150-fold greater than the time required for mixing.

4.1.2.1 Effects of ultrasound on cell viability

Power ultrasound has the potential to reduce viability in a population of cells (Radel *et al.*, 2000). Therefore, cell viability in sonicated and control fermentations was measured. Viability measurements were made using the methylene blue staining method (Section 3.1.7.4). As questions have been raised in the literature about the validity of this method (Mclean *et al.*, 2001; Trevors *et al.*, 1983), it was first validated against the reliable but cumbersome colony count method (Section 3.1.7.4). Thus, the viability of yeast cells in identical broth samples taken from some of the

early control fermentations and variously sonicated fermentations was measured by the methylene blue method and the colony count method. A comparison of the results (Figure 4.5) demonstrated an excellent agreement between these methods for the full range of sonication regimens (including controls) used in this work. These results suggest that the hemocytometer/methylene blue can be used to accurately estimate viable cell numbers (Sami *et al.*, 1994). As the hemocytometer/methylene blue method can be completed in less than 10 minutes compared to the 48-h required by the plate count method, the hemocytometer/methylene blue method was used in subsequent measurements of viable cell concentrations.

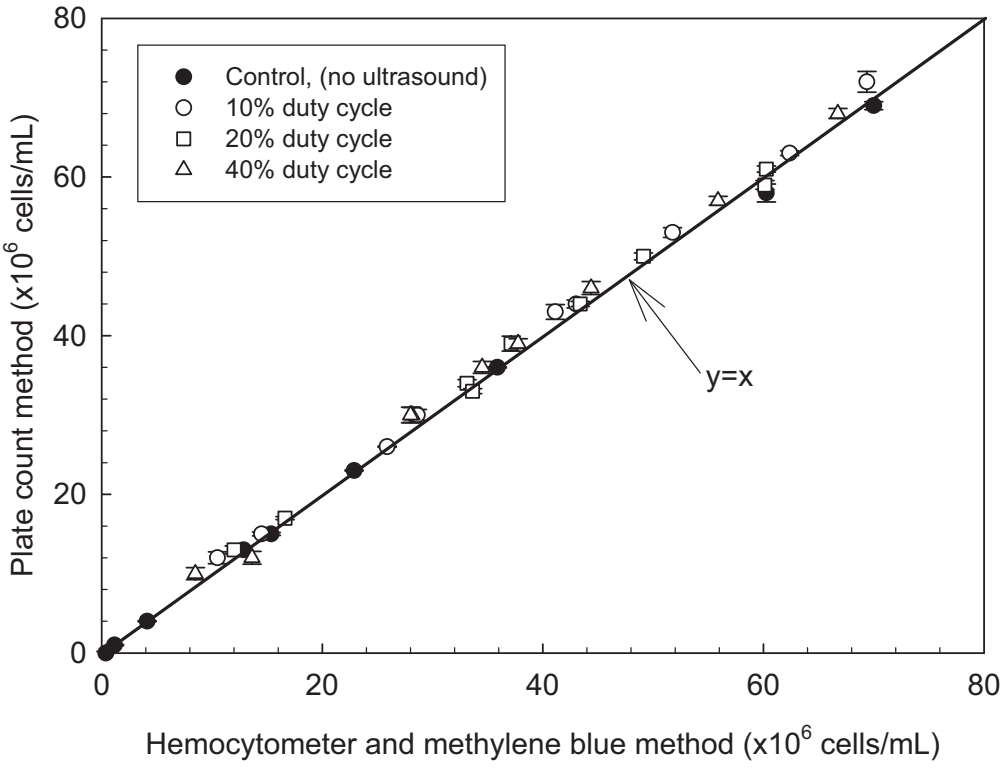

Figure 4.5 Comparison of hemocytometer/methylene blue and plate count methods for viable cells (sonication intensity = 11.8 W cm^{-2} where applicable)

Cell viability profiles for the fermentations profiled in Figure 4.2 and Figure 4.3 are shown in Figure 4.6. Prior to the beginning of sonication at 9.5 h, the cell viability in all fermentations exceeded >90%, but in all cases, the viability continuously declined as the fermentations progressed. For the control culture, this decline could be explained by a progressive accumulation of ethanol, a well known inhibitor of yeasts (Rosa and SaCorreia, 1996; Lucero *et al.*, 2000) including *K. marxianus* (Guimarães *et al.*, 2010). The beginning of the viability decline (Figure 4.6) coincided with the instance of the rapid increase in ethanol concentration around 9.5 h (Figure 4.1). The viability decline of the sonicated cultures was also due to accumulation of ethanol (Figure 4.3), but sonication appears to have been an additional contributing factor. Thus, at any instance after the sonication began, the viability was progressively reduced with the increasing value of the duty cycle of sonication (Figure 4.6). Although sonication enhanced the viability decline, by the end of the fermentation >65% of the yeast cells were still viable in the culture that was sonicated at a duty cycle of 40% (Figure 4.6). Ethanol is known to affect the structure of cell membranes (Lucero *et al.*, 2000) and this likely explained the increased susceptibility of cells to ultrasound once the ethanol concentration had increased.

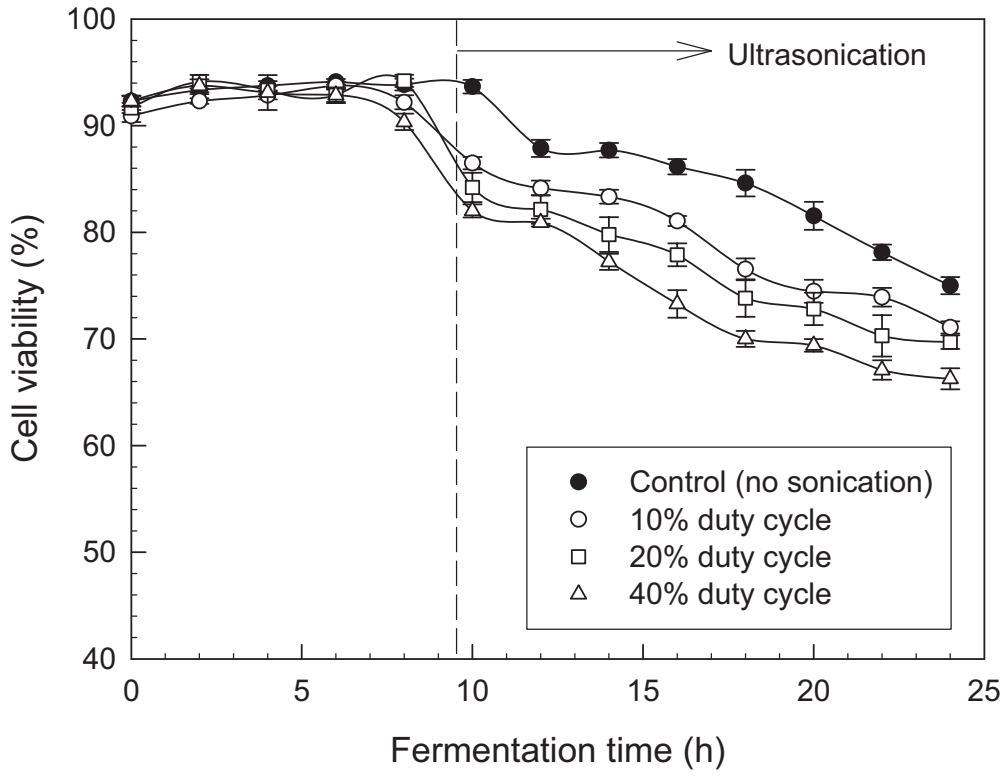

Figure 4.6 Cell viability profiles. The sonication intensity was 11.8 W cm^{-2} except for the nonsonicated control culture. Each of the profiles shown is an average of three independent fermentations.

Under certain conditions, ultrasound is known to affect the morphology of cells without causing a loss in viability (Radel *et al.*, 2000; Joyce *et al.*, 2003). Therefore, the cell morphology was examined photographically at 22 h of various fermentations (Figure 4.7). By this time the yeast broth had passed through the sonication chamber 50 times. Compared to nonsonicated culture (Figure 4.7a), no morphological changes were discerned in cells sonicated at 10 and 20% duty cycles (Figure 4.7b, 4.7c). However, the culture that had been sonicated at the 40% duty cycle contained many ghost cells (i.e. cells that had lost most or all of their contents) and cells with clearly broken envelopes (Figure 4.7d). This concurred with the lower biomass concentration (Figure 4.2a) and cell viability (Figure 4.6) in this fermentation, as discussed earlier.

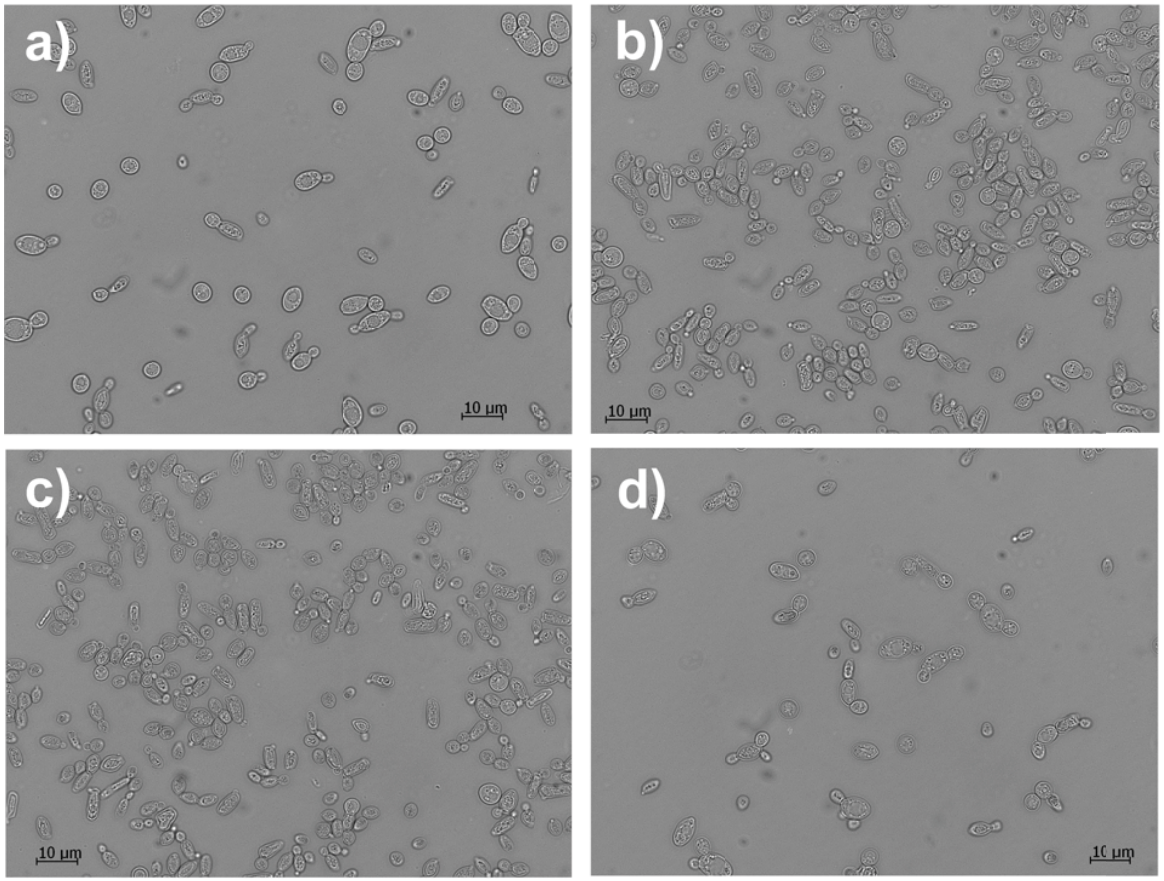

Figure 4.7 Yeast cell morphology (1000× magnification) at 22 h of fermentation: (a) control (no sonication); (b) sonication at 10% duty cycle; (c) sonication at 20% duty cycle; (d) sonication at 40% duty cycle. The sonication intensity was always 11.8 W cm^{-2}.

4.1.2.2 Effects of ultrasound on release of β-galactosidase

Transport of lactose into cells of *K. marxianus* is mediated by a lactose permease (Guimarães *et al.*, 2010). Once internalized, the lactose is hydrolyzed by β-galactosidase and the resulting glucose and galactose are metabolized by separate biochemical pathways (Guimarães *et al.*, 2010). As most of the lactose is hydrolyzed intracellularly, most of the β-galactosidase activity resides within the cells. The observed sonication-dependent changes in growth metabolism and ethanol production may be potentially linked to possible effects of sonication on the enzyme β-galactosidase. Considering this, the activity of the intercellular and extracellular β-galactosidase was measured in the various fermentations (Figure 4.8).

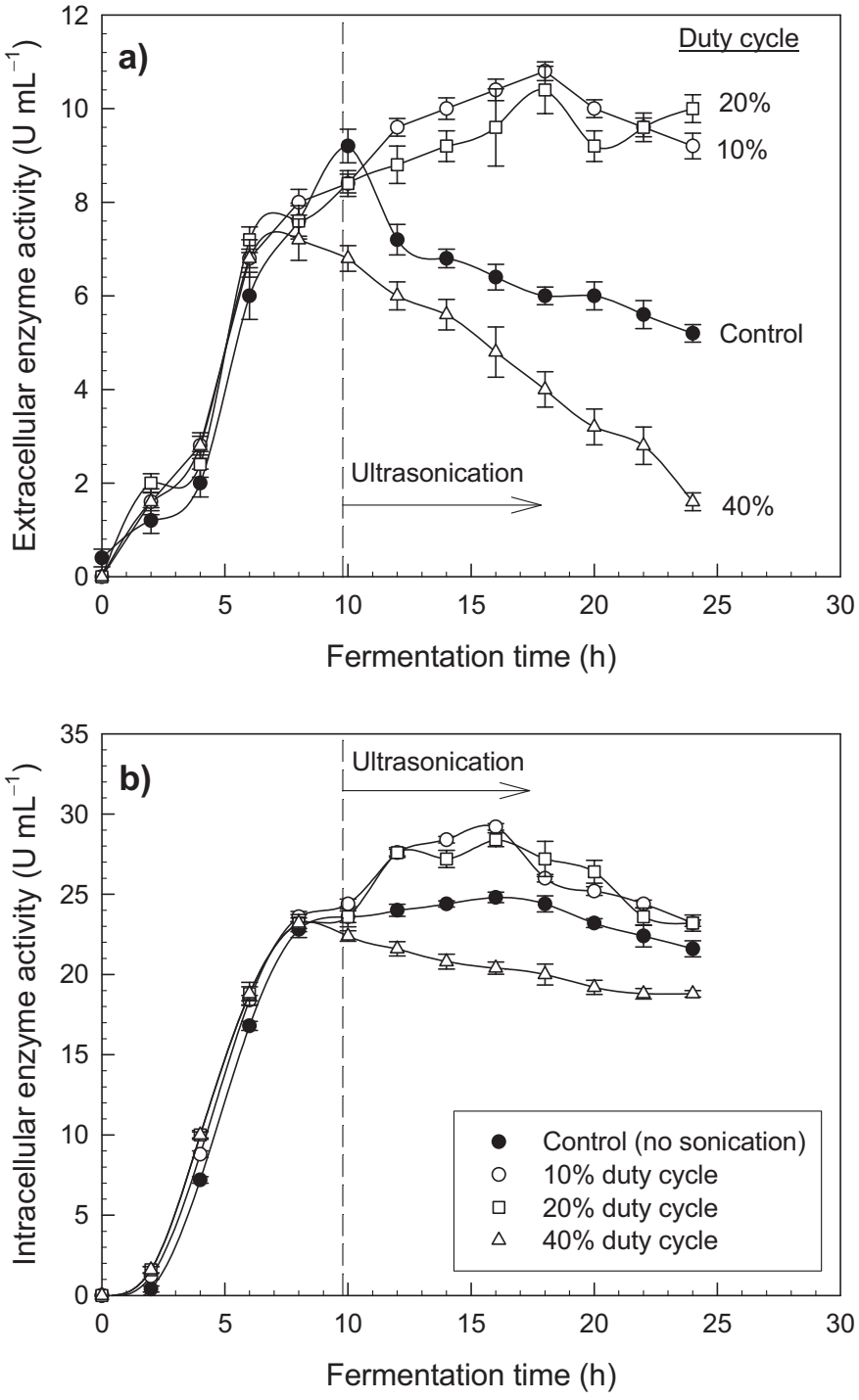

Figure 4.8 β-Galactosidase activity profiles during fermentation: a) extracellular enzyme activity; b) intracellular enzyme activity. The sonication intensity was 11.8 W cm^{-2} except for the nonsonicated control culture. Each of the profiles shown is an average of three independent fermentations.

Until the beginning of sonication at 9.5 h, the profiles for all fermentations were identical for both the extracellular and the intracellular enzyme activity (Figure 4.8). Irrespective of the fermentation, the extracellular enzyme activity was relatively small compared to the intracellular activity at any given instance (Figure 4.8), as expected. (β-Galactosidase is normally an intracellular enzyme.) The extracellular β-galactosidase was a consequence of either cell leakage or an ongoing lysis of a small fraction of the growing cell population. Sonication at 10 and 20% duty cycles appears to have stimulated the production of the enzyme inside the cells relative to control (Figure 4.8b), whereas sonication at the 40% duty cycle appears to have suppressed enzyme synthesis. In fact these apparent effects are entirely explained by the differences in the biomass concentrations of the various fermentations (Figure 4.2a) and not by any direct effect of sonication on the production or release of the enzyme. This is confirmed in Figure 4.9 where the measured extracellular and intracellular activities of β-galactosidase are plotted per unit of dry cell mass present at any given instance during fermentation. From 9.5 h onwards, all the sonicated cultures had nearly the same biomass specific enzyme activity as did the control culture. Therefore, sonication had no effect at all on production or release of β-galactosidase. During exponential growth, i.e. prior to 9.5 h, the biomass always had a much higher enzyme activity than later in the fermentation. This was likely because production of β-galactosidase was up regulated during rapid growth that demands a rapid hydrolysis of lactose to feed the resulting sugars into the energy consuming metabolic pathways.

In summary, therefore, ultrasound at any sonication regimen used did not affect the biomass specific production of β-galactosidase, nor the biomass specific release of β-galactosidase from the cells. Therefore, the observed effects of ultrasound on biomass growth profiles (Figure 4.2a), lactose consumption profiles (Figure 4.2b) and ethanol production profiles (Figure 4.3) cannot be attributed to any effect of ultrasound on production or release of β-galactosidase.

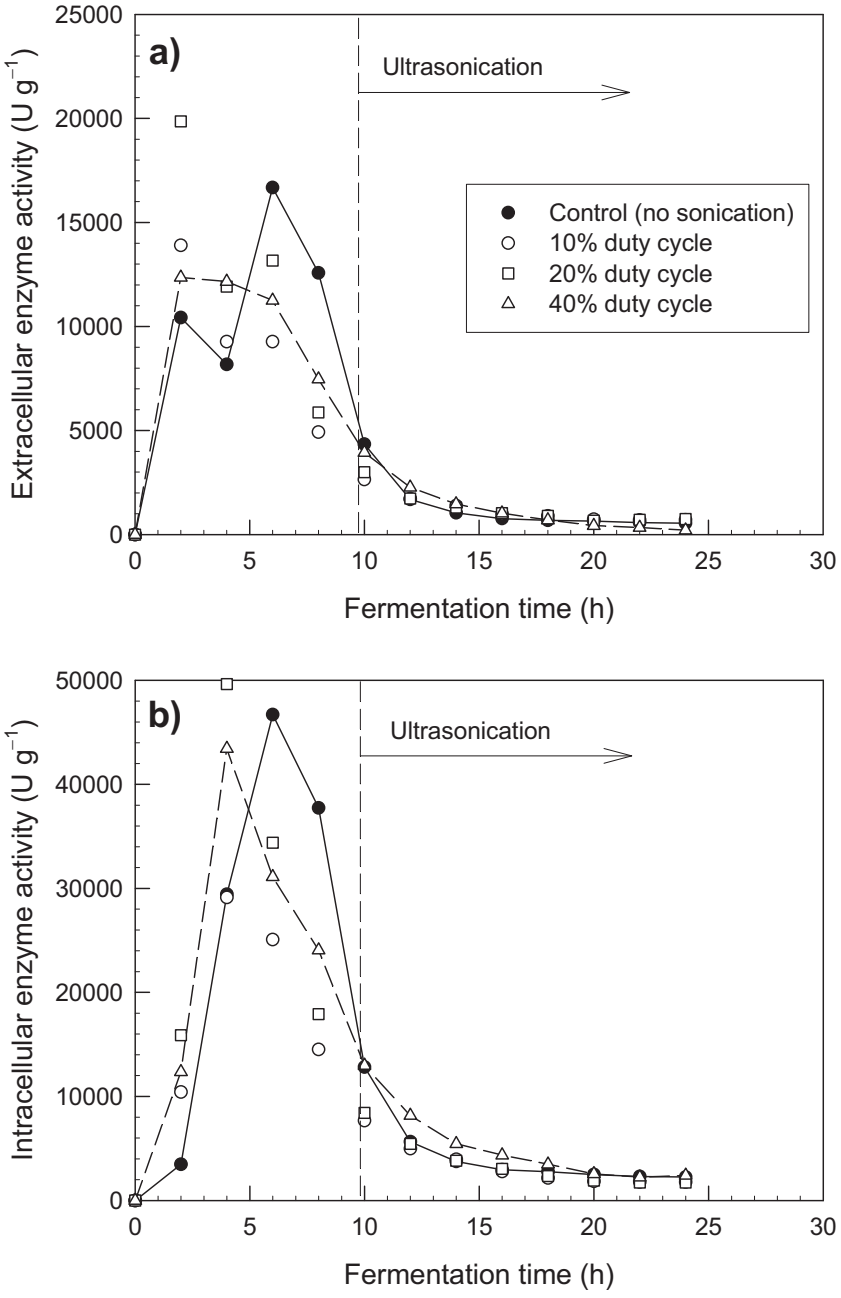

Figure 4.9 Biomass specific β-galactosidase activity profiles during fermentation: a) extracellular enzyme activity; b) intracellular enzyme activity. The sonication intensity was 11.8 W cm^{-2} except for the nonsonicated control culture. For clarity, lines are plotted only through the data for the control culture (solid lines) and the culture sonicated at the 40% duty cycle (dashed lines).

4.1.3 Continuous culture of *K. marxianus*

In this section, the effects of ultrasound on biomass, lactose and ethanol concentration profiles are discussed in continuous cultures of *K. marxianus*. The fermentation commenced as a batch culture that was switched to continuous feeding and harvest after 16 h of batch operation once a high concentration of biomass had been attained. In a ~1600 h long continuous culture, five dilution rates were tested. These were 0.05 h^{-1}, 0.075 h^{-1}, 0.1 h^{-1}, 0.15 h^{-1} and 0.2 h^{-1} and corresponded to residence times of 20 h, 13.3 h, 10 h, 6.7 h and 5 h, respectively. The maximum dilution rate used was less than the maximum specific growth rate μ_{max} that had been determined in earlier batch experiment (Table 4.1). This ensured that no wash out occurred at any of the dilution rates. At any given dilution rate, once three residence times had elapsed and the measured concentrations (biomass, ethanol, lactose) were stable within ±10% of the average value, a steady-state was assumed to exist. No sonication was used until a steady state had been attained at any given dilution rate. Sonication then began at a power intensity of 11.8 W cm^{-2} and 20% duty cycle, the condition that had been found to be optimal in batch fermentation experiments. Sonication then continued until the culture attained a new steady-state. After 4-5 residence time had elapsed at any steady-state, sonication was switched off, until the steady-state prior to commencing of sonication was re-established. This cycle was repeated twice for every dilution rate (sonicated and nonsonicated). A new dilution rate value was then set and the experiment continued.

The fermentation profiles of biomass, lactose and ethanol concentrations during 67 days of operation at increasing dilution rates are shown in Figure 4.10. The operation started after 16 h of batch fermentation at a 0.05 h^{-1} dilution rate. The dilution rate was then increased stepwise. At all dilution rates tested, use of ultrasound enhanced the steady state biomass concentration, lactose consumption and ethanol concentration relative to control. The values of the fermentation kinetic parameters at various steady states are shown in Table 4.2. The values were calculated as explained in Appendix 1.

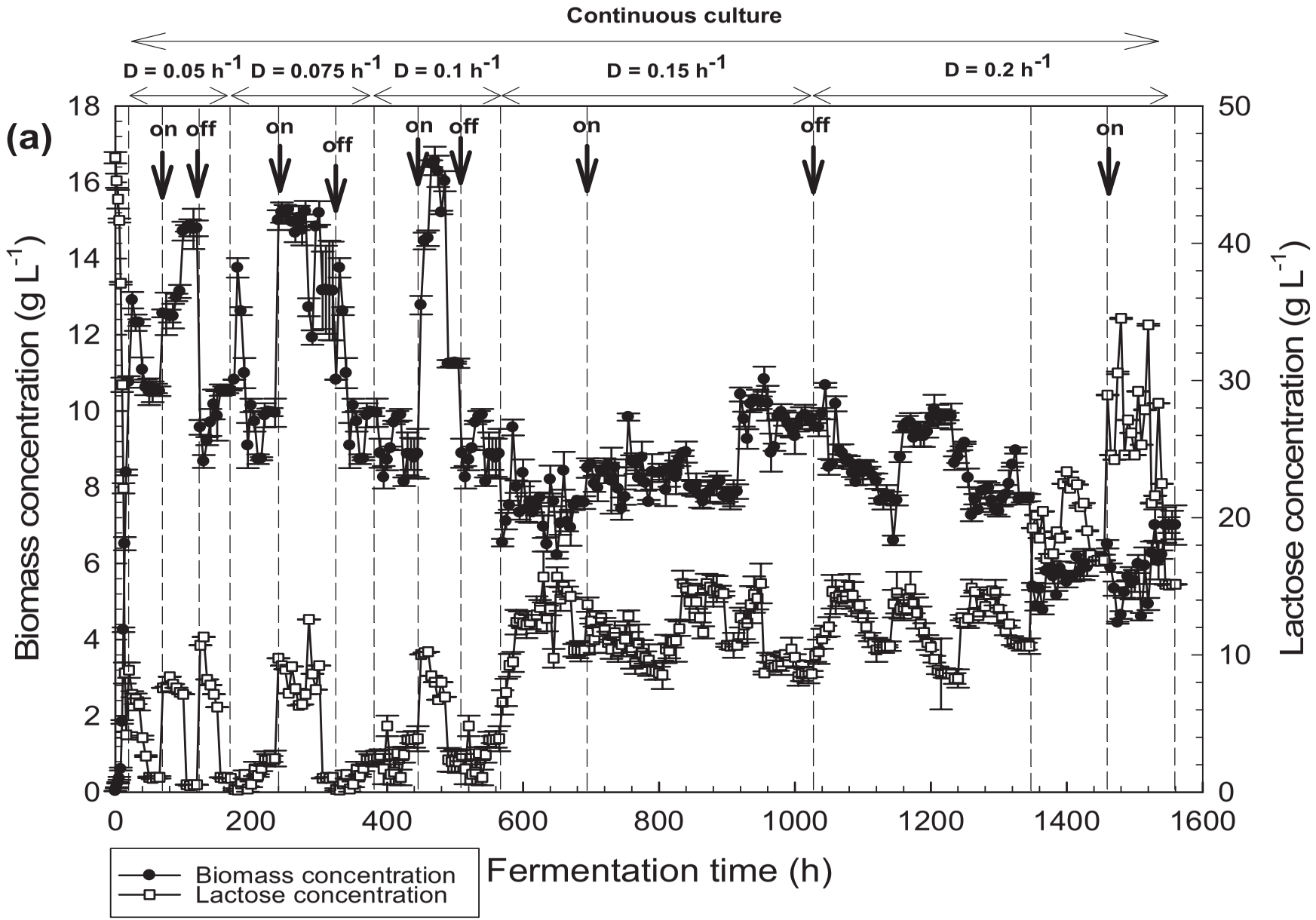
Continuous culture
D = 0.05 h-1
D = 0.075 h-1
D = 0.1 h-1
D = 0.15 h-1
D = 0.2 h-1
(a)
on
off
on
off
on
off
on
off
on
Biomass concentration (g L-1)
Lactose concentration (g L-1)
Fermentation time (h)
Biomass concentration
Lactose concentration
0
2
4
6
8
10
12
14
16
18
0
10
20
30
40
50
0
200
400
600
800
1000
1200
1400
1600

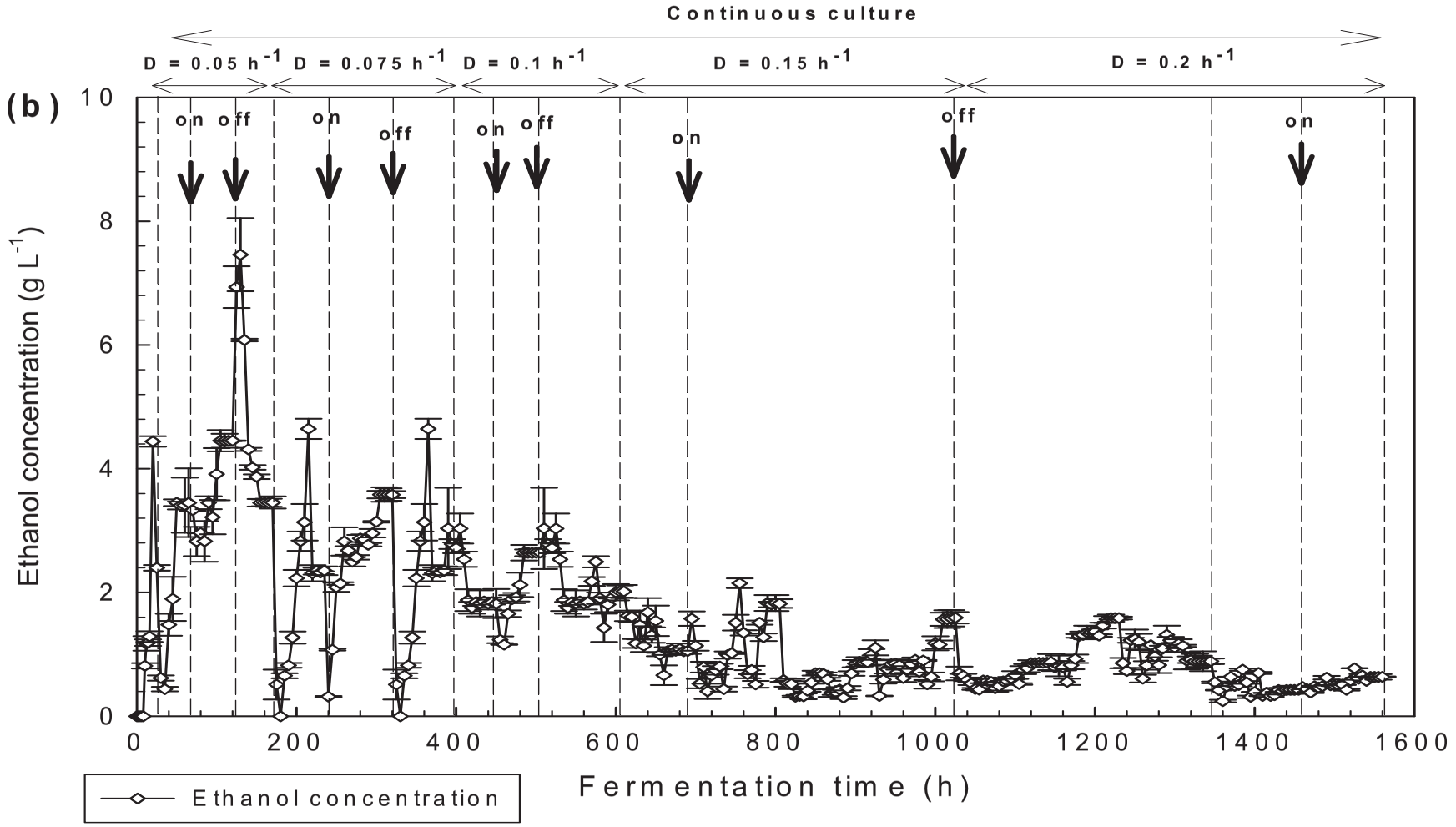

Figure 4.10 The continuous fermentation profiles: (a) biomass and lactose concentrations; and (b) ethanol concentration. When ultrasound was used, sonication intensity was 11.8 W cm^{-2} and duty cycle was 20%. Arrows mark the on/off sequence of sonication.

Table 4.2 Summary of steady state parameters from continuous cultures of *K. marxianus*

	Kinetic parameter[a]									
	Dilution rate, D (h^{-1})	Residual lactose concentration, S (g L^{-1})	Biomass concentration, X (g L^{-1})	Ethanol concentration, (g L^{-1})	Biomass yield on lactose, $Y_{x/s}$ (g g^{-1})	Biomass productivity, P_x (g L^{-1} h^{-1})	Ethanol yield on substrate, $Y_{p/s}$ (g L^{-1} h^{-1})	Ethanol productivity, P_E (g L^{-1} h^{-1})	Max. specific growth rate μ_{max} (h^{-1})	Monod coefficient, K_s (g L^{-1})
Control (no sonication)	0.05	1.06	10.48	3.43	0.21	0.52	0.07	0.17		
	0.075	2.43	9.95	2.33	0.21	0.75	0.049	0.17		
	0.1	3.85	8.85	1.84	0.19	0.88	0.04	0.18	0.19	3.15
	0.15	10.65	7.59	1.06	0.19	1.14	0.027	0.16		
	0.2	16.86	6.16	0.43	0.19	1.23	0.012	0.085		
Sonication (at 20% duty cycle)[a]	0.05	0.52	14.79	4.45	0.299	0.739	0.09	0.223		
	0.075	1.04	13.17	3.58	0.269	0.987	0.073	0.269		
	0.1	2.27	11.25	2.64	0.236	1.125	0.055	0.264	0.18	1.37
	0.15	8.65	9.86	1.59	0.238	1.478	0.038	0.238		
	0.2	15.14	7.01	0.64	0.20	1.40	0.02	0.13		

[a]Except for the control culture, the sonication power intensity was always 11.8 W cm^{-2}

The steady-state concentration of lactose, biomass and ethanol attained at various dilution rates in control and sonicated cultures (Figure 4.10) are plotted in Figure 4.11 as a function of dilution rate (i.e. the specific growth rate). Each data point in Figure 4.11 was obtained by averaging three steady-state measurements at a given dilution rate. The error bars in Figure 4.11 demonstrate an excellent stability of each steady-state.

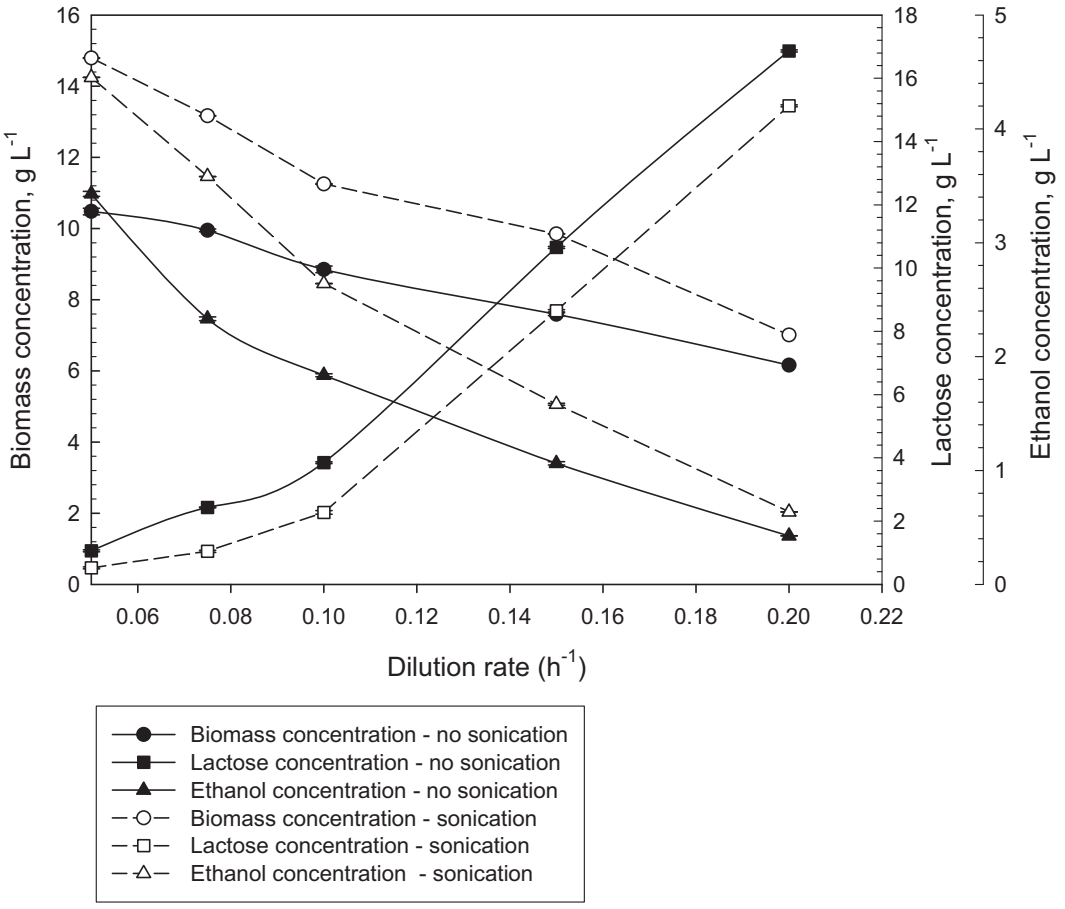

Figure 4.11 Steady state concentration of biomass, lactose and ethanol at various dilution rates in control (no sonication) and sonicated continuous cultures of *K. marxianus.*

As expected, as the dilution rate increased, biomass and ethanol concentration decreased steadily and residual lactose concentration increased in both control and sonicated fermentations. Sonication always enhanced the steady-state biomass concentration and ethanol concentration relative to the corresponding control (Figure 4.11). At lowest dilution rate (0.05 h^{-1}) the steady-state ethanol concentration in sonicated

culture was 4.45±0.004 g L^{-1} and ethanol yield on lactose was 0.09 g g^{-1} (Table 4.2) compared to a yield of 0.07 g g^{-1} for the control culture. The ethanol productivity of sonicated culture at dilution rate of 0.05 h^{-1} was 1.3-fold greater than for the control (Table 4.2). The ethanol productivity initially increased with increasing dilution rate and attained a maximum value of 0.18 g L^{-1} h^{-1} (nonsonicated) and 0.264 g L^{-1} h^{-1} (sonicated) at dilution rates of 0.1 h^{-1} and 0.075 h^{-1}, respectively (Figure 4.12). At these maximum values, the ethanol productivity was 1.5-fold greater than for the control.

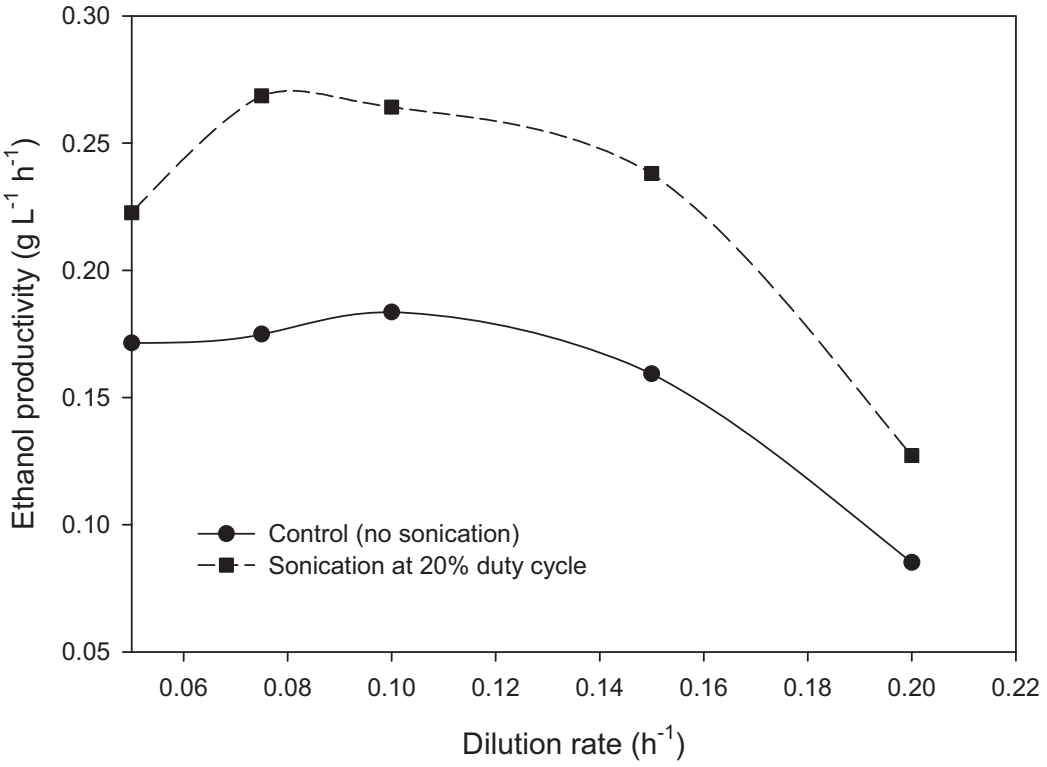

Figure 4.12 Steady state ethanol productivity at various dilution rates in control and sonicated cultures.

As shown in Table 4.2, at all dilution rates the biomass yield on lactose was 24–42% greater for the sonicated culture relative to control; the maximum biomass concentration was 14–41% greater; the maximum biomass productivity was 30–42% greater and the final ethanol yield on lactose was 1.3–1.7-fold greater (Table 4.2).

In continuous culture at a steady state, the specific growth rate equals the dilution rate (Scragg, 1991; Teixeira *et al.*, 1990). Therefore, the steady-state values of the substrate concentration S at various dilution rates (Figure 4.10) can be used to calculate the Monod growth kinetic parameters of the maximum specific growth rate (μ_{max}) and the saturation constant (K_s). Thus

$$\mu = D = \frac{\mu_{max}\, S}{K_s + S} \tag{4.3}$$

Therefore, a plot of 1/D versus 1/S (i.e., a Lineweaver-Burk plot) provides the values of μ_{max} and K_s. Lineweaver-Burk plots for the steady-state data are shown in Figure 4.13. Linear regression of the data for nonsonicated and sonicated fermentations gave values for μ_{max} and K_s as shown in Table 4.2. Sonication had almost no effect on μ_{max} relative to control (Table 4.2) but substantially lowered the K_s-value. Therefore, sonication enhanced the affinity of the yeast toward lactose, i.e. a lower concentration of lactose was sufficient to achieve a given biomass growth rate compared to control for substrate concentration levels of below saturation.

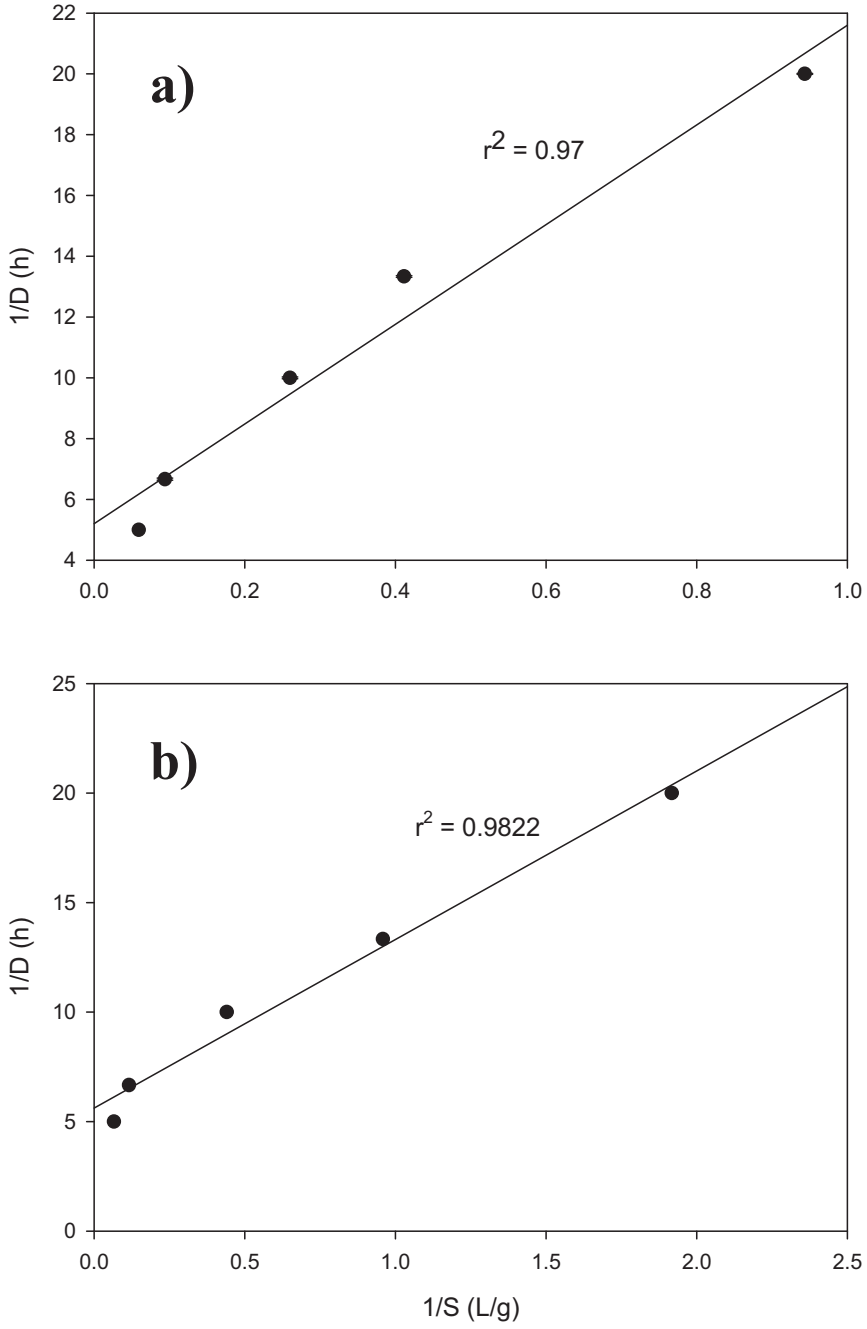

Figure 4.13 Lineweaver-Burk plots of continuous fermentation of lactose by *K. marxianus*: (a) control – no sonication; (b) sonication at 20% duty cycle with an intensity of 11.8 W cm^{-2}

The improvements in ethanol productivity and biomass production as a result of sonication were attributed to the changes in dissolved carbon dioxide concentration as a plausible cause. Production of CO_2 occurs as the fermentation proceeds and elevated concentrations of dissolved CO_2 are known to inhibit yeast fermentation and repress

ethanol formation. Ultrasound is known to improve gas–liquid mass transfer and likely contributed to the enhanced ethanol productivity by removing the soluble CO_2 from the broth.

4.1.4 Oxygen transfer studies in bioreactor

Ultrasonication is known to improve interfacial mass transfer and has been found to accelerate other diffusional processes (Chisti, 1999; Chisti, 2003; Chisti, 2010). To investigate the effects of ultrasound on the gas-liquid mass transfer, experiments were conducted in air-water and uninoculated air-lactose medium. These measurements were made to see if sonication would actually enhance gas-liquid mass transfer relative to control under conditions that were comparable to those used during batch fermentation of lactose by *K. marxianus*. Although gas-liquid oxygen transfer was measured, an enhanced oxygen transfer correlates directly with enhanced carbon dioxide mass transfer (Chisti, 1989). The methodology of the relevant measurements and calculation of k_La_L have been previously described (Section 3.1.8.2).

The dependence of k_La_L on air flow rate and agitation rate is shown in Figure 4.14 for the air-water system and air-uninoculated sugar systems (Martín *et al.*, 2010) in the absence of ultrasound. As expected, a steady increase in k_La_L with impeller speed and air flow rate is observed in both systems. This is because the gas-liquid interfacial area per unit liquid volume (a_L) increases with increasing speed of agitation and rate of aeration (Boodhoo *et al.*, 2008; Martín *et al.*, 2008). Mass transfer coefficient in the absence of sparging (i.e. 0 vvm; surface aeration only) was always low compared to the values for sparged aeration (Figure 4.14). Increasing the agitation rate increases impeller shear, thus increasing bubble breakup and increasing the interfacial area available for mass transfer. Increasing the sparging rate also increases the number of bubbles present in the liquid. For any given agitation speed and aeration rate, the k_La_L value in the lactose medium was a little lower than in water (Figure 4.14) in view of a higher viscosity of the lactose medium relative to water.

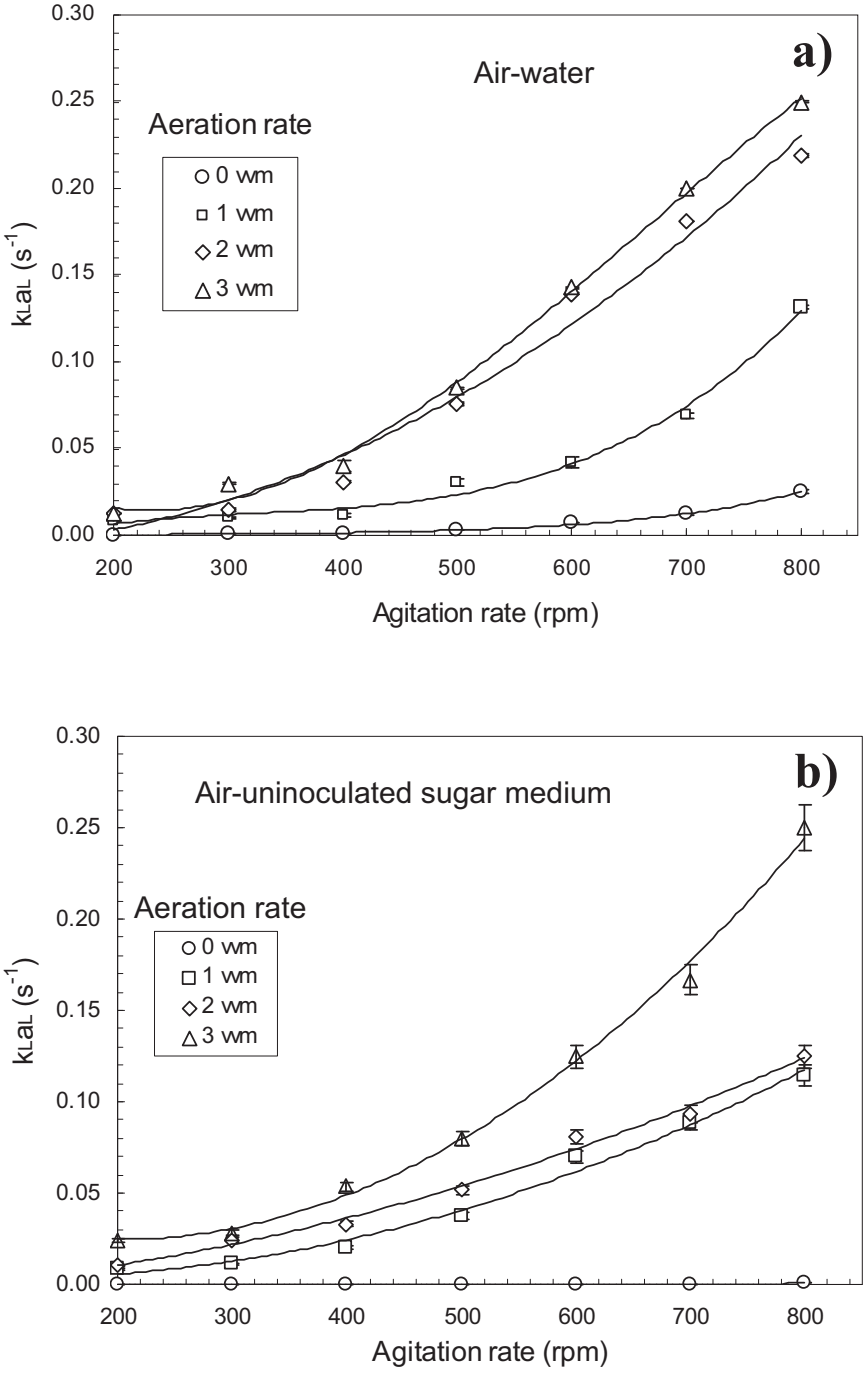

Figure 4.14 Dependence of mass transfer coefficient on agitation rate and aeration rate in the absence of ultrasound: (a) air-water system; and (b) air-uninoculated medium. All measurements were at 30 °C. Each profile shown is an average of three independent experiments.

Data in Figure 4.15 confirm that both low intensity sonication and high intensity sonication enhance mass transfer coefficient in both media relative to control. Effect of

sonication on k_La_L was relatively minor at agitation speeds of ≤ 400 rpm (Figure 4.15a, Figure 4.15b) but was substantial at higher agitation speeds. The data in Figure 4.15 are for a fixed aeration rate value of 2 vvm. The agitation speed used in *K. marxianus* fermentation was 500 rpm and the aeration rate was 2.67 vvm. At the highest agitation speed used, k_La_L under intense sonication was nearly double the control value. The observed effects can be attributed to the changes in the interfacial area caused by ultrasonic irradiation. In the presence of ultrasound, the bubbles produced from the sparger and by the impeller were of a smaller size and this increased the gas hold-up (i.e. the volume fraction of the gas in dispersion) and the interfacial area. The evidence provided here suggests that sonication under the conditions used in the fermentation did enhance gas–liquid mass transfer and therefore CO_2–mass transfer, compared to the case for control cultures.

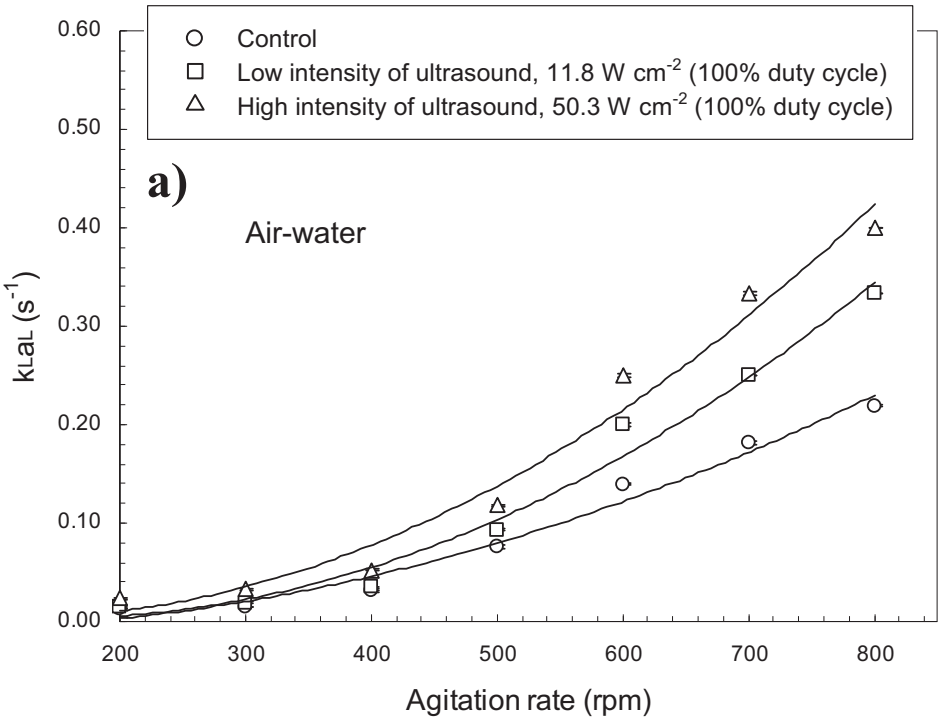

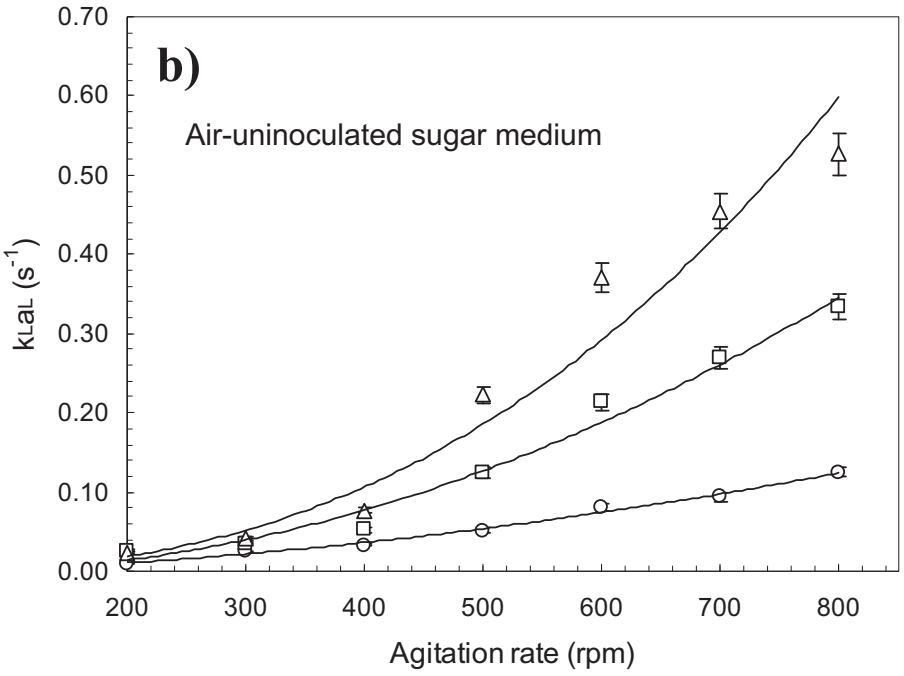

Figure 4.15 Dependence of mass transfer coefficient on agitation rate: (a) air-water system; and (b) air-uninoculated medium. In all cases the aeration rate was at 2 vvm and the temperature was 30 °C. Each profile shown is an average of three independent experiments.

4.2 Effect of ultrasound on β-galactosidase mediated-hydrolysis of lactose (cell-free system)

4.2.1 Introduction

The effect of ultrasound on β-galactosidase mediated hydrolysis of lactose was investigated in a cell-free system as this process is involved in *K. marxianus* fermentation where it occurs predominantly within the yeast cell and to a lesser extent outside the cell if the cells have released the normally intracellular β-galactosidase to the outside. In a homogenous system (i.e. a single phase without interfacial mass transfer effects) as in this case, ultrasound has the potential to influence enzyme–substrate binding/unbinding (Chisti, 2003b; Yang *et al.*, 2010). Ultrasound also has the potential to damage an enzyme (Chisti and Moo-Young, 1986). Therefore, β-galactosidase stability in substrate free buffer was characterized in separate experiments with and without sonication.

K. lactis β-galactosidase was used (Section 3.2). In addition to control (no sonication) various sonication duty cycles (10%, 20% and 40%) and sonication intensities (2.4 W cm^{-2}, 4.7 W cm^{-2}, 11.8 W cm^{-2}) were tested. Experiments were carried out in the same reactor as used in the fermentation (Section 3.1.4). In all cases, the temperature was carefully controlled at 37 °C and the pH was 6.5. Initial substrate concentration S_o varied (5–60 g L^{-1}). The initial enzyme concentration E_o was fixed at 1.0 mL L^{-1}. The recirculation flow rate between the bioreactor and the sonication chamber was fixed at 0.2 L min^{-1}.

4.2.2 Baseline determination (nonsonicated enzymatic hydrolysis of lactose)

Figure 4.16 shows the profiles of glucose production from lactose at seven initial lactose concentrations (5–60 g L^{-1}) in the absence of sonication. The conventional Michaelis-Menten kinetics can be used to describe the hydrolysis of lactose by β-galactosidase (Cavaille and Combes, 1995; Gekas and Lopez-Leiva, 1985; Santos *et al.*, 1998). As shown in Figure 4.16, the initial rate (i.e. the rate calculated at 2 min) of product formation (glucose) increased with increased initial substrate concentration. The final concentration of glucose also increased with increased initial concentration of lactose. The error bars in Figure 4.16 demonstrate a good reproducibility of the measurements.

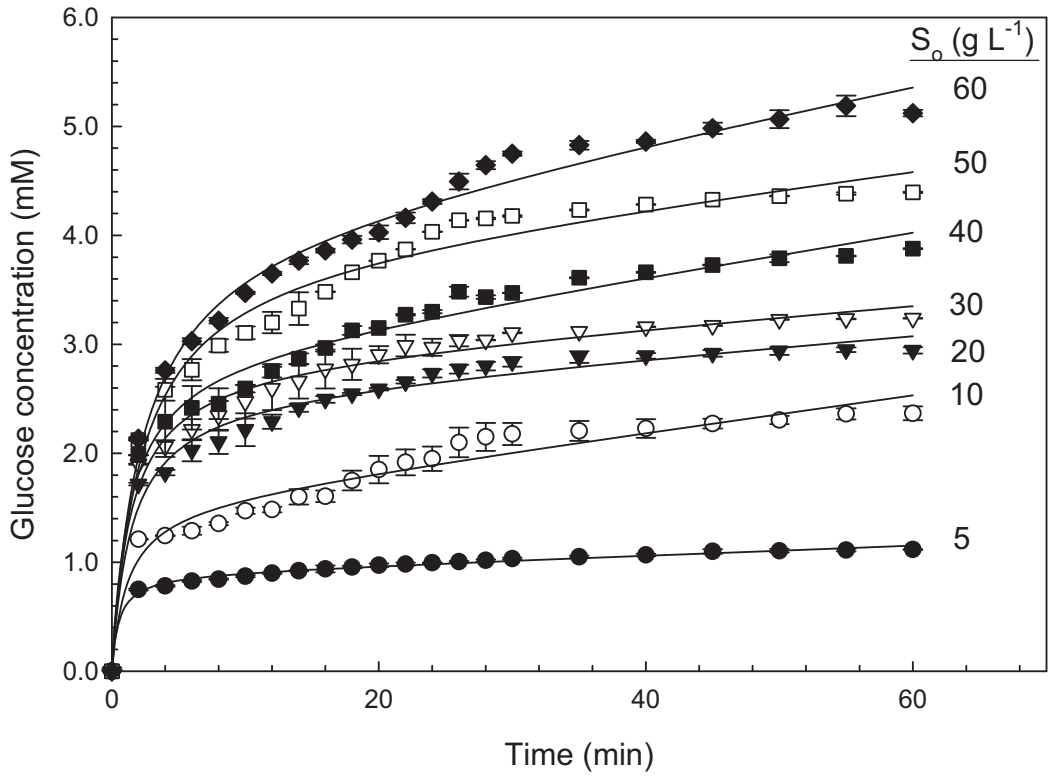

Figure 4.16 Glucose production from lactose during nonsonicated enzymatic hydrolysis. Initial substrate concentrations S_o were 5–60 g L^{-1}. Each profile shown is an average of three independent experiments.

Initial reaction rates V_i of the hydrolysis of lactose were determined from the initial slopes of product formation profiles (Figure 4.16) at various lactose concentrations. A plot of the initial rate versus the initial substrate concentration is shown in Figure 4.17. The hyperbolic curve (Figure 4.17) is clearly consistent with the expected Michaelis-Menten kinetics. The Michaelis-Menten kinetic parameters of the hydrolysis reaction were estimated by the direct linear method of Lineweaver-Burk plots (Figure 4.18) (Bailey and Ollis, 1986; Counotte and Prins, 1979; Fan *et al.*, 1987; Santos *et al.*, 1998; Shuler and Kargi, 2002). Thus, $1/V_i$ data were plotted against $1/S_o$ data, resulting in the expected straight line (Figure 4.18). The slope of the plot (Figure 4.18) provided a value of K_m/V_{max} and y-intercept provided the value of $1/V_{max}$ from which V_{max} and K_m could be calculated (Jurado *et al.*, 2002). The K_m value was 12.75±0.61 g L^{-1} and V_{max} was 2.24±0.02 × 10^{-5} M s^{-1}. This provided control data for comparison with the same reaction carried out under sonicated conditions.

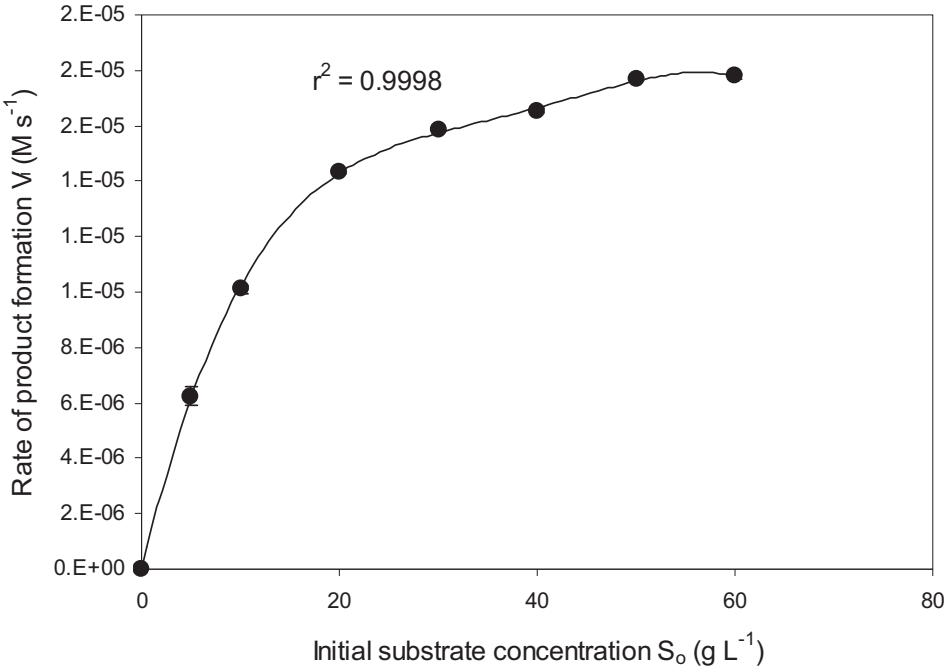

Figure 4.17 Effects of initial substrate concentration S_o on the initial rate (V_i) of lactose hydrolysis at various initial substrate concentrations (5.0–60.0 g L^{-1}).

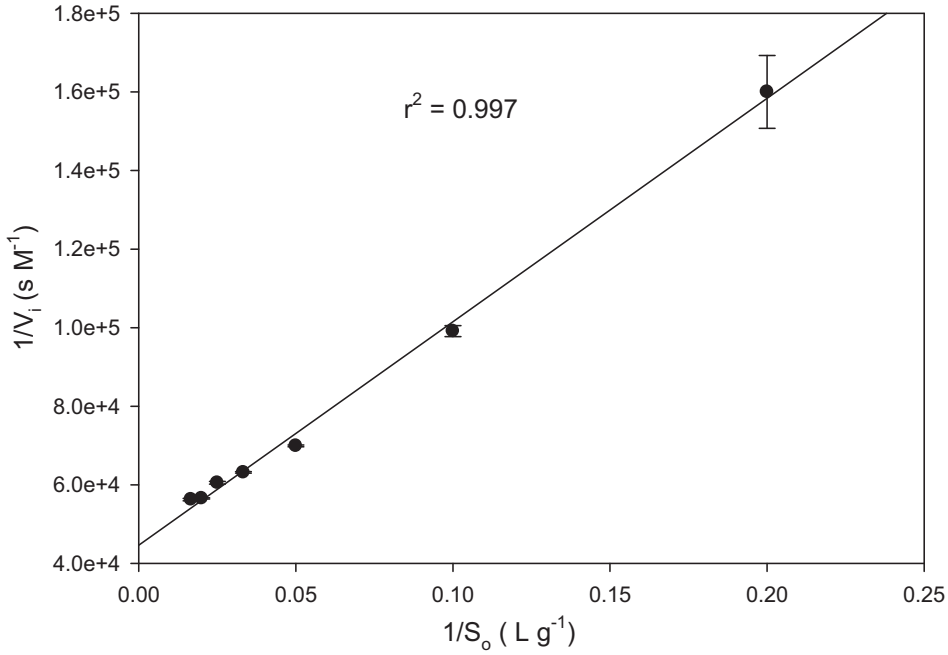

Figure 4.18 Double reciprocal (Lineweaver-Burk) plot of $1/V_i$ versus $1/S_o$ for enzymatic hydrolysis of lactose.

4.2.3 Effects of sonication on lactose hydrolysis

Figure 4.19 shows the effects of ultrasound on the rate of product formation at various combinations of sonication duty cycles and power intensities. Control data (no sonication) are also shown. The initial reaction rate increased relative to control for all duty cycles and power intensities applied (Figure 4.19). Irrespective of power intensity used, a duty cycle of 10% gave the highest values of the initial hydrolysis rate. At a high power intensity of 11.8 W cm^{-2}, as was used in *K. marxianus* fermentation (Section 3.1.4), an increasing duty cycle reduced the reaction rate relative to the values at the 10% duty cycle (Figure 4.19).

At a duty cycle of 10% in combination with a power intensity of 11.8 W cm^{-2}, the initial reaction rate was nearly 1.4-folds of the control rate (no sonication). From Figure 4.19, it is clear that a short irradiation pulse (i.e. 10% duty cycle) applied at the highest irradiation power, was most effective in enhancing the initial reaction rate, V_i. The effect of ultrasound was possibly due to an accelerated collision frequency of the enzyme and substrate molecules as a consequence of the microtubulence caused by sonication. Sonication also likely enhanced the diffusion of the product from the enzyme active site (Czechowska-Biskup *et al.*, 2005). Sonication at higher duty cycles of 20% and 40% was less effective because prolonged sonication tended to damage the enzyme as demonstrated later in Section 4.2.4.

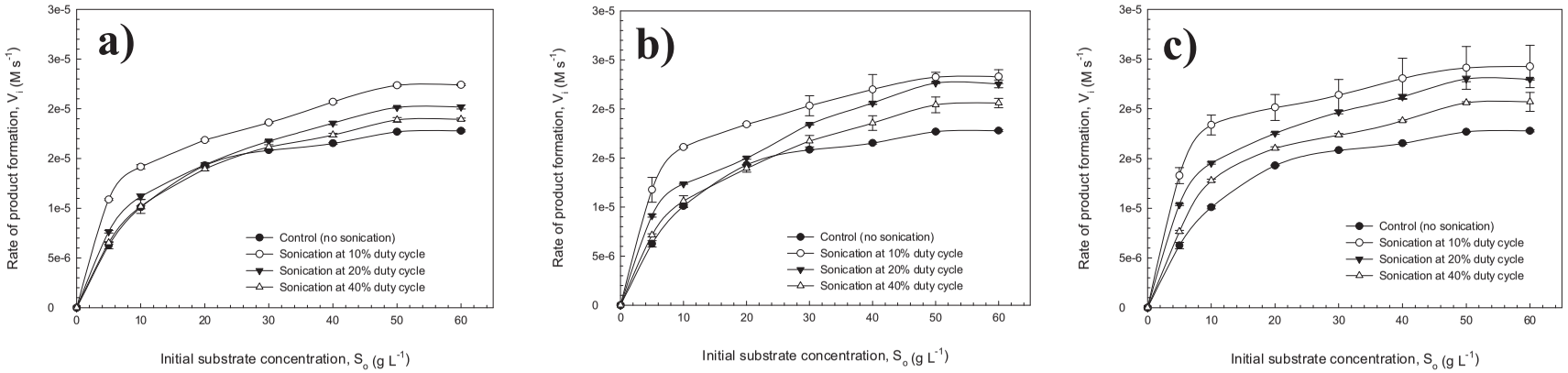

Figure 4.19 Effects of ultrasonication on initial reaction rate (V_i) at power intensities of: a) 2.4 W cm^{-2}; b) 4.7 W cm^{-2}; and c) 11.8 W cm^{-2}. Control reactors were not sonicated. Each profile shown is an average of three independent experiments.

The effects of sonication on the kinetic parameters V_{max} and K_m calculated using the data in Figure 4.18, are shown in Figure 4.20. Relative to control (no sonication), ultrasound enhanced V_{max} (Figure 4.20a) and reduced K_m (Figure 4.20b) at the optimal conditions of a 10% duty cycle and power intensity of 11.8 W cm^{-2}. At optimal sonication condition, the K_m value was 4.58±1.57 g L^{-1} and V_{max} was (2.57±0.331) × 10^{-5} M s^{-1}. A reduced value of K_m relative to control implies an increased affinity of the enzyme for the substrate, lactose. That is, the enzyme bound more readily to the substrate compared to the control case. The K_m values at any sonication intensity increased with increasing value of the sonication duty cycle (Figure 4.20b), but were lower than for the control under nearly all the sonication regimens tested. This suggests that ultrasound facilitated lactose binding to the active site of the enzyme, possibly by enhancing pulsating motions within the enzyme molecule (Butz *et al.*, 1988; Havsteen, 1989)

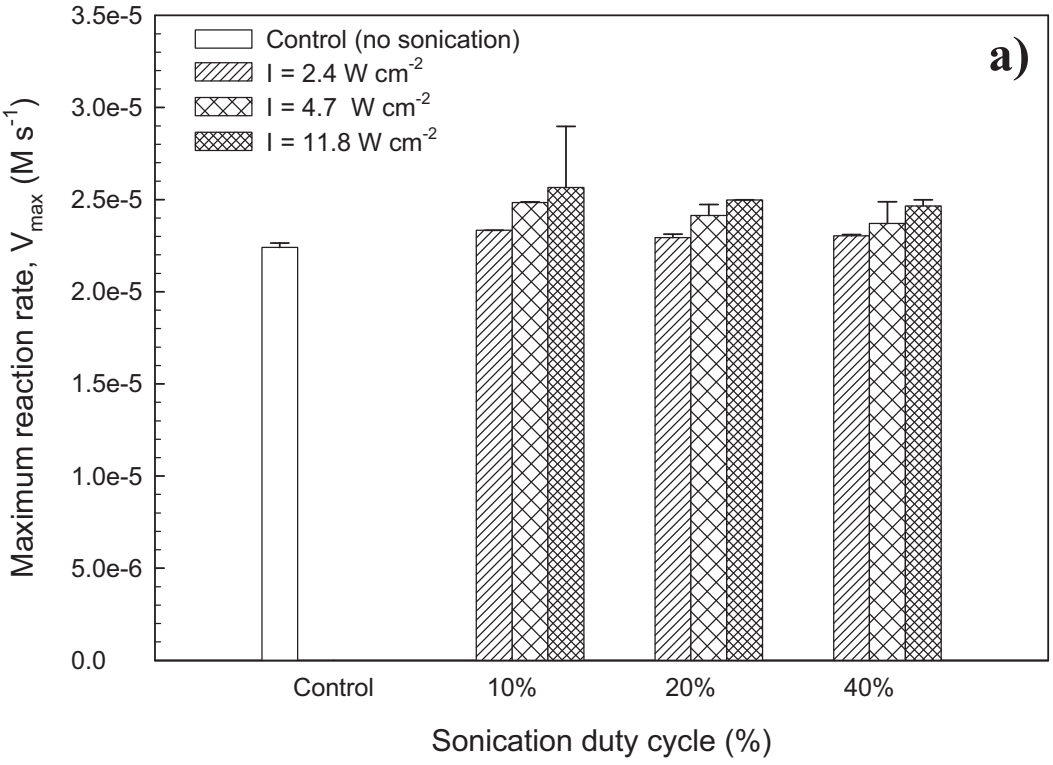

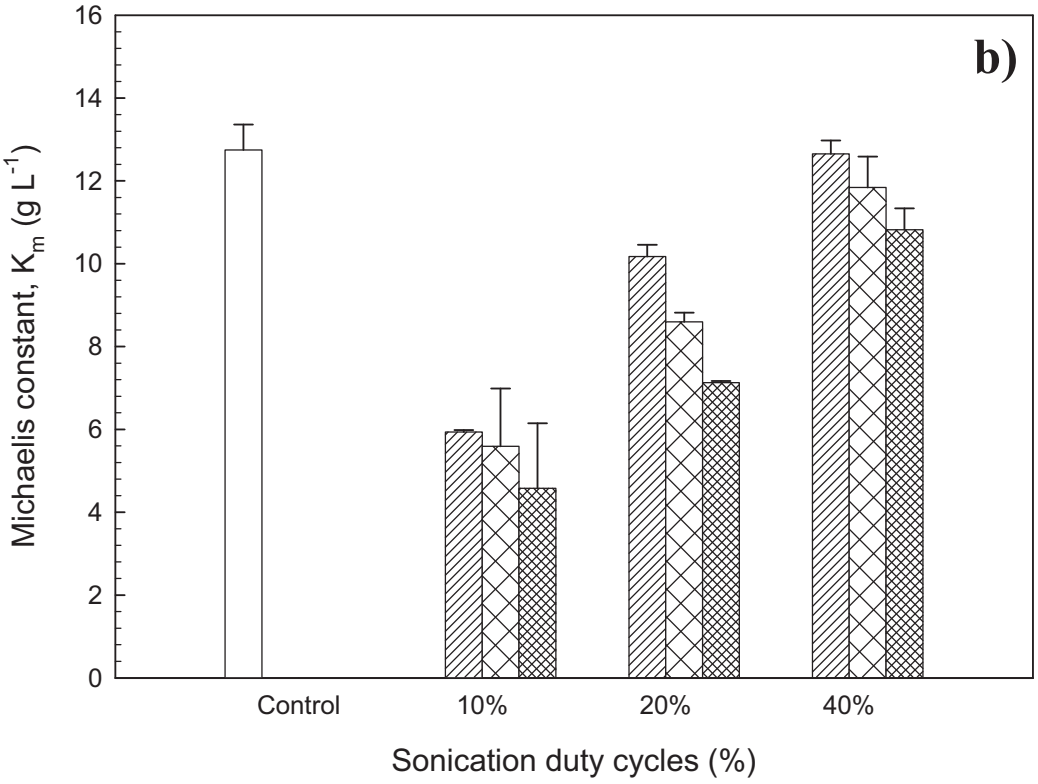

Figure 4.20 Effects of ultrasonication on: (a) maximum reaction rate (V_{max}); and (b) Michaelis constant (K_m) for hydrolysis of lactose at various sonication intensities (I) and duty cycles.

4.2.4 Effects of sonication on enzyme stability

β-Galactosidase stability was measured as percent (Özbek and Ülgen, 2000; Sener *et al.*, 2006) of the initial activity remaining after various periods of exposure to ultrasound at the power intensity of 11.8 W cm^{-2} and duty cycle values of 10%, 20% and 40%. The results are shown in Figure 4.21. In the absence of sonication, the enzyme was quite stable over the test period and no activity loss occurred (Figure 4.21). Sonication at the high power intensity clearly damaged the enzyme. The extent of damage increased with increasing time of exposure and increasing duty cycle (Figure 4.21). The ultrasound-induced vibrational motions within an enzyme molecule likely enhanced unfolding of the molecule to cause denaturation and activity loss.

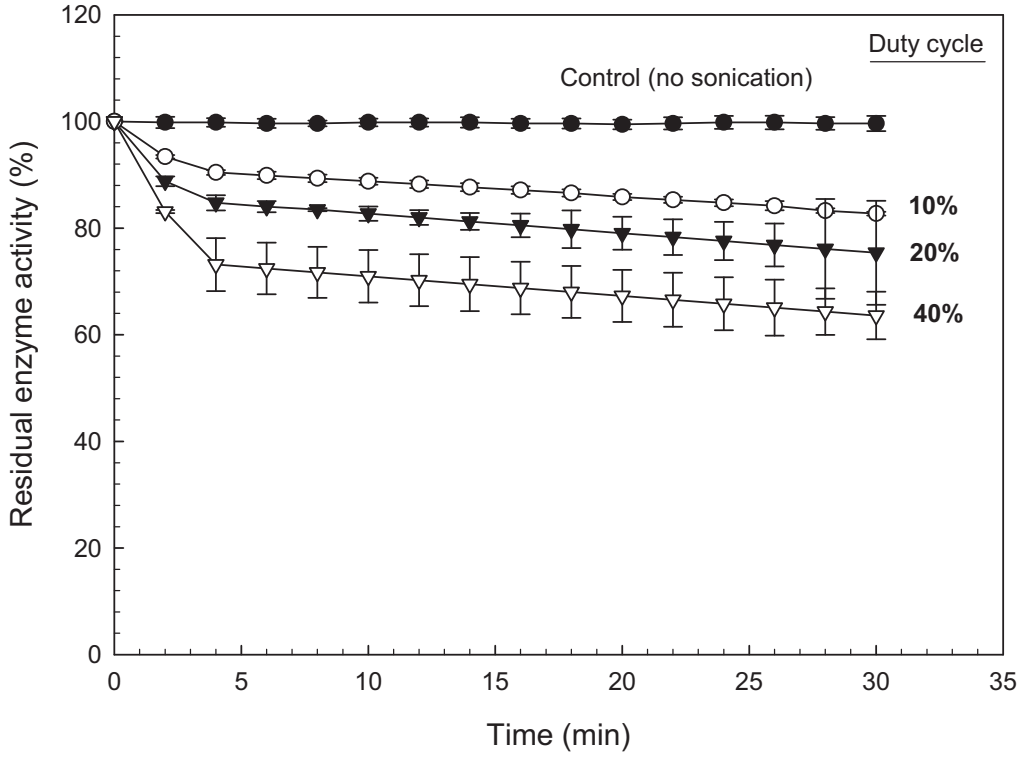

Figure 4.21 Residual enzyme activity (%) versus time at various sonication duty cycles. The sonication power intensity was fixed at 11.8 W cm^{-2} (37 °C, pH 6.5). Each profile shown is an average of three independent experiments.

4.3 Effect of ultrasound on enzymatic hydrolysis of cellulose

Here the focus was on assessing the effects of ultrasound on enzymatic hydrolysis of soluble and insoluble cellulose. The cellulose enzyme used was the commercial preparation *Accellerase 1000* (Section 3.3.2). Ultrasound power intensity values of 2.4 W cm^{-2}, 4.7 W cm^{-2} and 11.8 W cm^{-2} were tested at duty cycles of 10%, 20% and 40%. The control samples were not subjected to ultrasound. A soluble carboxymethyl-cellulose, CMC (non-crystalline) and insoluble cellulose of different particles sizes (Solka-Floc of 30μm, 60 μm and 290 μm average particle sizes) were used as model substrates. The experiments were conducted at an initial substrate concentrations S_o of 5–40 g L^{-1}. The initial enzyme concentration E_o was always 0.1 g L^{-1}. The temperature and pH value were 50 °C and 4.8, respectively. A 2-L stirred bioreactor (working volume 1-L) was used (Section 3.3.2).

4.3.1 Non-sonicated cellulose hydrolysis (baseline studies)

The results of duplicate nonsonicated cellulose hydrolysis experiments with various substrates are shown in Figure 4.22 as baseline data for comparison with the results for sonicated experiments. As expected, for a given initial substrate concentration, the initial rate of hydrolysis, i.e. the rate of production of glucose, decreased as the size of the substrate entity increased. The soluble substrate (CMC) was hydrolysed more rapidly than particulate cellulose. This was consistent with earlier studies (Ortega *et al.* 2001, Al-Zuhair, 2008; Yeh *et al.*, 2010). Many studies (Al-Zuhair, 2008; Lin *et al.*, 2010; Ortega and Busto, 2001; Yeh *et al.*, 2010) have discussed the reasons behind the reduced rate of hydrolysis with increasing crystallinity and particle size. A cellulase molecule can hydrolyze only that part of the substrate that it can directly contact. As the substrate 'particle' size increases from a soluble macromolecule to larger undissolved particle, the surface area of the substrate per unit mass decreases. Therefore, for a given mass of the substrate, the cellulase enzyme has a progressively reduced contact area to act on, as the substrate molecular size, or particle size is increased. This affects the rate of hydrolysis as in Figure 4.22. The error bars in Figure 4.22 demonstrate a good reproducibility of the measurements.

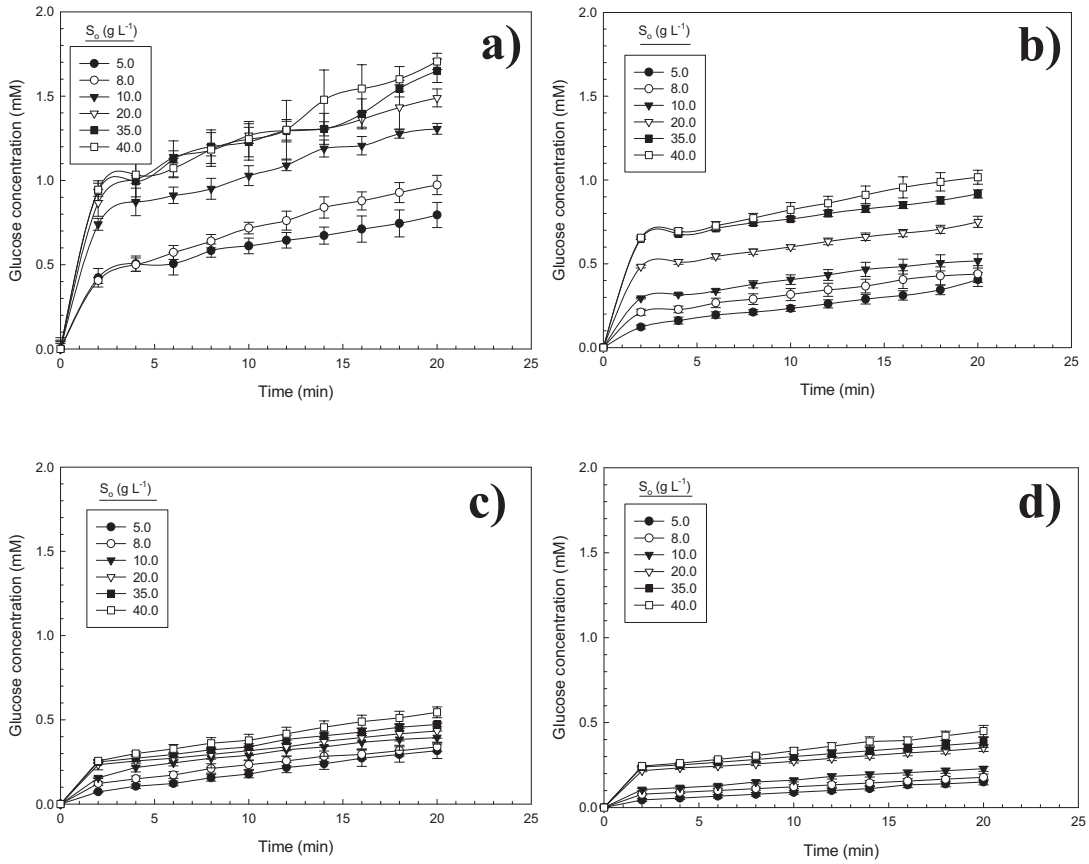

Figure 4.22 Time courses of the enzymatic hydrolysis of: (a) carboxymethyl cellulose (CMC); (b) Solka-Floc BH 300 (30 µm); (c) Solka-Floc BH 40 (60 µm); and (d) Solka-Floc CH 10 (290 µm). Nonsonicated controls at various initial substrate concentrations S_o, the initial enzyme concentration was always 0.1 g L^{-1}. Each profile shown is an average of three independent experiments.

4.3.2 Estimation of kinetic parameters of cellulose hydrolysis

Hydrolysis of cellulose produced glucose. Some typical glucose production profiles for various initial concentrations of the substrate (CMC) are shown in Figure 4.22a (nonsonicated hydrolysis). The cellulase-mediated hydrolysis of cellulose is known to follow Michaelis-Menten kinetics at low concentrations of glucose (Bailey and Ollis, 1986; Counotte and Prins, 1979). A plot of the initial reaction rate from Figure 4.22a against the initial CMC substrate concentration, produced the characteristic Michaelis-Menten profile (Figure 4.23), as expected. Therefore, the initial rate of glucose production was expected to depend on the initial substrate concentration S_o, as follows (Bailey and Ollis, 1986; Counotte and Prins, 1979; Fan *et al.*, 1987; Lineweaver and Burk, 1934; Shuler and Kargi, 2002):

$$\frac{1}{V_i} = \frac{K_m}{V_{max}} \frac{1}{S_o} + \frac{1}{V_{max}} \tag{4.4}$$

In Equation (4.4) V_i and V_{max} are the initial rate of product formation and the maximum rate of product formation (M s^{-1}), K_m is the Michaelis constant in g $L^{-1}$and S_o is the initial substrate concentration in g L^{-1}. Thus a plot of $1/V_i$ versus the reciprocal of CMC concentration should give straight line for experiments conducted at a fixed concentration of the enzyme. Such a plot was linear as shown in Figure 4.24. The slope and the intercept of the plot in Figure 4.24 were used to calculate the kinetic parameters V_{max} and K_m. The K_m value was 10.22±0.21 g L^{-1} and V_{max} was (0.92±0.003) × 10^{-5} M s^{-1}.

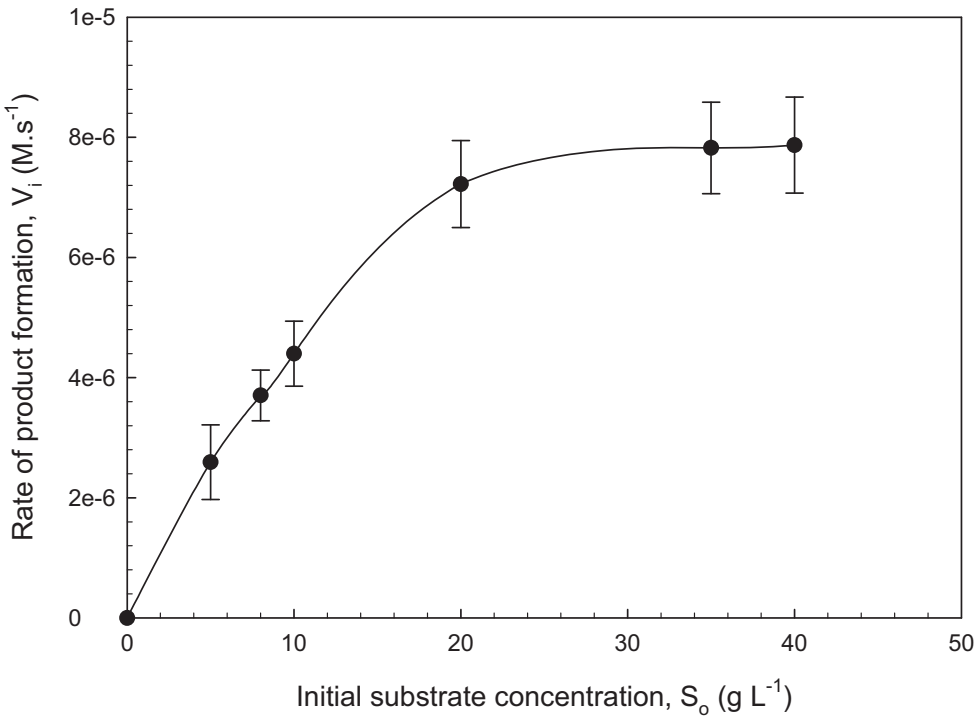

Figure 4.23 Effects of substrate concentration on the rate of enzyme-catalyzed hydrolysis of CMC (control, no sonication).

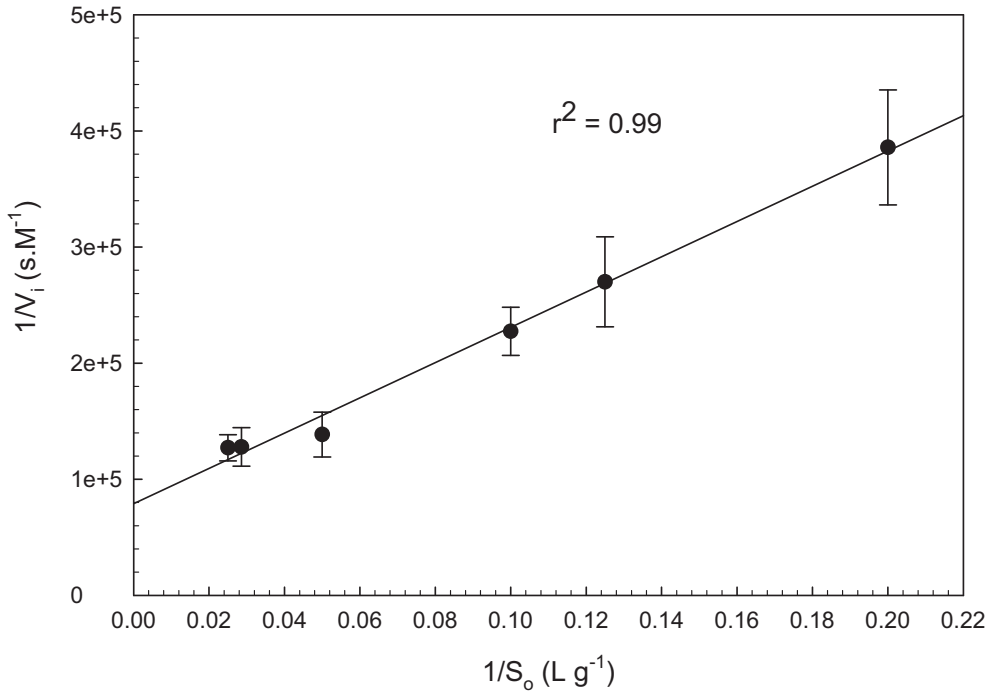

Figure 4.24 Plot of $1/V_i$ versus $1/S_o$ for enzymatic hydrolysis of CMC in the absence of ultrasonication (control).

4.3.3 Effects of ultrasound on cellulose hydrolysis

4.3.3.1 Soluble cellulose (CMC)

The initial hydrolysis rate of CMC at various initial substrate concentrations and under various sonication regimens (including control) is shown in Figure 4.25. In all cases the typical Michaelis-Menten kinetics were observed. Sonication at all power levels and duty cycles enhanced the rate of hydrolysis relative to control (Figure 4.25). At any given duty cycle, an increased intensity of sonication enhanced the rate of hydrolysis. The Michaelis constant (K_m) and the maximum reaction rate (V_{max}) calculated for the various operating conditions are given in Table 4.3. The same data in the form of Figure 4.26 allows for a clearer understanding of the effects of sonication on K_m and V_{max}.

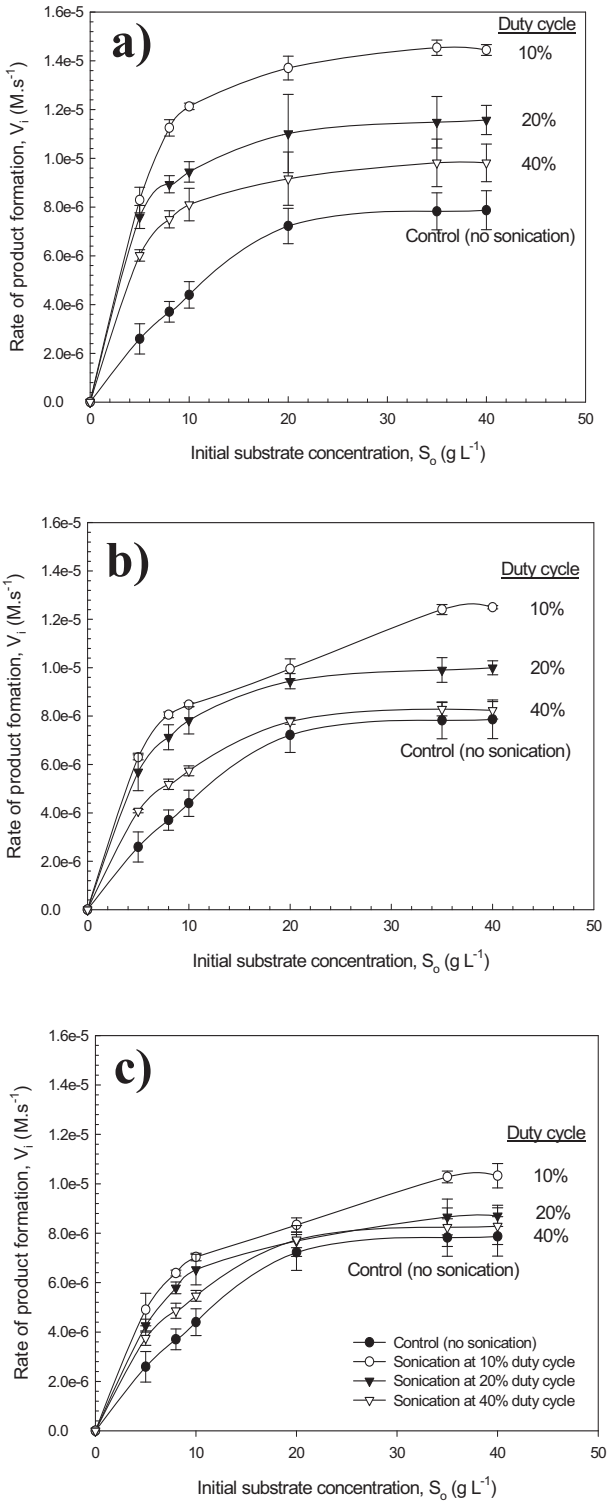

Figure 4.25 Effects of ultrasonication on initial reaction rate (V_i): (a) sonication intensity of 11.8 W cm^{-2}; (b) sonication intensity of 4.7 W cm^{-2}; (c) sonication intensity of 2.4 W cm^{-2}. The controls were not sonicated. The substrate was CMC. Each profile shown is an average of three independent experiments.

Table 4.3 Kinetic parameters for enzymatic hydrolysis of CMC*

Sonication power intensity (W cm^{-2})	Duty cycle (%)	K_m (g L^{-1})	V_{max} (M.s^{-1})
0 (control)	None	10.22 ± 0.21	(0.92 ± 0.0025) × 10^{-5}
2.4	10	7.20 ± 0.15	(1.20 ± 0.04) × 10^{-5}
	20	7.10 ± 0.35	(1.06 ± 0.02) × 10^{-5}
	40	9.07 ± 0.22	(1.05 ± 0.02) × 10^{-5}
4.7	10	6.12 ± 0.14	(1.39 ± 0.02) × 10^{-5}
	20	5.01 ± 0.09	(1.15 ± 0.02) × 10^{-5}
	40	7.43 ± 0.09	(1.01 ± 0.03) × 10^{-5}
11.8	10	4.82 ± 0.14	(1.70 ± 0.03) × 10^{-5}
	20	3.31 ± 0.09	(1.26 ± 0.01) × 10^{-5}
	40	3.99 ± 0.11	(1.10 ± 0.03) × 10^{-5}

*CMC was hydrolyzed with *Accellerase 1000* in 0.05 M acetate buffer at pH 4.8, 50 °C, at an initial enzyme concentration of 0.1 g L^{-1}

Relative to control, sonication always enhanced V_{max} (Figure 4.26a). At any given duty cycle, an increase in sonication intensity generally enhanced V_{max}. At any given sonication intensity, an increased duty cycle generally reduced the V_{max} value. In contrast, the K_m value relative to control was always reduced by sonication, irrespective of the power intensity and the duty cycle used (Figure 4.26b). In sonicated systems, at a given sonication power intensity, the K_m attained a minimum value at a duty cycle of 20% (Figure 4.26b); the K_m values were higher at higher and lower duty cycles. The lowest K_m value occurred at a sonication power intensity of 11.8 W cm^{-2} applied at a duty cycle of 20%. Changes in K_m reflect changes in the affinity of the enzyme towards the substrate. A low K_m value means a high affinity. Thus, a low K_m value is desirable in combination with a high value of V_{max}. In this study, the highest V_{max} value occurred at an irradiance power intensity of 11.8 W cm^{-2} but 10% duty cycle (Figure 4.26a). At this combination of power intensity and duty cycle, the K_m value was low compared to control (Figure

4.26b), but not the lowest. Overall, the optimal sonication regimen for enhancing the hydrolysis of CMC relative to control was considered to be the one corresponding to an irradiance power of 11.8 W cm^{-2} at a duty cycle of 10%.

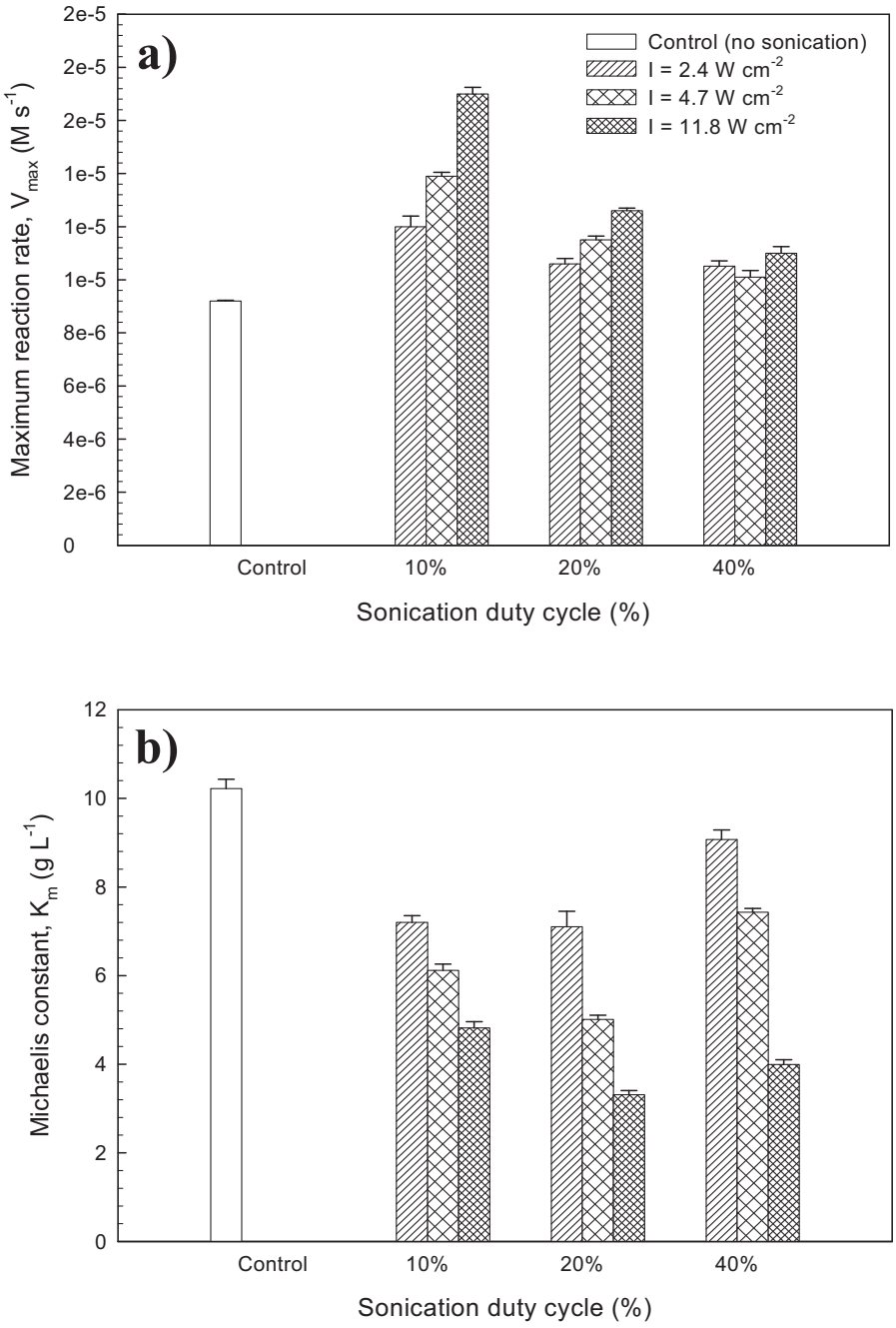

Figure 4.26 Effect of sonication on: (a) maximum reaction rate V_{max} and (b) Michaelis constant K_m for hydrolysis of CMC. The control was not sonicated. (*I* is sonication intensity.)

At the highest intensity, ultrasound likely affected the V_{max} value by improving the rate of diffusion of the macromolecular substrate to and from the enzyme (also a macromolecule) as a consequence of velocity gradients produced by cavitation (Mason and Lorimer, 1988; Mason and Lorimer, 2002). The effects of ultrasound on K_m are explained by ultrasound influencing the dynamic adsorption-desorption of the substrate at the active site of the enzyme as a consequence of acoustic streaming, local microturbulence and possibly motions induced within the enzyme molecule. At the optimal sonication conditions (i.e. a power intensity of 11.8 W cm^{-2} and a 10% duty cycle), V_{max} value was 85% greater than for the control and the Michaelis constant K_m was 53% reduced relative to control (Table 4.3). Ultrasound may also act by loosening the network of cellulose molecules in solution to enhance access of the enzyme to them (Xiao *et al.*, 2005; Xiao *et al.*, 2010).

At any power intensity, an extension of the duty cycle tended to reduce V_{max} because extended sonication had also a damaging effect on the enzyme as shown in a later part of this thesis.

4.3.3.2 Particulate cellulose

To determine the effect of ultrasound on hydrolysis of particulate cellulose, the reaction was carried out under the sonication regimen of a 10% duty cycle and a power intensity 11.8 W cm^{-2} as had been found optimal for hydrolysis of soluble cellulose (Section 4.3.3.1). Concentration of the product (glucose) was measured as the reaction progressed. The data are shown in Figure 4.27. From Figure 4.27, the following are clear: 1) at any given substrate concentration, an increase in particle size reduces the rate of reaction irrespective of whether sonication is used; 2) at any given substrate concentration and particle size, sonication always enhances the rate of reaction relative to control; 3) for any given set of conditions, the glucose concentration data are highly reproducible and follow a consistent pattern. As the substrate is a suspended solid, and the surface area per unit mass of the different grades of the substrate is different, a comparison of kinetics in terms of V_{max} and K_m for different grades of Solka Floc is not meaningful. The faster conversion of substrate with a smaller particle size is attributed to a larger surface area available for the enzyme to act (Basedow and Ebert, 1977; Yeh *et al.*, 2010) (Figure 4.28). For a given particle size of substrate, the enhancement caused by sonication is likely a combination of

enhanced solid-liquid mass transfer (Ahamed and Vermette, 2010; Chisti, 2003; Hagenson and Doraiswamy, 1998; Li *et al.*, 2005; van Wyk, 1997; Várnai *et al.*, 2010) (mass transfer of the enzyme to and from the surface of the substrate) (Figure 4.28) and possibly a reduced value of K_m as was seen for the hydrolysis of soluble cellulose (Section 4.3.3.1).

Ultrasound used alone (i.e. no enzyme present) also has the potential to reduce particle size and hydrolyse cellulose and other polymers. This however generally occurs only under sonication that is much more intense than used in this work.

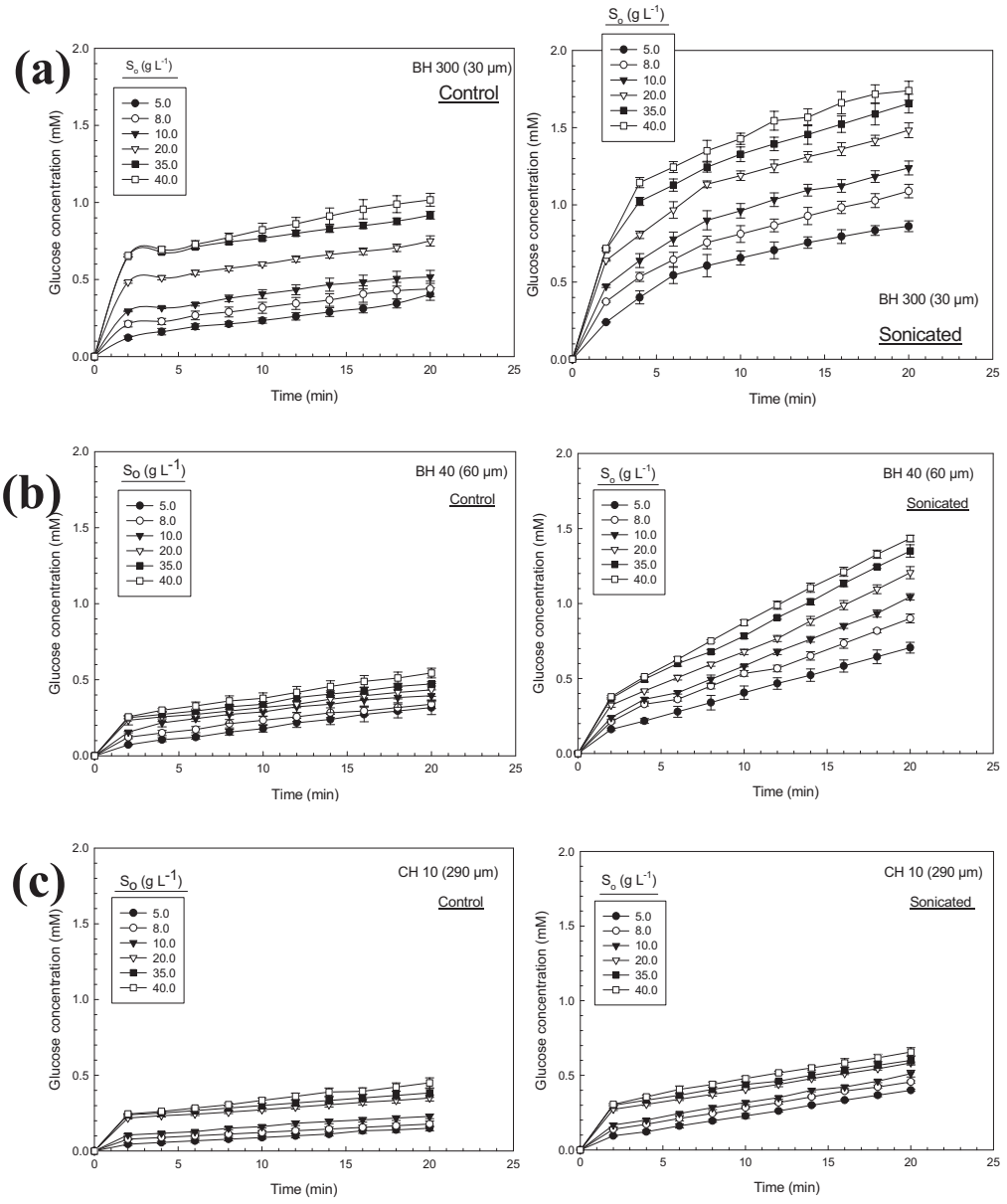

Figure 4.27 Glucose production from Solka-Floc particulate cellulose of different particle sizes: (a) 30 µm; (b) 60 µm; and (c) 290 µm. In all cases the sonication duty cycle was 10% and the power intensity was 11.8 W cm^{-2}. Control runs were not sonicated. S_o is initial substrate concentration. Each profile shown is an average of three independent experiments.

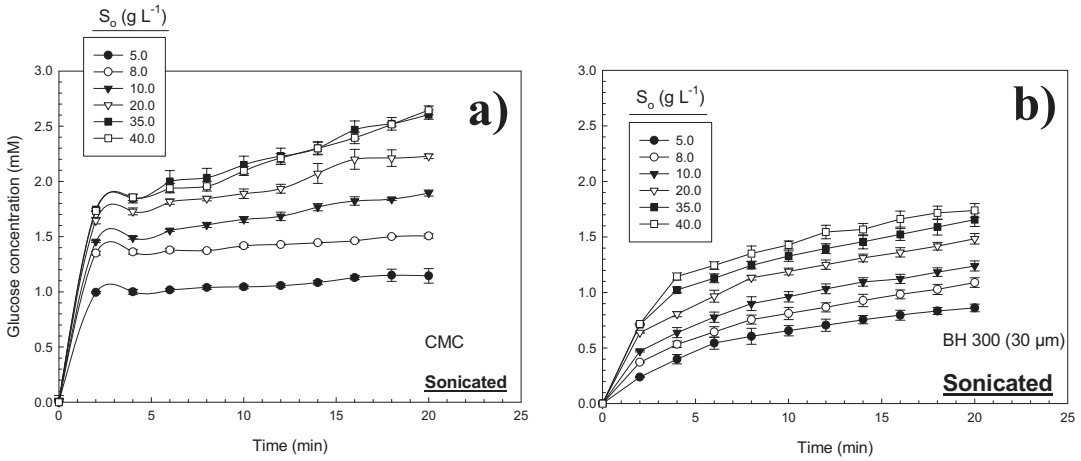

Figure 4.28 Glucose production by hydrolysis of: (a) CMC; (b) particulate cellulose at particle size of 30 µm. In all cases the sonication duty cycle was 10% and the power intensity was 11.8 W cm^{-2}. S_o is initial substrate concentration. Each profile shown is an average of three independent experiments.

4.3.3.3 Effects of ultrasound on stability of cellulase

As evidenced in earlier sections, certain sonication regimens certainly enhance the rates of an enzymatic reaction, but ultrasound also damages enzyme if the intensity of exposure or the duration of exposure are high. Only a few reports have recorded an increased enzyme activity in the presence of ultrasound for enzymes dissolved in a buffer (Yachmenev *et al.*, 2002), whereas numerous reports have recorded a decreased enzyme activity (Basto *et al.*, 2007; Kardos and Luche, 2001). In some cases, an increase of activity occurred at low sonication intensities but a decrease at higher intensities (Rokhina *et al.*, 2009; Sinisterra, 1992). In view of this, the stability of cellulase was examined at various sonication intensities and duty cycles. The enzyme was dissolved in 0.05 M acetate buffer, pH 4.8, without the substrate and stability was tested at 50 °C.

Figure 4.29 shows the results in terms of the percentage of initial activity (i.e. the activity calculated at 2 min) remaining after a given period of exposure to ultrasound. Control data (no sonication) are also shown. Clearly, all combinations of sonication intensities and duty cycles enhanced enzyme activity loss relative to control (Figure 4.29). As expected, a lower intensity sonication (Figure 4.29a) was less damaging compared to higher intensity sonication (Figure 4.29 b, c). At any fixed sonication intensity, an increased duty cycle generally enhanced the damage by prolonging the cumulative period

of exposure. Each measurement was replicated six times and the results were quite consistent and reproducible (Figure 4.29). There was a slight decline in activity of the control enzyme, but this would occur at the relatively high temperature (50 ºC) used in the study.

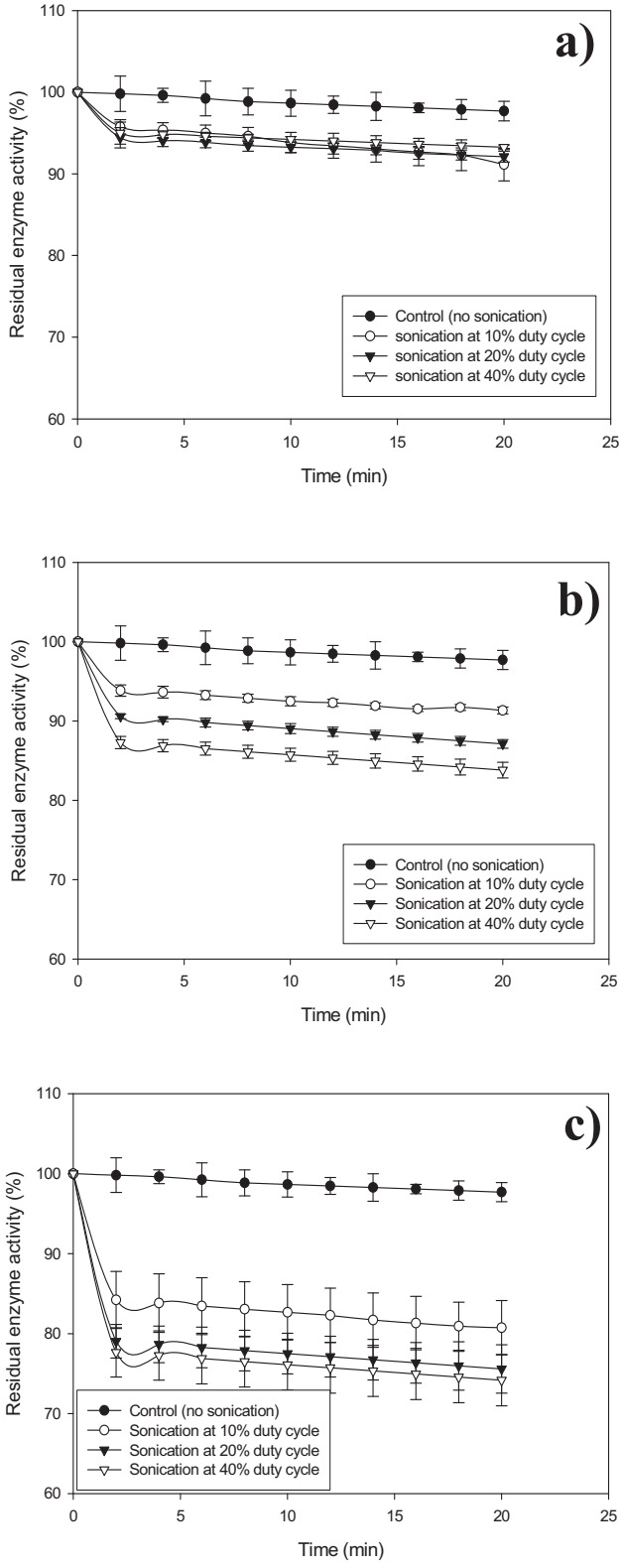

Figure 4.29 Effects of ultrasound on the residual enzyme activity (%): (a) sonication intensity of 2.4 W cm^{-2}; (b) sonication intensity of 4.7 W cm^{-2}; (c) sonication intensity of 11.8 W cm^{-2}. Controls were not sonicated. Each profile shown is an average of three independent experiments.

4.4 Effects of sonication on various bioreaction systems (a unified analysis)

The purpose of this study was to examine the unified effects of ultrasound on various model bioprocesses for explaining the possible causes of ultrasound-induced enhancement in diverse model reaction situations. The model processes investigated included: 1) a fermentation involving cells and gas-liquid mass transfer effects; 2) cell-free enzyme catalysed hydrolysis of a small molecule that was not likely to encounter any major mass transfer limitations; 3) enzyme-mediated hydrolysis of a macromolecular substrate in which the size of the substrate entity could be varied substantially and solid-liquid mass transfer limitations occurred.

In all the model processes tested, under suitable sonication regimens, ultrasound improved the process in terms of the rate of product formation and productivity relative to nonsonicated control. Sonication regimens that produced process enhancements, did damage enzymes such as β-galactosidase and cellulase. This suggests that ultrasound-induced enhancements in production rates more than compensated for productivity loss associated with enzyme damage. In all cases, the process enhancing effects of ultrasound—whether enhanced gas-liquid mass transfer, improved solid-liquid mass transfer, enhanced interactions of dissolved macromolecules (i.e. soluble cellulose and cellulase), and alterations in affinity of enzyme towards its substrate—could be linked to cavitation-associated acoustic turbulence, or microstreaming in the fluid.

As evidenced by reduced values of K_m relative to control, sonication improved the affinity (or ease of binding and unbinding) of both a small substrate (i.e. lactose) and a macromolecular substrate (i.e. dissolved cellulose) to enzymes. In addition to microstreaming, this may be linked to ultrasound directly influencing the adsorption-desorption dynamics of the substrates at the active sites of the enzymes by inducing pulsating motions within the enzyme molecules. Sonication reduced the value of the Monod constant K_s in the yeast fermentations, suggesting an enhanced affinity of the yeast cell towards the substrate, lactose. Sonication apparently also enhanced carbon dioxide removal in this fermentation. Thus, in some cases at least, multiple factors linked to sonication appear to contribute to the observed process enhancements.

The observed effects of sonication in the model reaction systems tested suggest a substantial commercial potential for ultrasound in enhancing bioprocesses.

CHAPTER 5

CONCLUSIONS

5.1 Conclusions

Based on the results of this study, the following are the main conclusions:

1. Intermittent sonication with power ultrasound (20 kHz, 11.8 W cm^{-2}) at duty cycles of ≤20% in batch fermentations effectively stimulates biomass production, lactose utilization and ethanol production by *K. marxianus* relative to control. An increase in the duty cycle to 40% adversely impacts the yeast compared to duty cycles of < 40%.

2. Under the best conditions in the sonicated batch fermentation, sonication enhanced the final ethanol concentration by nearly 3.5-fold relative to control. This corresponded to a 3.5-fold enhancement in ethanol productivity, but required 952 W of additional power input per cubic meter of broth through sonication.

3. In continuous fermentations, increasing the dilution rate, reduced the steady-state biomass and ethanol concentrations both in control and sonicated fermentations, as expected. At a fixed dilution rate of 0.1 h^{-1} and sonication at 11.8 W cm^{-2} and 20% duty cycle, sonication enhanced the maximum ethanol productivity by nearly 1.5-fold relative to control.

4. In cell-free systems, ultrasound was shown to increase the gas-liquid mass transfer coefficient in a stirred bioreactor relative to controls. At the highest agitation speed (800 rpm) and 2 vvm aeration rate, the mass transfer coefficient under intense sonication (50.3 W cm^{-2}, continuous sonication) was nearly twice that of the control.

5. In the cell-free hydrolysis of lactose by β-galactosidase, a sonication regimen of a 10% duty cycle and a power intensity of 11.8 W cm^{-2}, was most effective in enhancing the initial reaction rate. In this sonication regimen the reaction rate was enhanced nearly 1.4-fold relative to control. Under the same conditions, the enzyme lost 27% of its activity relative to control in 30 min. A 40% duty cycle at 11.8 W cm^{-2}, adversely affected the enzyme activity.

6. Hydrolysis of both soluble and insoluble cellulose followed Michaelis-Menten kinetics.

7. In the hydrolysis of soluble cellulose, ultrasound enhanced the maximum reaction rate V_m and reduced the value of Michaelis constant K_m under optimal sonication conditions of a 10% duty cycle and a power intensity of 11.8 W cm^{-2}, relative to control. Using optimal sonication, the maximum reaction rate was nearly doubled relative to control.

8. In the hydrolysis of insoluble cellulose of different particle sizes, an increasing particle size reduced the rate of hydrolysis. At any fixed particle size, sonication at 10% duty cycle and 11.8 W cm^{-2} , power intensity improved the rate of hydrolysis relative to controls.

9. The activity of cellulase dissolved in phosphate buffer in the absence of the substrate was lost by ~20% in 20 min under sonication conditions (a 10% duty cycle and a power intensity of 11.8 W cm^{-2}) that had enhanced the rate of substrate hydrolysis relative to controls in separate experiments. Thus, despite an increased rate of enzyme degradation under sonication, ultrasound can be used to achieve an overall improvement in rates of hydrolysis of soluble and insoluble substrates relative to controls.

CHAPTER 6

RECOMMENDATIONS

6.1 Recommendations

Sonication under suitable regimens has a clear potential for enhancing the productivity of different kinds of bioreaction systems as well as other operations such as product recovery. Whether sonication is useful or not and the suitable sonication regimens if any, can only be established experimentally on a case-by-case basis. In view of the diversity of bioprocesses, a substantial scope exists for future studies of ultrasound-induced enhancements. Two recommendation for future work relating to the present study are the following:

1. Effect of sonication on an anaerobic fermentation of lactose should be examined relative to controls, under conditions that provide a maximum ethanol productivity.

2. Designs of new ultrasonic equipment need to be evaluated for biotechnology research because the equipment used currently (i.e. probe type horns) has been adapted from the chemical industry and its design does not consider that living systems cannot survive extreme localized sonication conditions. Equipment that distributes the sound energy cover a broad area should be fabricated and evaluated. Such a system may provide an even distribution of ultrasonic energy and allow better control on the sonication process.

LIST OF PUBLICATIONS

This work has been published or presented in part as follows:

1. Ahmad Ziad Sulaiman, Azilah Ajit, Rosli Mohd Yunus, Yusuf Chisti, Ultrasound-assisted fermentation enhances bioethanol productivity, Biochemical Engineering Journal, Volume 54, Issue 3, May 2011, Page 141-150.

2. Ahmad Ziad Sulaiman, Azilah Ajit, Rosli Mohd Yunus, Yusuf Chisti, Effects of ultrasound on enzymatic hydrolysis of soluble cellulose, Presented at 14th International Biotechnology Symposium and Exhibition, Rimini, Italy, 14-18th September, 2010. Abstract published in Journal of Biotechnology, Volume 150, Supplement 1, November 2010, Page 135.

3. Ahmad Ziad Sulaiman, Rosli Mohd Yunus, Yusuf Chisti, Effects of ultrasound on ethanol production by *Kluyveromyces marxianus*, Presented at 3rd International Conference on Chemical & Bioprocess Engineering (ICCBPE 2010), Sabah, Malaysia, August 16-18th August, 2009.

REFERENCES

Ahamed A, Vermette P. 2010. Effect of mechanical agitation on the production of cellulases by *Trichoderma reesei* RUT-C30 in a draft-tube airlift bioreactor. Biochemical Engineering Journal 49:379-387.

Al-Zuhair S. 2008. The effect of crystallinity of cellulose on the rate of reducing sugars production by heterogeneous enzymatic hydrolysis. Bioresource Technology 99:4078-4085.

Aliyu M, Hepher MJ. 2000. Effects of ultrasound energy on degradation of cellulose material. Ultrasonics Sonochemistry 7:265-268.

Anderson JM. 1953. Effects of ultrasonic radiation on growth and fermentation in yeast, *Saccharomyces cerevisiae*. Biochimica et Biophysica Acta 11:122-137.

Ashokkumar M, Lee J, Kentish S, Grieser F. 2007. Bubbles in an acoustic field: an overview. Ultrasonics Sonochemistry 14:470-475.

Badino AC, Facciotti MCR, Schmidell W. 2000. Improving k(L)a determination in fungal fermentation, taking into account electrode response time. Journal of Chemical Technology and Biotechnology 75:469-474.

Bailey JE, Ollis DF. 1986. Biochemical Engineering Fundamentals. New York: McGraw-Hill, pp. 610-758.

Bakken AP, Hill Jr CG, Amundson CH. 1992. Hydrolysis of lactose in skim milk by immobilized β-galactosidase (*Bacillus circulans*). Biotechnology and Bioengineering 39:408-417.

Baldascini H, Ganzeveld KJ, Janssen DB, Beenackers AACM. 2001. Effect of mass transfer limitations on the enzymatic kinetic resolution of epoxides in a two-liquid-phase system. Biotechnology and Bioengineering 73:45-54.

Bandyopadhyay B, Humphrey AE, Taguchi H. 1967. Dynamic measurement of the volumetric oxygen transfer coefficient in fermentation systems. Biotechnology and Bioengineering 9:533-544.

Bar R. 1988. Ultrasound enhanced bioprocesses: Cholesterol oxidation by *Rhodococcus erythropolis*. Biotechnology and Bioengineering 32:655-663.

Barberis SE, Segovia RF. 1997. Dissolved oxygen concentration controlled feeding of substrate into *Kluyveromyces fragilis* culture. Biotechnology Techniques 11:797-799.

Basedow AM, Ebert KH. 1977. Ultrasonic degradation of polymers in solution. In: Cantow HJ, Dall'asta G, Dusek K, Ferry JD, H.Fujita, Gordon M, Kern W, Natta G, Okamura S, Overberger CG and others, editors. Advances in Polymer Science. New York: Springer, pp. 88-97.

Basedow AM, Ebert KH. 1979. Effects of mechanical stress on the reactivity of polymers: activation of acid hydrolysis of dextran by ultrasound. Polymer Bulletin 1:299-306.

Basto C, Silva CJ, Gübitz G, Cavaco-Paulo A. 2007. Stability and decolourization ability of *Trametes villosa* laccase in liquid ultrasonic fields. Ultrasonics Sonochemistry 14:355-362.

Beldman G, Voragen AGJ, Rombouts FM, Searle-van Leeuwen MF, Pilnik W. 1987. Adsorption and kinetic behavior of purified endoglucanases and exoglucanases from *Trichoderma viride*. Biotechnology and Bioengineering 30:251-257.

Belem MAF, Lee BH. 1998. Production of Bioingredients from *Kluyveromyces marxianus* grown on whey: An alternative. Critical Reviews in Food Science and Nutrition 38:565-598.

Bisset F, Sternberg D. 1978. Immobilization of *Aspergillus* beta-glucosidase on chitosan. Applied and Environmental Microbiology 35:750-755.

Böhm H, Anthony P, Davey MR, Briarty LG, Power JB, Lowe KC, Benes E, Gröschl M. 2000. Viability of plant cell suspensions exposed to homogeneous ultrasonic fields of different energy density and wave type. Ultrasonics 38:629-632.

Bojorge N, Valdman B, Acevedo F, Gentina JC. 1999. A semi-structured model for the growth and β-galactosidase production by fed-batch fermentation of *Kluyveromyces marxianus*. Bioprocess and Biosystems Engineering 21:313-318.

Boodhoo KVL, Vicevic M, Cartwright CD, Toogood EC. 2008. Intensification of gas-liquid mass transfer using a rotation bed of porous packings for application to an *E. coli* batch fermentation process. Chemical Engineering Journal 135:141-150.

Boyd AR, Gunasekera TS, Attfield PV, Simic K, Vincent SF, Veal DA. 2003. A flow-cytometric method for determination of yeast viability and cell number in a brewery. FEMS Yeast Research 3:11-16.

Butz P, Greulich KO, Ludwig H. 1988. Volume changes during enzyme reactions: indications of enzyme pulsation on fumarase catalysis. Biochemistry 27: 1556-1563.

Carbajal RI, Tecante A. 2004. On the applicability of the dynamic pressure step method for kLa determination in stirred Newtonian and non-Newtonian fluids, culture media and fermentation broths. Biochemical Engineering Journal 18:185-192.

Carrara CR, Rubiolo AC. 1996. Determination of kinetics parameters for free and immobilized [beta]-galactosidase. Process Biochemistry 31:243-248.

Cavaille D, Combes D. 1995. Characterization of beta-galactosidase from *Kluyveromyces lactis*. Biotechnology and Applied Biochemistry 22:55-64.

Chandel AK, Chan ES, Rudravaram R, Narasu ML, Rao LV, Ravindra P. 2007. Economics and environmental impact of bioethanol production technologies: an appraisal. Biotechnology and Molecular Biology Reviews 2:14-32.

Chisti Y. 1989. Airlift Bioreactors. New York, Elsevier.

Chisti Y. 1999. Mass transfer. Encyclopedia of Bioprocess Technology: Fermentation, biocatalysis, and bioseparation, Wiley, pp. 1607-1640.

Chisti Y. 2003a. Ultrasound-the power of a silent gong. Biotechnology Advances 21:1-2.

Chisti Y. 2003b. Sonobioreactors: using ultrasound for enhanced microbial productivity. Trends in Biotechnology 21:89-93.

Chisti Y. 2010. Mass Transfer. in Encyclopedia of Industrial Biotechnology, Bioprocess, Bioseparation, and Cell Technology, edited by Michael Flickinger. Oxford: Wiley-Blackwell: Seven volume set. ISBN: 978-0471-79930-6. pp. 5248

Chisti Y, Moo-Young M. 1986. Disruption of microbial cells for intracellular products. Enzyme and Microbial Technology 8:194-204.

Chisti Y, Moo-Young M. 2002. Bioreactors. In: Encyclopedia of Physical Science and Technology, edited by Meyers, R.A., vol. 2, Academic Press, San Diego, pp. 247-271.

Choi JH, Kim SB. 1994. Effect of ultrasound on sulfuric acid-catalysed hydrolysis of starch. Korean Journal of Chemical Engineering 11:178-184.

Chu J, Li B, Zhang S, Li Y. 2000. On-line ultrasound stimulates the secretion and production of gentacimin by *Micromonospora echinospora*. Process Biochemistry 35:569-572.

Chuanyun D, Bochu W, Chuanren D, Sakanishi A. 2003. Low ultrasonic stimulates fermentation of riboflavin producing strain *Ecemothecium ashbyii*. Colloids and Surfaces B: Biointerfaces 30:37-41.

Chuanyun D, Bochu W, Huan Z, Conglin H, Chuanren D, Wangqian L, Toyama Y, Sakanishi A. 2004. Effect of low frequency ultrasonic stimulation on the secretion of siboflavin produced by *Ecemothecium ashbyii*. Colloids and Surfaces B: Biointerfaces 34:7-11.

Counotte GHM, Prins RA. 1979. Calculation of K_m and V_{max} from substrate concentration versus time plot. Applied and Environmental Microbiology 38:758-760.

Cruz AJG, Silva AS, Araujo M, Giordano RC, Hokka CO. 1999. Estimation of the volumetric oxygen tranfer coefficient (kLa) from the gas balance and using a neural network technique. Brazilian Journal of Chemical Engineering 16:179-183.

Czechowska-Biskup R, Rokita B, Lotfy S, Ulanski P, Rosiak JM. 2005. Degradation of chitosan and starch by 360-kHz ultrasound. Carbohydrate Polymers 60:175-184.

Demirhan E, Ozbek B. 2009. A modelling study on hydrolysis of lactose recovered from whey and β-galactosidase stability under sonic treatment. Chemical Engineering Communications 196:767-787.

Doran PM. 1995. Bioprocess Engineering Principles. San Diego, Academic Press, pp. 439

Dunn IJ, Einsele A. 1975. Oxygen transfer coefficients by the dynamic method. Journal of Applied Chemistry and Biotechnology 25:707-720.

Ensminger, D. 1988. Ultrasonics: fundamentals, technology, application. Portland, CRC Press, pp. 580.

Fadavi A, Chisti Y. 2005. Gas-liquid mass transfer in a novel forced circulation loop reactor. Chemical Engineering Journal 112:73-80.

Fan LT, Gharpuray MM, Lee YH. 1987. Cellulose hydrolysis. Biotechnology Monographs, vol. 3, pp. 25, New York: Springer-Verlag.

Fasano JB, Penney WR. 1991. Avoid blending mix-ups. Chemical Engineering Progress. 87:56-63.

Filson PB, Dawson-Andoh BE. 2009. Sono-chemical preparation of cellulose nanocrystals from lignocellulose derived materials. Bioresource Technology 100:2259-2264.

Floros JD, Liang H. 1994. Acoustically assisted diffusion through membranes and biomaterials. Food Technology 48:79-84.

Fonseca GG, Heinzle E, Wittmann C, Gombert AK. 2008. The yeast *Kluyveromyces marxianus* and its biotechnological potential. Applied Microbiology and Biotechnology 79:339-354.

Furlan SA, Schneider A.L.S., Merkle R, Carvalho-Jonas MF, Jonas R. 2001. Optimization of pH, temperature and inoculum ratio for the production of β-D-galactosidase by *Kluyveromyces marxianus* using a lactose-free medium. Acta Biotechnologica 1:57-64.

Gekas V, Lopez-Leiva M. 1985. Hydrolysis of lactose: a literature review. Process Biochemistry 20:2-12.

Gogate PR, Kabadi AM. 2009. A review of applications of cavitation in biochemical engineering/biotechnology. Biochemical Engineering Journal 44:60-72.

Gogate PR, Pandit AB. 1999. Survey of measurement techniques for gas-liquid mass transfer coefficient in bioreactors. Biochemical Engineering Journal 4:7-15.

Grba S, Stehlik-Tomas V, Stanzer D, Vaheie N, ŠKrlin A. 2002. Selection of yeast strain *Kluyveromyces marxianus* for alcohol and biomass production on whey. Journal of Chemical Technology and Biotechnology 16:13-16.

Guimarães PMR, Teixeira JA, Domingues L. 2010. Fermentation of lactose to bio-ethanol by yeasts as part of integrated solutions for the valorisation of cheese whey. Biotechnology Advances 28:375-384.

Hagenson LC, Doraiswamy LK. 1998. Comparison of the effects of ultrasound and mechanical agitation on a reacting solid-liquid system. Chemical Engineering Science 53:131-148.

Hansen PJ. 2000. Use of a hemacytometer. Florida: University of Florida.

Havsteen BH. 1989. A new principle of enzyme catalysis: coupled vibrations facilitate conformational changes. Journal of Theoretical Biology 140:101-127.

Herrán NS, López JLC, Pérez JAS, Chisti Y. 2008. Effects of ultrasound on culture of *Aspergillus terreus*. Journal of Chemical Technology and Biotechnology 83:593-600.

Hewitt GM, Wassink JWDG. 1984. Simultaneous production of inulase and lactase in batch and continous cultures of *Kluyveromyces fragilis*. Enzyme and Microbial Technology 6:263-270.

Howell JA, Stuck JD. 1975. Kinetics of Solka Floc cellulose hydrolysis by *Trichoderma viride* cellulase. Biotechnology and Bioengeering 17:873-893.

Huang W-C, Cheng S-J, Chen TL. 2006. The role of dissolved oxygen and function of agitation in hyaluronic acid fermentation. Biochemical Engineering Journal 32:239-243.

Husain Q. 2010. β-Galactosidases and their potential applications: a review. Critical Reviews in Biotechnology 30:1-22.

Iida Y, Tuziuti T, Yasui K, Kozuka T, Towata A. 2008. Protein release from yeast cells as an evaluation method of physical effects in ultrasonic field. Ultrasonics-Sonochemistry 15:995-1000.

Imai M, Ikari K, Suzuki I. 2004. High-performance hydrolysis of cellulose using mixed cellulase species and ultrasonication pretreatment. Biochemical Engineering Journal 17:79-83.

Jian S, Wenyi T, Wuyong C. 2008. Ultrasound-accelerated enzymatic hydrolysis of solid leather waste. Journal of Cleaner Production 16:591-597.

Jomdecha C, Prateepasen P. 2006. The research of low-ultrasonic affects to yeast growth in fermentation process. 12th A-PCNDT 2006 - Asia Pacific Conference on non-descructive testing. Auckland, New Zealand.

Jones RP, Greenfield PF. 1982. Effect of carbon dioxide on yeast growth and fermentation. Enzyme and Microbial Technology 4:210-223.

Joyce E, Phull SS, Lorimer JP, Mason TJ. 2003. The development and evaluation of ultrasound for the treatment of bacterial suspensions. A study of frequency, power and sonication time on cultured *Bacillus* species. Ultrasonics Sonochemistry 10:315-318.

Jurado E, Camacho F, Luzon G, Vicaria JM. 2002. A new kinetic model proposed for enzymatic hydrolysis of lactose by a [beta]-galactosidase from *Kluyveromyces fragilis*. Enzyme and Microbial Technology 31:300-309.

Kardos N, Luche J-L. 2001. Sonochemistry of carbohydrate compounds. Carbohydrate Research 332:115-131.

Khanal SK, Montalbo M, van Leeuwen JH, Srinivasan G, Grewell D. 2007. Ultrasound enhanced glucose release from corn in ethanol plants. Biotechnology and Bioengineering 98:978-985.

Kilby NJ, Hunter CS. 1990. Repeated harvest of vacuole-located secondary product from in vitro grown plant cells using 1.02 MHz ultrasound. Applied Microbiology and Biotechnology 33:448-451.

Kim JK, Tak KT, Moon JH. 1998. A continuous fermentation of *Kluyveromyces fragilis* for the production of a highly nutritious protein diet. Aquacultural Engineering 18:41-49.

Knorr D, Zenker M, Heinz V, Lee DU. 2004. Applications and potential of ultrasonics in food processing. Trends in Food Science and Technology 15:261-266.

Koda S, Mori H, Matsumoto K, Nomura H. 1994. Ultrasonic degradation of water-soluble polymers. Polymer(Guildford) 35:30-33.

Kristol DS, Khamis AA, Parker RC. 1984. Effect of ultrasound on the acid hydrolysis of dextran. Industrial and Engineering Chemistry Process and Development 23:74-78.

Krzystek L, Ledakowicz S. 2000. Stoichiometric analysis of *Kluyveromyces fragilis* growth on lactose. Journal of Chemical Technology and Biotechnology 75:1110-1118.

Kumar A, Gogate PR, Pandit AB, Delmas H, Wilhelm AM. 2004. Gas-liquid mass transfer studies in sonochemical reactors. Industrial and Engineering Chemistry Research 43:1812-1819.

Ladero M, Santos A, Garcia-Ochoa F. 2000. Kinetic modeling of lactose hydrolysis with an immobilized [beta]-galactosidase from *Kluyveromyces fragilis*. Enzyme and Microbial Technology 27:583-592.

Lamping SR, Zhang H, Allen B, Shamlou PA. 2003. Design of a prototype miniature bioreactor for high throughput automated bioprocessing. Chemical Engineering Science 58:747-758.

Lanchun S, Bochu W, Lianchai Z, Jie L, Yanhong Y, Chuanren D. 2003a. The influence of low intensity ultrasonic on some physiological characteristics of *Saccharomyces cerevisae*. Colloids and Surfaces B: Biointerfaces 30:61-66.

Lanchun S, Bochu W, Zhiming L, Chuanren D, Chuanyun D, A.Sakanishi. 2003b. The research into the influence of low intensity ultrasonic on the growth of *S. cerevisiaes*. Colloids and Surfaces B: Biointerfaces 30:43-49.

Lane MM, Morrissey JP. 2010. *Kluyveromyces marxianus*: A yeast emerging from its sister's shadow. Fungal Biology Reviews 12:17-26.

Lee SB, Shin HS, Ryu DDY, Mandels M. 1982. Adsorption of cellulase on cellulose: Effect of physicochemical properties of cellulose on adsorption and rate of hydrolysis. Biotechnology and Bioengineering 24:2137-2153.

Leeuwen CV. 1979. Dynamic measurement of the overall volumetric mass transfer coefficient in air sparged systems. Biotechnology and Bioengineering 21:2125-2131.

Leighton TG. 2007. What is ultrasound? Progress in Biophysics and Molecular Biology 93:3-83.

Li C, Yoshimoto M, Ogata H, Tsukuda N, Fukunaga K, Nakao K. 2005. Effects of ultrasonic intensity and reactor scale on kinetics of enzymatic saccharification of various waste papers in continuously irradiated stirred tanks. Ultrasonics Sonochemistry 12:373-384.

Li C, Yoshimoto M, Tsukuda N, Fukunaga K, Nakao K. 2004. A kinetic study on enzymatic hydrolysis of a variety of pulps for its enhancement with continuous irradiation. Biochemical Engineering Journal 19:155-164.

Lii C, Chen CH, Yeh AI, Lai VMF. 1999. Preliminary study on the degradation kinetics of agarose and carrageenans by ultrasound. Food Hydrocolloids 13:477-481.

Lin L, Yan R, Liu Y, Jiang W. 2010. In-depth investigation of enzymatic hydrolysis of biomass wastes based on three major components: Cellulose, hemicellulose and lignin. Bioresource Technology 101:8217-8223.

Linek V, Vacek V, Benes P. 1987. A critical review and experimental verification of the correct use of the dynamic method for the determination of oxygen transfer in aerated agitated vessels to water, electrolyte solutions and viscous liquids. Chemical Engineering Journal 34:11-34.

Lineweaver H, Burk D. 1934. The determination of enzyme dissociation constants. Journal of the American Chemical Society 56:658-666.

Liu H, Yan Y, Wang W, Yu Y. 2007. Low intensity ultrasound stimulates biological activity of aerobic activated sludge. Frontiers of Environmental Science and Engineering in China 1:67-72.

Lockner D. 1993. The role of acoustic emission in the study of rock fracture. International Journal of Rock Mechanics and Mining Sciences and Geomechanics Abstracts 30:883-899.

Lucero P, Penalver E, Moreno E, Lagunas R. 2000. Internal trehalose protects endocytosis from inhibition by ethanol in Saccharomyces cerevisiae. Applied and Environmental Microbiology 66:44-56.

Lukondeh T, Ashbolt NJ, Rogers PL. 2005. Fed-batch fermentation for production of *Kluyveromyces marxianus* FII510700 cultivated on a lactose-based medium. Journal of Industrial Microbiology and Biotechnology 32:284-288.

Mandels M, Hontz L, Nystrom J. 2004. Enzymatic hydrolysis of waste cellulose. Biotechnology and Bioengineering 16:1471-1493.

Marison I, Stockar Uv. 1987. A calorimetric investigation of the aerobic cultivation of *Kluyveromyces fragilis* on various substrates. Enzyme and Microbial Technology 9:33-43.

Marquez LDS, Sousa GDB, Assis AJ, Ribeiro EJ. 2005. Synthesis of β-galactosidase in aerobic fermentation by *Kluyveromyces marxianus*. 2nd Mercosur Congress on Chemical Engineering and 4th Mercosur Congress on Process Systems Engineering. Rio de Janeiro.

Martín M, Montes FJ, Galán MA. 2008. Bubbling process in stirred tank reactors II: Agitator effect on the mass transfer rates. Chemical Engineering Science 63:3223-3234.

Martín M, Montes FJ, Galán MA. 2010. Mass transfer rates from bubbles in stirred tanks operating with viscous fluids. Chemical Engineering Science 65:3814-3824.

Mason TJ, Lorimer JP. 1988. Sonochemistry: theory, applications and uses of ultrasound in chemistry. Chichester: Ellis Horwood.

Mason TJ, Lorimer JP. 2002. Applied Sonochemistry: The uses of power ultrasound in chemistry and processing. Berlin: Wiley.

Mason TJ, Paniwnyk L, Lorimer JP. 1996. The uses of ultrasound in food technology. Ultrasonics Sonochemistry 3:253-260.

Matsuura K, Hirotsune M, Nunokawa Y, Satoh M, Honda K. 1994. Acceleration of cell growth and ester formation by ultrasonic wave irradiation. Journal of Fermentation and Bioengineering 77:36-40.

Mclean D, Holcomb J, Maxwell K, Somes JB. 2001. A novel method for quantitation of active yeast cells. Cheney, WA, http://www.genprime.com/ downloads/ EasyCountTechPaper.pdf.

Mecozzi M, Acquistucci R, Amici M, Cardarilli D. 2002. Improvement of an ultrasound assisted method for the analysis of total carbohydrate in environmental and food samples. Ultrasonics Sonochemistry 9:219-223.

Mehaia MA, Cheryan M. 1984. Hollow fibre bioreactor for ethanol production: application to the conversion of lactose by *Kluyveromyces fragilis*. Enzyme and Microbial Technology 6:117-120.

Melo EHM, Kennedy JF. 1993. Cellulose derivatives: an enzymatic approach to their modification. Carbohydrate Polymers 22:233-237.

Miller GL. 1959. Use of dinitrosalicylic acid reagent for determination of reducing sugar. Analytical Chemistry 31:426–428.

Monod J. 1949. The growth of bacterial cultures. Annual Review of Microbiology 3:371-394.

Moresi M, Trunfio A, Parente E. 1990. Kinetics of continuous whey fermentation by *Kluyveromyces fragilis*. Journal of Chemical Technology and Biotechnology 49:205-22.

Mueller JA, Boyle WC, Lightfoot EN. 1967. Effect of the response time of a dissolved oxygen probe on the oxygen uptake rate. Applied Microbiology 15:674-676.

Muralidhara HS, Ensminger D, Putnam A. 1985. Acoustic dewatering and drying (low and high frequency): state of the art review. Drying Technology 529-566.

Nakanoh M, Yoshida F. 1980. Gas absorption by Newtonian and Non-Newtonian liquids in a bubble column. Industrial Engineering Chemistry Process Design Development 19:190-195.

Neis U. 2002. Intensification of biological and chemical processes by ultrasound. TU Hamburg-Harburg Reports on Sanitary Engineering 35:79-90.

Nguyen TMP, Lee YK, Zhou W. 2009. Stimulating fermentative activities of bifidobacteria in milk by high - intensity ultrasound. International Dairy Journal 19:410-416.

Nitayavardhana S, Shrestha P, Rasmussen ML, Lamsal BP, van Leeuwen JH, Khanal SK. 2010. Ultrasound improved ethanol fermentation from cassava chips in cassava-based ethanol plants. Bioresource Technology 101:2741-2747.

Nor ZM, Tamer MI, Scharer JM, Moo-Young M, Jervis EJ. 2001. Automated fed-batch culture of *Kluyveromyces fragilis* based on a novel method for on-line estimation of cell specific growth rate. Biochemical Engineering Journal 9:221-231.

Norton JS, Krauss RW. 1972. The inhibition of cell division in *Saccharomyces cerevisiae* (Meyen) by carbon dioxide. Plant and Cell Physiology 13:139-149.

Novalin S, Neuhaus W, Kulbe K. 2005. A new innovative process to produce lactose-reduced skim milk. Journal of Biotechnology 119:212-218.

Nyborg WL. 1982. Ultrasonic microstreaming and related phenomena. The British Journal of Cancer. Supplement 5:156.

Ortega N, Busto D. 2001. Kinetics of cellulose saccharification by *Trichoderma reesei* cellulases. International Biodeterioration and Biodegradation 47:7-14.

Özbek B, Ülgen K. 2000. The stability of enzymes after sonication. Process Biochemistry 35:1037-1043.

Ozilgen M, D.F.Ollis, Ogrydziak D. 1988. Kinetics of batch fermentations with *Kluyveromyces fragilis*. Enzyme and Microbial Technology 10:165-172.

Painting K, Kirsop B. 1990. A quick method for estimating the percentage of viable cells in a yeast population, using methylene blue staining. World Journal of Microbiology and Biotechnology 6:346-347.

Patist A, Bates D. 2008. Ultrasonic innovations in the food industry: From the laboratory to commercial production. Innovative Food Science and Emerging Technologies 9:147-154.

Pessela BCC, Mateo C, Fuentes M, Vian A, García JL, Carrascosa AV, Guisán JM, Fernández-Lafuente R. 2003. The immobilization of a thermophilic [beta]-galactosidase on Sepabeads supports decreases product inhibition: Complete hydrolysis of lactose in dairy products. Enzyme and Microbial Technology 33:199-205.

Philichi TL, Stenstrom MK. 1989. Effects of dissolved oxygen probe lag on oxygen transfer parameter estimation. Water Pollution Control 61:83-86.

Potapovich MV, Eryomin AN, Metelitza DI. 2005. Ultrasonic and thermal inactivation of catalases from bovine liver, the methylotrophic yeast *Pichia pastoris*, and the fungus *Penicillium piceum*. Applied Biochemistry and Microbiology 41:529-537.

Radel S, McLoughlin AJ, Gherardini L, Doblhoff-Dier O, Benes E. 2000. Viability of yeast cells in well controlled propagating and standing ultrasonic plane waves. Ultrasonics 38:633-637.

Rokhina EV, Lens P, Virkutyte J. 2009. Low-frequency ultrasound in biotechnology: state of the art. Trends in Biotechnology 27:298-306.

Rolz C. 1986. Ultrasound effect on enzymatic saccharification. Biotechnology Letters 8:131-136.

Rosa MF, S Correia I. 1996. Intracellular acidification does not account for inhibition of Saccharomyces cerevisiae growth in the presence of ethanol. FEMS Microbiology Letters 135:271-274.

Ruchti G, Dunn IJ, Bourne JR. 1981. Comparison of dynamic oxygen electrode methods for the measurement of KLa. Biotechnology and Bioengineering 23:277-290.

Runyan CM, Carmen JC, Beckstead BL, Nelson JL, Robinson RA, Pitt WG. 2006. Low-frequency ultrasound increases outer permeability of *Pseudomonas aeruginosa*. Journal Genetic Applied Microbiology 52:295-301.

Sainz Herrán N, Casas López JL, Sánchez Pérez JA, Chisti Y. 2010. Influence of ultrasound amplitude and duty cycle on fungal morphology and broth rheology of *Aspergillus terreus*. World Journal of Microbiology and Biotechnology 26:1409–1418.

Sakakibara M, Wang D, Ikeda K, Suzuki K. 1994. Effect of ultrasonic irradiation on production of fermented milk with *Lactobacillus delbrueckii*. Ultrasonics Sonochemistry 1:S107-S110.

Sakakibara M, Wang D, Takahashi R, Takahashi K, Mori S. 1996. Influence of ultrasound irradiation on hydrolysis of sucrose catalyzed by invertase. Enzyme and Microbial Technology 18:444-448.

Sami M, Ikeda M, Yabuuchi S. 1994. Evaluation of the alkaline methylene blue staining method for yeast activity determination. Journal of Fermentation and Bioengineering 78:212-216.

Santos A, Ladero M, Garcia-Ochoa F. 1998. Kinetic modeling of lactose hydrolysis by a [beta]-galactosidase from *Kluyveromyces fragilis*. Enzyme and Microbial Technology 22:558-567.

Schläfer O, Sievers M, Klotzbucher H, Onyeche TI. 2000. Improvement of biological activity by low energy ultrasound assisted bioreactors. Ultrasonics 38:711-716.

Schuchardt U, Joekes I, Duarte HC. 1987. Hydrolysis of sugar cane bagasse with hydrochloric acid, promoted by ultrasound. Journal of Chemical Technology and Biotechnology 39:115-24.

Scragg AH. 1991. Bioreactors in Biotechnology: a practical approach. Chichester: Ellis Horwood, pp 63 – 86.

Sener N, KilIç Apar D, Özbek B. 2006. A modelling study on milk lactose hydrolysis and [beta]-galactosidase stability under sonication. Process Biochemistry 41:1493-1500.

Shewale SD, Pandit AB. 2009. Enzymatic production of glucose from different qualities of grain sorghum and application of ultrasound to enhance the yield. Carbohydrate Research 344:52-60.

Shuler ML, Kargi F. 1992. Bioprocess Engineering: basic concepts: Englewood Cliffs: Prentice Hall.

Sigma. 1994. Enzymatic assay of β-galactosidase. Sigma Aldrich Corporation.

Sinisterra JV. 1992. Application of ultrasound to biotechnology: an overview. Ultrasonics 30:180-185.

Sreenath HK. 1993. Hydrolysis of carboxymethyl celluloses by cellulases. Lebensmittel Wissenschaft Technologie 26:224-228.

Sulaiman AZ, Ajit A, Yunus RM, Chisti Y. 2011. Ultrasound-assisted fermentation enhances bioethanol productivity. Biochemical Engineering Journal 54:141-150

Suslick KS. 1988. Ultrasound: its chemical, physical and biological effects. New York: VCH Publishers.

Suslick KS. 1989. The chemical effects of ultrasound. Scientific American 260:80-86.

Suslick KS. 1990. Sonochemistry. Science 247:1439-1445.

Suslick KS, Nyborg WL. 1990. Ultrasound: its chemical, physical and biological effects. The Journal of the Acoustical Society of America 87:919-920.

Suslick KS, Didenko Y, Fang MM, Hyeon T, Kolbeck KJ, McNamara III WB, Mdleleni MM, Wong M. 1999. Acoustic cavitation and its chemical consequences. Philosophical Transactions: Mathematical, Physical and Engineering Sciences 357:335-353.

Suslick KS, Price GJ. 1999. Applications of ultrasound to materials chemistry. Annual Review of Materials Science 29:295-326.

Teixeira JA, Mota M, Goma G. 1990. Continuous ethanol production by a flocculating strain of *Kluyveromyces marxianus*: bioreactor performance. Bioprocess and Biosystems Engineering 5:123-127.

Thompson LH, Doraiswamy LK. 1999. Sonochemistry: science and engineering. Industrial and Engineering Chemistry Research 38:1215-1249.

Tomaska M., Stredansky M., Gemeiner P., Sturdik E. 1995. Improvement of the thermostability of β-galactosidase form *Kluyveromyces marxianus*. Process Biochemistry 30:649-652.

Trevors JT, Merrick RL, Russell I, Stewart GG. 1983. A comparison of methods for assessing yeast viability. Biotechnology Letters 5:131-134.

Tribe LA, Briens CL, Margaritis A. 1995. Determination of the volumetric mass transfer coefficient (k_La) using the dynamic"gasout-gas-in" method: analysis of errors caused by dissolved oxygen probes. Biotechnology and Bioengineering 46:388-392.

Tuulmets A, Raik P. 1999. Ultrasonic acceleration of ester hydrolyses. Ultrasonics-Sonochemistry 6:85-87.

Vallet C, Masud Z, Martin ML. 1998. Isotropic characterization of the bioconversion of lactose into ethanol. Food Chemistry 63:115-123.

van Wyk JPH. 1997. Cellulase adsorption-desorption and cellulose saccharification during enzymatic hydrolysis of cellulose materials. Biotechnology Letters 19:775-778.

Van't Riet K. 1979. Review of measuring methods and results in nonviscous gas-liquid mass transfer in stirred vessels. Industrial and Engineering Chemistry Process Design and Development 18:357-364.

Várnai A, Viikari L, Marjamaa K, Siika-aho M. 2010. Adsorption of monocomponent enzymes in enzyme mixture analysed quantitatively during hydrolysis of lignocellulose substrates. Bioresource Technology 102:1220-1227.

Wang D, Sakakibara M, Kondoh N, Suzuki K. 1996. Ultrasound-enhanced lactose hydrolysis in milk fermentation with *Lactobacillus bulgaricus*. Journal of Chemical Technology and Biotechnology 2:86-92.

Wang D, Sakakibara M. 1997. Lactose hydrolysis and β-galactosidase activity in sonicated fermentation with *Lactobacillus* strains. Ultrasonics Sonochemistry 4:255-261.

Wang NS. 2007. Experiment N0.9C: Measurements of cell biomass concentration. Maryland: University of Maryland.

Wood BE, Aldrich HC, Ingram LO. 1997. Ultrasound stimulates ethanol production during the simultaneous saccharification and fermentation of mixed waste office paper. Biotechnology Progress 13:232-237.

Wu H, Hulbert GJ, Mount JR. 2000. Effects of ultrasound on milk homogenization and fermentation with yogurt starter. Innovative Food Science and Emerging Technologies 1:211-218.

Xiao Y, Wu Q, Cai Y, Lin X. 2005. Ultrasound-accelerated enzymatic synthesis of sugar esters in nonaqueous solvents. Carbohydrate Research 340:2097-2103.

Xiao Y, Yang L, Mao P, Zhao Z, Lin X. 2010. Ultrasound-promoted enzymatic synthesis of troxerutin esters in nonaqueous solvents. Ultrasonics Sonochemistry 18:303-309.

Xie B, Liu H, Yan Y. 2009. Improvement of the activity of anaerobic sludge by low-intensity ultrasound. Journal of Environmental Management 90:260-264.

Yachmenev VG, Bertoniere NR, Blanchard EJ. 2002. Intensification of the bio-processing of cotton textiles by combined enzyme/ultrasound treatment. Journal of Chemical Technology and Biotechnology 77:559-567.

Yachmenev VG, Blanchard EJ, Lambert AH. 2004. Use of ultrasonic energy for intensification of the bio-preparation of greige cotton. Ultrasonics 42:87-91.

Yang F, Li L, Li Q, Tan W, Liu W, Xian M. 2010. Enhancement of enzymatic in situ saccharification of cellulose in aqueous-ionic liquid media by ultrasonic intensification. Carbohydrate Polymers 81:311-316.

Yang ST, Okos MR. 1989. A new graphical method for determining parameters in Michaelis–Menten type kinetics for enzymatic lactose hydrolysis. Biotechnology and Bioengineering 34:763-773.

Yeh AI, Huang YC, Chen SH. 2010. Effect of particle size on the rate of enzymatic hydrolysis of cellulose. Carbohydrate Polymers 79:192-199.

Zabaneh M, Bar R. 1991. Ultrasound-enhanced bioprocess. II: Dehydrogenation of hydrocortisone by *Arthrobacter simplex*. Biotechnology and Bioengineering 37:998-1003.

Zafar S, Owais M, Saleemuddin M, Husain S. 2005. Batch kinetics and modelling of ethanolic fermentation of whey. International Journal of Food Science and Technology 40:597-604.

APPENDIX 1

a) Kinetic parameters calculation for a batch fermentation (Doran, 1995)

The equations used in calculating the kinetic parameters of the fermentation:

i. Specific growth rate, μ

$$\mu = \frac{1}{(t_2 - t_1)} \ln\left(\frac{X_2}{X_1}\right)$$

where X_1 is the biomass concentration at t_2 (=8 h) and X_2 is the biomass concentration at time t_1 (=14 h) during exponential growth.

ii. Average specific lactose consumption rate, q_s

$$q_s = -\frac{\Delta S}{\Delta X t}$$

where ΔS is the substrate consumed by time t (= 22 h) and ΔX is the increase in biomass concentration by time *t*.

iii. Maximum biomass yield on substrate, $Y_{x/s}$

$$Y_{x/s} = -\frac{\Delta X}{\Delta S}$$

where $Y_{x/s}$ is calculated at the maximum biomass concentration X_{max}

iv. Maximum biomass productivity, P_x

$$P_{\mathrm{x}} = \frac{X_{\max} - \mathrm{X}_0}{t}$$

where P_{x} is calculated at the instance t of the maximum biomass concentration $\mathrm{X}_{\max}$ in the fermentation. X_o is the biomass concentration at the beginning of the fermentation.

v. Final ethanol yield on substrate, $\mathrm{Y}_{\mathrm{p/s}}$

$$Y_{p/s} = -\frac{\Delta P}{\Delta S}$$

where ΔP is the change in ethanol concentration during the fermentation (at final ethanol concentration).

vi. Final ethanol productivity, P_E

$$P_{\mathrm{E}} = \frac{E_f - \mathrm{E}_0}{t_f}$$

where E_0 is the initial concentration of ethanol, E_f is the final concentration of ethanol and t_f is the duration of the fermentation.

vii. Average specific ethanol production rate, q_p

$$q_p = \frac{\Delta E}{\Delta X_{\max} t}$$

where q_p is calculated at the instance *t* of the maximum biomass concentration. ΔE is the increase in ethanol concentration by time *t* during the fermentation.

b) Kinetic parameters calculation for a continuous fermentation

The equations used in calculating the kinetic parameters of the fermentation:

i. Specific growth rate, μ

$$\mu = \mathrm{D}$$

for continuous culture at steady state.

ii. Average specific lactose consumption rate, q_s

$$q_s = \frac{(S_o - S_e)}{X} D$$

where (S_o – S_e) is the substrate consumed and X is the biomass concentration at steady state at dilution rate D.

iii. Maximum biomass yield on substrate, $Y_{x/s}$

$$Y_{x/s} = \frac{X}{(S_o - S_e)}$$

where $Y_{x/s}$ is calculated at the steady state biomass concentration X.

iv. Maximum biomass productivity, P_x

$$P_{\mathrm{x}} = D.X$$

where P_{x} is calculated at the steady state biomass concentration X in the fermentation. D is the dilution rate.

v. Final ethanol yield on substrate, $Y_{p/s}$

$$Y_{p/s} = \frac{E}{(S_o - S_e)}$$

Where *E* is the steady state ethanol concentration.

vi. Final ethanol productivity, P_E

$$P_{\mathrm{E}} = D \,.\, E$$

Where *E* is the steady state ethanol concentration and *D* is the dilution rate.

vii. Average specific ethanol production rate, q_p

$$q_p = \frac{E}{X} D$$

where q_p is calculated at the steady state ethanol concentration *E*, steady state biomass concentration *X* and *D* is the dilution rate.

APPENDIX 2

The equations used in calculating the standard deviation of kinetic parameters and other derived data

(http://www.ecs.umass.edu/cee/reckhow/courses/572/572bk23/572BK23.html)

Addition or subtraction of two numbers (x_1,x_2) with significant errors (s_1, s_2)

$$(x_1 \pm s_1) + (x_2 \pm s_2) = (x_1 + x_2) \pm \sqrt{s_1^2 + s_2^2}$$

$$(x_1 \pm s_1) - (x_2 \pm s_2) = (x_1 - x_2) \pm \sqrt{s_1^2 + s_2^2}$$

Multiplication or division by a constant

$$n(x \pm s) = nx \pm ns$$

Where n is a constant

Multiplication or division of two numbers (x_1,x_2) with significant errors (s_1, s_2)

$$(x_1 \pm s_1)(x_2 \pm s_2) = (x_1 \times x_2) \pm (x_1 \times x_2)\sqrt{\left(\frac{s_1}{x_1}\right)^2 + \left(\frac{s_2}{x_2}\right)^2}$$

$$\frac{(x_1 \pm s_1)}{(x_2 \pm s_2)} = \frac{x_1}{x_2} \pm \left(\frac{x_1}{x_2}\right)\sqrt{\left(\frac{s_1}{x_1}\right)^2 + \left(\frac{s_2}{x_2}\right)^2}$$

APPENDIX 3

A3.1 A typical control fermentation profiles of *K. marxianus* at initial lactose concentration of 50 g L^{-1}, 30 °C, pH 5.0 and inoculum size of 5% by volume (Figure 4.1)

Fermentation time (h)	Average biomass concentration (g L^{-1})	Standard deviation (n=6)
0.0	0.03	0.01
2.0	0.12	0.01
4.0	0.24	0.02
6.0	0.36	0.04
8.0	0.60	0.04
10.0	1.84	0.05
12.0	4.26	0.06
14.0	6.52	0.17
16.0	8.39	0.07
18.0	8.85	0.06
20.0	9.30	0.07
22.0	9.71	0.08
24.0	9.57	0.12

Fermentation time (h)	Average lactose concentration (g L^{-1})	Standard deviation (n=6)
0.0	46.24	0.41
2.0	44.56	0.52
4.0	43.21	0.69
6.0	41.66	0.14
8.0	37.09	0.10
10.0	29.68	0.52
12.0	22.14	0.37
14.0	8.68	0.76
16.0	4.17	0.21
18.0	3.57	0.09
20.0	2.76	0.31
22.0	2.15	0.15
24.0	2.29	0.10

Fermentation time (h)	Average ethanol concentration (g L^{-1})	Standard deviation (n=6)
0.0	0.00	0.00
2.0	0.00	0.00
4.0	0.00	0.00
6.0	0.00	0.00
8.0	0.00	0.00
10.0	0.82	0.04
12.0	1.18	0.12
14.0	1.29	0.06
16.0	1.49	0.12
18.0	1.62	0.14
20.0	1.71	0.12
22.0	1.69	0.05
24.0	1.48	0.04

A3.2 Effects of sonication on: (a) biomass concentration; (b) lactose concentration; and (c) dissolved oxygen concentration. (Figure 4.2)

a) Biomass concentration (g L^{-1})

Fermentation time (h)	Control		10% duty cycle		20% duty cycle		40% duty cycle	
	Average data	Standard deviation	Average data	Standard deviation	Average data	Standard deviation	Average data	Standard deviation
0.0	0.03	0.01	0.07	0.02	0.04	0.03	0.09	0.01
2.0	0.12	0.01	0.12	0.01	0.10	0.01	0.13	0.01
4.0	0.24	0.02	0.30	0.02	0.20	0.02	0.23	0.03
6.0	0.36	0.04	0.73	0.03	0.55	0.03	0.60	0.04
8.0	0.60	0.04	1.63	0.69	1.30	0.04	0.96	0.06
10.0	1.84	0.05	3.18	0.16	2.81	0.02	1.73	0.08
12.0	4.26	0.06	5.55	0.35	5.08	0.10	2.65	0.10
14.0	6.52	0.17	7.21	0.08	7.12	0.11	3.83	0.35
16.0	8.39	0.07	10.50	0.33	9.35	0.05	4.69	0.45
18.0	8.85	0.06	12.06	0.24	11.55	0.25	5.74	0.05
20.0	9.30	0.07	13.73	0.28	13.81	0.44	7.53	0.26
22.0	9.71	0.08	13.76	0.85	13.60	0.25	8.39	0.31
24.0	9.57	0.12	13.12	0.22	13.40	0.36	7.80	0.28

b) Lactose concentration (g L^{-1})

Fermentation time (h)	Control		10% duty cycle		20% duty cycle		40% duty cycle	
	Average data	Standard deviation	Average data	Standard deviation	Average data	Standard deviation	Average data	Standard deviation
0.0	46.24	0.41	45.97	0.14	47.79	0.47	47.79	0.38
2.0	44.56	0.52	45.03	0.27	45.23	0.51	45.23	0.25
4.0	43.21	0.69	44.02	0.15	44.49	0.20	44.49	0.26
6.0	41.66	0.14	40.52	0.38	41.19	0.43	41.19	0.21
8.0	37.09	0.10	34.60	0.15	35.40	0.98	35.94	0.72
10.0	29.68	0.52	25.24	0.14	25.51	1.24	31.90	0.65
12.0	22.14	0.37	19.45	0.23	19.45	0.26	30.49	1.00
14.0	8.68	0.76	7.00	0.31	7.47	0.20	23.02	0.62
16.0	4.17	0.21	2.15	0.20	3.50	0.77	18.44	1.91
18.0	3.57	0.09	0.94	0.13	1.68	0.15	13.53	0.62
20.0	2.76	0.31	0.27	0.76	0.40	0.11	12.45	1.02
22.0	2.15	0.15	0.20	1.00	0.27	0.91	9.49	0.83
24.0	2.29	0.10	0.07	0.05	0.20	0.22	9.42	0.39

c) Dissolved oxygen level (%)

Fermentation time (h)	Control	10% duty cycle	20% duty cycle	40% duty cycle
0.0	100.8	100.0	99.1	100.1
0.2	99.1	98.7	99.0	99.9
0.4	99.5	99.4	98.9	99.9
0.6	99.4	99.3	98.9	99.8
0.8	99.3	99.2	98.8	99.7
1.0	99.3	99.2	98.8	99.5
1.2	99.2	99.1	98.9	99.5
1.4	99.1	99.0	98.9	99.4
1.6	99.1	98.9	98.9	99.4
1.8	99.0	98.9	98.9	99.3
2.0	99.0	98.8	98.8	99.2
2.2	99.0	98.7	98.9	99.1
2.4	99.0	98.5	98.9	98.9
2.6	98.9	98.5	98.8	98.9
2.8	98.9	98.3	98.7	98.7
3.0	98.8	98.1	98.7	98.6
3.2	98.8	98.0	98.6	98.6
3.4	98.6	97.7	98.5	98.5
3.6	98.6	97.6	98.4	98.3
3.8	98.4	97.4	98.4	98.1
4.0	98.4	97.4	98.3	98.0
4.2	98.3	97.2	98.2	98.0
4.4	98.1	97.0	98.0	97.8
4.6	97.9	96.8	97.9	97.6
4.8	97.8	96.6	97.6	97.5
5.0	97.6	96.3	97.4	97.3
5.2	97.4	96.0	97.3	97.1
5.4	97.2	95.9	96.9	96.9
5.6	97.0	95.8	96.6	96.7
5.8	96.7	95.5	96.4	96.4
6.0	96.3	95.3	96.1	96.1
6.2	96.0	95.2	95.8	95.9
6.4	95.6	94.8	95.3	95.5
6.6	95.1	94.5	94.9	95.0
6.8	94.5	94.2	94.5	94.7
7.0	93.7	93.8	94.0	94.3
7.2	92.9	93.5	93.3	93.6
7.4	92.1	93.0	92.7	93.1
7.6	91.0	92.6	92.0	92.4
7.8	90.0	92.0	91.2	92.1
8.0	88.6	91.5	90.3	91.2
8.2	87.4	90.7	89.3	90.2

8.4	85.9	90.1	88.4	89.5
8.6	84.6	89.3	87.3	88.6
8.8	82.9	88.5	86.8	87.3
9.0	81.4	87.6	85.7	85.8
9.2	80.4	86.4	84.5	84.6
9.4	79.7	85.3	83.5	83.1
9.6	79.3	83.7	81.9	81.3
9.8	78.4	82.3	80.7	79.7
10.0	76.6	81.0	79.6	77.6
10.2	75.2	79.2	78.7	76.6
10.4	74.6	77.8	77.9	74.8
10.6	72.7	76.2	77.7	73.0
10.8	70.8	74.8	77.6	72.3
11.0	68.3	73.9	76.8	70.8
11.2	65.2	72.9	74.9	69.4
11.4	64.6	72.0	73.9	67.1
11.6	73.1	71.1	73.2	65.0
11.8	72.8	70.0	72.3	62.3
12.0	71.0	68.7	71.8	59.6
12.2	68.3	67.4	70.9	58.3
12.4	66.6	67.0	70.0	56.8
12.6	65.1	66.2	68.2	60.9
12.8	63.5	64.3	77.1	62.3
13.0	63.0	62.8	81.2	61.1
13.2	61.9	60.4	80.1	58.5
13.4	58.6	58.1	78.3	54.2
13.6	55.3	54.6	76.6	49.5
13.8	51.3	51.9	75.2	45.4
14.0	50.4	48.7	74.0	42.0
14.2	53.3	45.6	71.9	40.9
14.4	35.3	43.5	69.9	42.8
14.6	39.7	41.6	67.8	42.0
14.8	35.2	41.5	66.8	40.9
15.0	32.2	45.3	64.6	43.0
15.2	32.5	47.2	63.1	51.0
15.4	34.0	43.5	58.5	55.9
15.6	45.9	40.0	55.5	59.2
15.8	21.0	36.6	49.3	62.3
16.0	14.1	36.0	45.3	64.4
16.2	13.7	32.0	43.6	66.8
16.4	13.6	30.8	40.1	69.6
16.6	14.0	29.1	36.6	73.0
16.8	13.3	27.2	36.5	74.6
17.0	32.6	26.1	33.3	77.6
17.2	23.2	24.2	29.9	80.2
17.4	21.1	21.9	28.1	81.8
17.6	23.9	20.7	28.5	83.8
17.8	25.6	18.8	26.6	85.7

18.0	33.1	19.6	27.6	87.1
18.2	34.0	18.4	26.9	88.3
18.4	35.2	18.3	28.5	89.3
18.6	34.9	19.6	29.2	90.2
18.8	36.6	21.9	30.3	90.8
19.0	38.6	21.6	33.4	91.3
19.2	55.3	23.9	35.8	91.6
19.4	43.3	25.4	39.1	92.0
19.6	41.8	28.7	40.3	92.1
19.8	46.3	31.5	44.1	92.3
20.0	49.4	35.4	47.7	92.5
20.2	53.3	38.0	49.7	92.6
20.4	56.5	42.2	52.7	92.6
20.6	60.5	46.5	54.2	98.6
20.8	63.6	49.8	56.9	96.0
21.0	67.3	54.4	58.8	96.2
21.2	71.2	57.3	60.4	96.3
21.4	74.9	60.9	62.9	96.3
21.6	78.2	63.1	64.3	96.4
21.8	80.8	65.3	65.3	96.6
22.0	83.4	67.6	66.9	96.7
22.2	84.9	69.6	68.1	96.8
22.4	86.2	71.3	69.5	96.8
22.6	87.5	73.3	71.6	97.1
22.8	88.5	74.9	73.4	97.1
23.0	89.2	76.4	75.3	97.2
23.2	89.5	78.1	77.6	97.3
23.4	89.8	79.1	79.9	97.3
23.6	90.3	80.1	81.5	97.4
23.8	91.2	80.3	83.2	97.4
24.0	91.7	80.8	84.4	97.7

A3.3 Ethanol concentration profiles (g L^{-1}) (Figure 4.3)

Fermentation time (h)	Control		10% duty cycle		20% duty cycle		40% duty cycle	
	Average data	Standard deviation	Average data	Standard deviation	Average data	Standard deviation	Average data	Standard deviation
0.0	0.00	0.00	0.00	0.00	0.00	0.00	0.00	0.00
2.0	0.00	0.00	0.00	0.00	0.00	0.00	0.00	0.00
4.0	0.00	0.00	0.00	0.00	0.00	0.00	0.00	0.00
6.0	0.00	0.00	0.04	0.00	0.05	0.01	0.05	0.01
8.0	0.00	0.00	0.08	0.00	0.10	0.01	0.53	0.03
10.0	0.82	0.04	2.31	0.37	2.11	0.18	1.27	0.12
12.0	1.18	0.12	3.99	0.13	3.98	0.45	1.62	0.14
14.0	1.29	0.06	4.15	0.10	4.75	0.35	1.82	0.15
16.0	1.49	0.12	4.25	0.14	4.94	0.06	1.85	0.14
18.0	1.62	0.14	4.44	0.30	5.18	0.38	1.94	0.25
20.0	1.71	0.12	4.65	0.41	5.34	0.52	2.12	0.22
22.0	1.69	0.05	4.65	0.45	5.25	0.34	2.11	0.20
24.0	1.48	0.04	4.42	0.40	5.20	0.68	2.00	0.09

A3.4 Cell viability profiles (%) (Figure 4.6)

Fermentation time (h)	Control		10% duty cycle		20% duty cycle		40% duty cycle	
	Average data	Standard deviation	Average data	Standard deviation	Average data	Standard deviation	Average data	Standard deviation
0.0	92.31	0.47	90.91	0.57	91.67	0.47	92.31	0.53
2.0	93.33	0.38	92.31	0.26	94.12	0.64	93.75	0.61
4.0	93.75	0.44	92.86	0.38	93.33	0.39	93.10	1.64
6.0	94.12	0.25	93.75	0.36	92.86	0.64	92.86	0.73
8.0	93.85	0.55	92.19	0.65	94.20	0.58	90.36	0.78
10.0	93.65	0.63	86.49	0.58	84.21	1.37	82.00	0.61
12.0	87.88	0.80	84.15	0.71	82.14	1.34	80.91	0.37
14.0	87.69	0.68	83.33	0.65	79.79	1.62	77.24	0.75
16.0	86.15	0.72	81.05	0.47	77.88	1.07	73.28	1.29
18.0	84.62	1.25	76.53	1.02	73.83	1.75	70.00	0.75
20.0	81.54	1.32	74.47	1.09	72.82	1.52	69.39	0.59
22.0	78.13	0.73	73.91	0.88	70.30	1.94	67.09	0.92
24.0	75.00	0.80	71.08	0.57	69.70	0.65	66.27	0.99

A3.5 β-Galactosidase activity profiles during fermentation (Figure 4.8)

a) Extracellular enzyme activity (Unit mL^{-1})

Fermentation time (h)	Control		10% duty cycle		20% duty cycle		40% duty cycle	
	Average data	Standard deviation	Average data	Standard deviation	Average data	Standard deviation	Average data	Standard deviation
0.0	0.40	0.19	0.00	0.00	0.00	0.00	0.00	0.00
2.0	1.20	0.27	1.60	0.19	2.00	0.20	1.60	0.27
4.0	2.00	0.30	2.80	0.27	2.40	0.27	2.80	0.20
6.0	6.00	0.50	6.80	0.20	7.20	0.27	6.80	0.40
8.0	7.60	0.38	8.00	0.27	7.60	0.33	7.20	0.44
10.0	9.20	0.36	8.40	0.20	8.40	0.27	6.80	0.27
12.0	7.20	0.33	9.60	0.19	8.80	0.40	6.00	0.30
14.0	6.80	0.20	10.00	0.23	9.20	0.33	5.60	0.33
16.0	6.40	0.27	10.40	0.23	9.60	0.82	4.80	0.54
18.0	6.00	0.19	10.80	0.20	10.40	0.50	4.00	0.38
20.0	6.00	0.30	10.00	0.19	9.20	0.33	3.20	0.38
22.0	5.60	0.30	9.60	0.31	9.60	0.20	2.80	0.40
24.0	5.20	0.19	9.20	0.27	10.00	0.30	1.60	0.19

b) Intracellular enzyme activity (Unit mL^{-1})

Fermentation time (h)	Control		10% duty cycle		20% duty cycle		40% duty cycle	
	Average data	Standard deviation	Average data	Standard deviation	Average data	Standard deviation	Average data	Standard deviation
0.0	0.00	0.00	0.00	0.00	0.00	0.00	0.00	0.00
2.0	0.40	0.19	1.20	0.19	1.60	0.20	1.60	0.20
4.0	7.20	0.20	8.80	0.20	10.00	0.27	10.00	0.19
6.0	16.80	0.27	18.40	0.30	18.80	0.44	18.80	0.72
8.0	22.80	0.50	23.60	0.33	23.20	0.54	23.20	0.33
10.0	23.60	0.63	24.40	0.30	23.60	0.36	22.40	0.33
12.0	24.00	0.38	27.60	0.20	27.60	0.30	21.60	0.44
14.0	24.40	0.19	28.40	0.20	27.20	0.54	20.80	0.46
16.0	24.80	0.33	29.20	0.20	28.40	0.43	20.40	0.38
18.0	24.40	0.50	26.00	0.23	27.20	1.10	20.00	0.65
20.0	23.20	0.27	25.20	0.27	26.40	0.71	19.20	0.44
22.0	22.40	0.68	24.40	0.23	23.60	0.54	18.80	0.33
24.0	21.60	0.50	23.20	0.20	23.20	0.50	18.80	0.20

A3.6 Biomass specific β-galactosidase activity profiles during fermentation (Figure 4.9)

a) Extracellular enzyme activity (Unit g^{-1})

Fermentation time (h)	Control		10% duty cycle		20% duty cycle		40% duty cycle	
	Average data	Standard deviation	Average data	Standard deviation	Average data	Standard deviation	Average data	Standard deviation
0.0	0.00	0.00	0.00	0.00	0.00	0.00	0.00	0.00
2.0	10425.72	2.70	13900.96	2.09	19860.97	2.39	12355.21	2.40
4.0	8176.61	1.37	9265.39	1.02	11916.58	1.64	12163.34	1.79
6.0	16680.57	2.26	9266.83	0.49	13167.52	0.87	11252.69	0.98
8.0	12576.53	0.99	4920.35	2.09	5868.73	0.32	7468.88	0.64
10.0	4995.38	0.23	2641.59	0.15	2993.80	0.10	3938.38	0.24
12.0	1690.54	0.08	1728.48	0.12	1732.59	0.09	2266.29	0.14
14.0	1043.26	0.04	1387.23	0.04	1291.72	0.05	1463.17	0.16
16.0	762.95	0.03	990.14	0.04	1026.46	0.09	1023.32	0.15
18.0	678.05	0.02	895.70	0.02	900.12	0.05	696.74	0.07
20.0	645.51	0.03	728.51	0.02	666.04	0.03	425.24	0.05
22.0	576.59	0.03	697.91	0.05	706.03	0.02	333.79	0.05
24.0	543.46	0.02	701.10	0.02	746.51	0.03	205.17	0.03

b) Intracellular enzyme activity (Unit g^{-1})

Fermentation time (h)	Control		10% duty cycle		20% duty cycle		40% duty cycle	
	Average data	Standard deviation	Average data	Standard deviation	Average data	Standard deviation	Average data	Standard deviation
0.0	0.00	0.00	0.00	0.00	0.00	0.00	0.00	0.00
2.0	3475.24	1.69	10425.72	1.90	15888.78	2.26	12355.21	1.91
4.0	29435.81	2.38	29119.79	1.62	49652.43	4.03	43440.49	5.65
6.0	46705.59	5.04	25074.95	1.16	34381.86	2.03	31110.38	2.32
8.0	37729.60	2.43	14515.04	6.14	17915.06	0.74	24066.39	1.49
10.0	12814.25	0.48	7673.20	0.40	8411.15	0.14	12973.47	0.61
12.0	5635.13	0.12	4969.39	0.32	5434.03	0.13	8158.64	0.34
14.0	3743.48	0.10	3939.74	0.05	3818.99	0.09	5434.64	0.51
16.0	2956.43	0.05	2780.00	0.09	3036.62	0.05	4349.12	0.42
18.0	2757.40	0.06	2156.32	0.05	2354.16	0.11	3483.71	0.12
20.0	2495.97	0.03	1835.85	0.04	1911.26	0.08	2551.43	0.10
22.0	2306.38	0.07	1773.85	0.11	1735.66	0.05	2241.16	0.09
24.0	2257.45	0.06	1767.98	0.03	1731.90	0.06	2410.69	0.09

A3.7 The continuous fermentation profiles (a) biomass and lactose; and (b) ethanol production with and without ultrasound (Figure 4.10)

a.1) Biomass concentration (g L^{-1}) at dilution rate of 0.05 h^{-1} for control (no sonication) and with sonication at 20% duty cycle (intensity at 11.8 W cm^{-2})

Fermentation time (h)	Average data	Standard deviation	Dilution rate (h^{-1})
0.0	0.03	0.01	Batch fermentation
2.0	0.12	0.01	
4.0	0.24	0.02	
6.0	0.36	0.04	
8.0	0.60	0.04	
10.0	1.84	0.05	
12.0	4.26	0.06	
14.0	6.52	0.17	
16.0	8.39	0.07	
20.0	10.76	0.15	D = 0.05 (no sonication)
25.0	12.91	0.22	
30.0	12.32	0.22	
35.0	12.32	0.09	
40.0	11.08	0.32	
45.0	10.62	0.20	
50.0	10.50	0.35	
55.0	10.50	0.27	
60.0	10.59	0.12	
65.0	10.52	0.13	
70.0	12.56	0.10	D=0.05 (sonication at 20% duty cycle)
75.0	12.55	0.56	
80.0	12.49	0.17	
85.0	12.49	0.32	
90.0	12.98	0.10	
95.0	13.14	0.17	
100.0	14.72	0.25	
105.0	14.79	0.09	
110.0	14.81	0.22	
115.0	14.78	0.53	
120.0	14.79	0.21	
125.0	9.57	0.19	D=0.05 (no sonication)
130.0	8.68	0.17	
135.0	9.21	0.11	
140.0	9.70	0.35	
145.0	10.17	0.39	
150.0	9.87	0.65	

155.0	10.55	0.15	
160.0	10.53	0.11	
165.0	10.53	0.06	
170.0	10.55	0.01	

a.2) Biomass concentration (g L^{-1}) at dilution rate of 0.075 h^{-1} for control (no sonication) and with sonication at 20% duty cycle (intensity at 11.8 W cm^{-2})

Fermentation time (h)	Average data	Standard deviation	Dilution rate (h^{-1})
175.0	10.82	0.00	D=0.075 (no sonication)
180.0	13.76	0.25	
185.0	12.62	0.11	
190.0	10.99	0.40	
195.0	9.09	0.59	
200.0	10.14	0.18	
205.0	9.73	0.27	
210.0	8.73	0.13	
215.0	8.75	0.04	
220.0	9.88	0.32	
225.0	9.99	0.08	
230.0	9.97	0.11	
235.0	9.95	0.37	
240.0	15.01	0.26	D=0.075 (sonication at 20% duty cycle)
245.0	15.21	0.27	
250.0	15.18	0.23	
255.0	15.28	0.09	
260.0	14.96	0.05	
265.0	14.68	0.25	
270.0	15.06	0.32	
275.0	14.75	0.41	
280.0	15.24	0.27	
285.0	12.72	0.24	
290.0	11.93	0.19	
295.0	14.83	0.01	
300.0	15.19	0.31	
305.0	13.17	1.02	
310.0	13.18	1.16	
315.0	13.17	1.30	
320.0	13.15	1.30	
325.0	10.82	0.00	D=0.075 (no sonication)
330.0	13.76	0.25	
335.0	12.62	0.11	
340.0	10.99	0.40	

345.0	9.09	0.59	
350.0	10.14	0.18	
355.0	9.73	0.27	
360.0	8.73	0.13	
365.0	8.75	0.04	
370.0	9.88	0.32	
375.0	9.99	0.08	
380.0	9.97	0.11	
385.0	9.95	0.37	

a.3) Biomass concentration (g L^{-1}) at dilution rate of 0.1 h^{-1} for control (no sonication) and with sonication at 20% duty cycle (intensity at 11.8 W cm^{-2})

Fermentation time (h)	Average data	Standard deviation	Dilution rate (h^{-1})
390.0	8.89	0.38	D=0.1 (no sonication)
395.0	8.26	0.30	
400.0	8.72	0.27	
405.0	9.02	0.05	
410.0	9.70	0.04	
415.0	9.86	0.14	
420.0	9.90	0.15	
425.0	8.14	0.11	
430.0	8.87	0.56	
435.0	8.88	0.42	
440.0	8.77	0.50	
445.0	8.88	0.66	
450.0	12.78	0.24	D=0.1 (sonication at 20% duty cycle)
455.0	14.46	0.22	
460.0	14.53	0.20	
465.0	16.49	0.09	
470.0	16.56	0.37	
475.0	16.29	0.41	
480.0	15.21	0.04	
485.0	16.03	0.26	
490.0	11.24	0.10	
495.0	11.25	0.08	
500.0	11.27	0.03	
505.0	11.25	0.12	
510.0	8.89	0.38	D=0.1 (no sonication)
515.0	8.26	0.30	
520.0	8.72	0.27	
525.0	9.02	0.05	
530.0	9.70	0.04	

535.0	9.86	0.14	
540.0	9.90	0.15	
545.0	8.14	0.11	
550.0	8.87	0.56	
555.0	8.88	0.42	
560.0	8.77	0.50	
565.0	8.88	0.66	

a.4) Biomass concentration (g L^{-1}) at dilution rate of 0.15 h^{-1} for control (no sonication) and with sonication at 20% duty cycle (intensity at 11.8 W cm^{-2})

Fermentation time (h)	Average data	Standard deviation	Dilution rate (h^{-1})
570.0	6.55	0.10	D=0.15 (no sonication)
575.0	7.11	0.21	
580.0	7.53	0.12	
585.0	9.57	0.21	
590.0	8.01	0.16	
595.0	7.34	0.19	
600.0	8.37	0.35	
605.0	7.42	0.33	
610.0	7.61	0.54	
615.0	7.34	0.01	
620.0	7.50	0.24	
625.0	7.73	0.14	
630.0	6.96	0.29	
635.0	6.50	0.18	
640.0	8.20	0.37	
645.0	7.63	0.12	
650.0	6.22	0.09	
655.0	7.05	0.30	
660.0	8.43	0.50	
665.0	7.09	0.25	
670.0	6.94	0.47	
675.0	7.53	0.12	
680.0	7.64	0.02	
685.0	7.60	0.03	
690.0	7.60	0.17	
695.0	8.50	0.26	D=0.15 (sonication at 20% duty cycle)
700.0	8.60	0.09	
705.0	8.09	0.21	
710.0	7.99	0.36	
715.0	8.45	0.12	
720.0	8.43	0.33	

725.0	8.58	0.07	
730.0	8.17	0.87	
735.0	8.52	0.21	
740.0	7.96	0.57	
745.0	7.44	0.29	
750.0	7.74	0.20	
755.0	9.84	0.10	
760.0	8.68	0.16	
765.0	8.62	0.27	
770.0	8.24	0.20	
775.0	8.78	0.42	
780.0	8.12	0.21	
785.0	7.61	0.05	
790.0	8.40	0.46	
795.0	8.37	0.07	
800.0	8.37	0.24	
805.0	8.40	0.21	
810.0	7.93	0.42	D=0.15 (no sonication)
815.0	8.46	0.44	
820.0	8.55	0.04	
825.0	8.26	0.44	
830.0	8.73	0.18	
835.0	8.89	0.07	
840.0	8.92	0.28	
845.0	8.01	0.18	
850.0	7.97	0.19	
855.0	8.06	0.30	
860.0	7.80	0.33	
865.0	7.63	0.19	
870.0	7.83	0.21	
875.0	7.88	0.30	
880.0	8.04	0.23	
885.0	8.10	0.32	
890.0	8.16	0.15	
895.0	7.77	0.21	
900.0	7.78	0.17	
905.0	7.71	0.29	
910.0	7.84	0.34	
915.0	7.88	0.19	
920.0	10.43	0.18	D=0.15 (sonication at 20% duty cycle)
925.0	9.78	0.20	
930.0	9.27	0.26	
935.0	10.19	0.22	
940.0	10.30	0.10	
945.0	10.29	0.27	
950.0	10.22	0.16	
955.0	10.83	0.33	
960.0	10.20	0.46	

965.0	8.91	0.50	
970.0	9.05	0.10	
975.0	9.86	0.08	
980.0	9.97	0.21	
985.0	9.81	0.20	
990.0	9.65	0.31	
995.0	9.54	0.23	
1000.0	9.34	0.47	
1005.0	9.63	0.16	
1010.0	9.81	0.28	
1015.0	9.90	0.26	
1020.0	9.78	0.14	
1025.0	9.81	0.19	
1030.0	9.58	0.10	D=0.15 (no sonication)
1035.0	9.57	0.23	
1040.0	9.93	0.15	
1045.0	10.68	0.06	
1050.0	8.53	0.21	
1055.0	8.60	0.11	
1060.0	10.19	0.20	
1065.0	8.99	0.13	
1070.0	8.89	0.23	
1075.0	8.71	0.14	
1080.0	8.68	0.14	
1085.0	8.37	0.11	
1090.0	8.13	0.08	
1095.0	8.59	0.12	
1100.0	8.39	0.32	
1105.0	8.58	0.09	
1110.0	8.43	0.11	
1115.0	8.29	0.07	
1120.0	8.16	0.20	
1125.0	7.64	0.07	
1130.0	7.67	0.26	
1135.0	7.80	0.26	
1140.0	7.76	0.13	
1145.0	6.60	0.13	D=0.15 (sonication at 20% duty cycle)
1150.0	7.65	0.13	
1155.0	8.79	0.13	
1160.0	9.58	0.14	
1165.0	9.68	0.19	
1170.0	9.70	0.25	
1175.0	9.30	0.23	
1180.0	9.58	0.14	
1185.0	9.34	0.27	
1190.0	9.34	0.28	
1195.0	9.45	0.15	
1200.0	9.83	0.12	

1205.0	10.04	0.38	
1210.0	9.86	0.31	
1215.0	9.84	0.20	
1220.0	9.84	0.16	
1225.0	9.86	0.10	
1230.0	9.86	0.34	
1235.0	8.63	0.18	D=0.15 (no sonication)
1240.0	8.79	0.16	
1245.0	9.02	0.05	
1250.0	9.17	0.03	
1255.0	8.24	0.24	
1260.0	7.27	0.16	
1265.0	7.68	0.14	
1270.0	7.40	0.04	
1275.0	7.90	0.06	
1280.0	7.93	0.23	
1285.0	7.99	0.13	
1290.0	7.65	0.08	
1295.0	7.41	0.13	
1300.0	7.37	0.14	
1305.0	7.70	0.20	
1310.0	7.80	0.26	
1315.0	8.09	0.35	
1320.0	8.59	0.05	
1325.0	8.96	0.08	
1330.0	7.68	0.14	
1335.0	7.73	0.13	
1340.0	7.73	0.11	
1345.0	7.73	0.10	

a.5) Biomass concentration (g L^{-1}) at dilution rate of 0.2 h^{-1} for control (no sonication) and with sonication at 20% duty cycle (intensity at 11.8 W cm^{-2})

Fermentation time (h)	Average data	Standard deviation	Dilution rate (h^{-1})
1350.0	5.40	0.09	D=0.2 (no sonication)
1355.0	4.88	0.11	
1360.0	5.32	0.05	
1365.0	4.78	0.12	
1370.0	5.80	0.05	
1375.0	5.97	0.10	
1380.0	5.65	0.18	
1385.0	5.17	0.11	
1390.0	5.87	0.18	

1395.0	5.71	0.06	
1400.0	5.51	0.14	
1405.0	5.61	0.09	
1410.0	5.67	0.14	
1415.0	6.17	0.15	
1420.0	5.80	0.22	
1425.0	5.97	0.41	
1430.0	5.90	0.23	
1435.0	6.14	0.07	
1440.0	6.16	0.15	
1445.0	6.16	0.04	
1450.0	6.16	0.08	
1455.0	6.16	0.07	
1460.0	6.50	0.11	D=0.2 (sonication at 20% duty cycle)
1465.0	5.88	0.11	
1470.0	5.34	0.19	
1475.0	4.45	0.03	
1480.0	4.65	0.10	
1485.0	5.24	0.14	
1490.0	5.65	0.10	
1495.0	5.48	0.43	
1500.0	5.54	0.29	
1505.0	5.99	0.24	
1510.0	4.60	0.10	
1515.0	5.94	0.48	
1520.0	4.94	0.16	
1525.0	6.27	0.30	
1530.0	7.01	0.41	
1535.0	6.06	0.48	
1540.0	6.23	0.11	
1545.0	7.01	0.47	
1550.0	7.01	0.21	
1555.0	7.01	0.37	
1560.0	7.01	0.52	

b.1) Lactose concentration (g L^{-1}) at dilution rate of 0.05 h^{-1} for control (no sonication) and with sonication at 20% duty cycle (intensity at 11.8 W cm^{-2})

Fermentation time (h)	Average data	Standard deviation	Dilution rate (h^{-1})
0.0	46.24	0.41	Batch fermentation
2.0	44.56	0.52	
4.0	43.21	0.69	
6.0	41.66	0.14	

8.0	37.09	0.10	
10.0	29.68	0.52	
12.0	22.14	0.37	
14.0	8.68	0.76	
16.0	4.17	0.21	
20.0	8.88	0.56	D=0.05 (no sonication)
25.0	7.13	0.22	
30.0	6.80	0.38	
35.0	6.39	0.44	
40.0	3.97	0.15	
45.0	2.63	0.06	
50.0	1.08	0.06	
55.0	1.01	0.07	
60.0	1.08	0.08	
65.0	1.08	0.08	
70.0	7.61	0.00	D=0.05 (sonication at 20% duty cycle)
75.0	7.67	0.00	
80.0	8.41	0.00	
85.0	7.88	0.00	
90.0	7.61	0.00	
95.0	7.27	0.00	
100.0	7.13	0.00	
105.0	0.54	0.00	
110.0	0.47	0.00	
115.0	0.54	0.00	
120.0	0.54	0.00	
125.0	10.70	0.00	D=0.05 (no sonication)
130.0	11.31	0.00	
135.0	8.21	0.00	
140.0	7.81	0.00	
145.0	7.13	0.00	
150.0	6.19	0.01	
155.0	1.08	0.00	
160.0	1.01	0.00	
165.0	1.08	0.00	
170.0	1.01	0.00	

b.2) Lactose concentration (g L^{-1}) at dilution rate of 0.075 h^{-1} for control (no sonication) and with sonication at 20% duty cycle (intensity at 11.8 W cm^{-2})

Fermentation time (h)	Average data	Standard deviation	Dilution rate (h^{-1})
175.0	0.20	0.08	D=0.075 (no sonication)
180.0	0.15	0.09	
185.0	0.60	0.13	
190.0	1.29	0.29	
195.0	0.23	0.20	
200.0	0.57	0.21	
205.0	1.69	0.52	
210.0	1.20	0.10	
215.0	1.74	0.21	
220.0	2.45	0.53	
225.0	2.41	0.36	
230.0	2.42	0.21	
235.0	2.45	0.58	
240.0	9.76	0.01	D=0.075 (sonication at 20% duty cycle)
245.0	9.22	0.00	
250.0	8.95	0.01	
255.0	7.20	0.00	
260.0	9.15	0.01	
265.0	7.54	0.00	
270.0	6.33	0.00	
275.0	6.39	0.01	
280.0	7.13	0.00	
285.0	12.59	0.00	
290.0	8.62	0.00	
295.0	7.47	0.00	
300.0	9.22	0.01	
305.0	1.01	0.01	
310.0	1.08	0.00	
315.0	1.01	0.00	
320.0	1.08	0.00	
325.0	0.20	0.08	D=0.075 (no sonication)
330.0	0.15	0.09	
335.0	0.60	0.13	
340.0	1.29	0.29	
345.0	0.23	0.20	
350.0	0.57	0.21	
355.0	1.69	0.52	
360.0	1.20	0.10	
365.0	1.74	0.21	
370.0	2.45	0.53	
375.0	2.41	0.36	

380.0	2.42	0.21	
385.0	2.45	0.58	

b.3) Lactose concentration (g L^{-1}) at dilution rate of 0.1 h^{-1} for control (no sonication) and with sonication at 20% duty cycle (intensity at 11.8 W cm^{-2})

Fermentation time (h)	Average data	Standard deviation	Dilution rate (h^{-1})
390.0	2.68	0.44	D=0.1 (no sonication)
395.0	1.68	1.11	
400.0	4.83	0.75	
405.0	1.30	0.72	
410.0	1.47	0.93	
415.0	2.81	0.47	
420.0	1.07	0.57	
425.0	2.73	0.58	
430.0	3.82	0.57	
435.0	3.83	0.25	
440.0	3.84	0.61	
445.0	3.89	0.91	
450.0	10.03	0.00	D=0.1 (sonication at 20% duty cycle)
455.0	10.16	0.00	
460.0	10.23	0.00	
465.0	8.48	0.00	
470.0	8.01	0.00	
475.0	6.73	0.00	
480.0	8.01	0.00	
485.0	6.93	0.00	
490.0	2.36	0.86	
495.0	2.22	0.75	
500.0	2.29	0.81	
505.0	2.22	0.82	
510.0	2.68	0.44	D=0.1 (no sonication)
515.0	1.68	1.11	
520.0	4.83	0.75	
525.0	1.30	0.72	
530.0	1.47	0.93	
535.0	2.81	0.47	
540.0	1.07	0.57	
545.0	2.73	0.58	
550.0	3.82	0.57	
555.0	3.83	0.25	
560.0	3.84	0.61	
565.0	3.89	0.91	

b.4) Lactose concentration (g L^{-1}) at dilution rate of 0.15 h^{-1} for control (no sonication) and with sonication at 20% duty cycle (intensity at 11.8 W cm^{-2})

Fermentation time (h)	Average data	Standard deviation	Dilution rate (h^{-1})
570.0	6.54	0.89	D=0.15 (no sonication)
575.0	7.26	0.99	
580.0	9.24	0.83	
585.0	9.49	0.73	
590.0	12.38	0.90	
595.0	12.65	0.52	
600.0	12.32	0.37	
605.0	12.18	0.96	
610.0	12.38	0.52	
615.0	12.86	0.30	
620.0	12.92	1.34	
625.0	13.46	0.54	
630.0	15.68	1.85	
635.0	12.65	0.94	
640.0	13.33	0.44	
645.0	9.76	0.68	
650.0	15.68	0.70	
655.0	14.07	0.86	
660.0	15.01	0.41	
665.0	14.61	0.37	
670.0	14.27	0.21	
675.0	10.34	0.46	
680.0	10.34	0.57	
685.0	10.27	0.74	
690.0	10.34	0.31	
695.0	13.66	0.52	D=0.15 (sonication at 20% duty cycle)
700.0	12.47	0.19	
705.0	11.11	0.96	
710.0	11.69	0.27	
715.0	12.70	0.49	
720.0	11.82	0.88	
725.0	10.91	0.77	
730.0	10.41	0.70	
735.0	11.63	0.82	
740.0	10.29	0.80	
745.0	10.75	0.86	
750.0	11.15	1.00	
755.0	12.84	0.40	
760.0	10.34	1.33	

765.0	9.41	0.79	
770.0	10.88	1.34	
775.0	10.14	0.94	
780.0	9.81	0.44	
785.0	9.63	1.15	
790.0	8.88	0.22	
795.0	8.82	0.63	
800.0	8.68	0.46	
805.0	8.55	1.03	
810.0	10.43	1.03	D=0.15 (no sonication)
815.0	10.30	0.55	
820.0	10.97	0.43	
825.0	11.04	1.54	
830.0	11.91	0.52	
835.0	15.21	0.93	
840.0	14.88	0.60	
845.0	13.87	1.32	
850.0	14.74	0.25	
855.0	13.87	0.50	
860.0	12.72	0.35	
865.0	11.64	0.44	
870.0	15.21	0.70	
875.0	14.94	0.14	
880.0	14.67	1.15	
885.0	14.81	0.95	
890.0	14.61	0.43	
895.0	14.47	0.17	
900.0	10.70	0.11	
905.0	10.63	0.22	
910.0	10.70	0.91	
915.0	10.70	0.08	
920.0	12.72	0.72	D=0.15 (sonication at 20% duty cycle)
925.0	12.18	1.03	
930.0	12.32	1.43	
935.0	13.66	1.36	
940.0	14.40	1.32	
945.0	14.13	0.81	
950.0	15.21	1.44	
955.0	8.68	0.11	
960.0	9.83	0.33	
965.0	9.69	0.27	
970.0	9.09	0.08	
975.0	9.22	0.37	
980.0	9.22	0.68	
985.0	10.03	0.23	
990.0	9.49	0.32	
995.0	10.43	0.83	
1000.0	9.83	0.22	

1005.0	8.41	0.66	
1010.0	8.62	0.52	
1015.0	8.68	0.28	
1020.0	8.75	0.82	
1025.0	8.62	0.22	
1030.0	9.96	0.47	
1035.0	10.23	0.88	
1040.0	11.17	0.73	
1045.0	11.71	0.41	
1050.0	12.05	0.70	
1055.0	14.61	1.22	
1060.0	14.20	1.23	
1065.0	14.27	0.71	
1070.0	14.07	0.10	
1075.0	14.27	0.41	
1080.0	15.08	0.81	D=0.15
1085.0	14.34	0.98	(no sonication)
1090.0	13.13	0.29	
1095.0	13.60	0.42	
1100.0	12.72	0.30	
1105.0	12.05	0.63	
1110.0	11.31	0.30	
1115.0	10.90	0.33	
1120.0	10.37	0.88	
1125.0	10.63	0.47	
1130.0	10.57	0.41	
1135.0	10.63	0.08	
1140.0	10.63	0.35	
1145.0	13.73	1.00	
1150.0	14.54	1.51	
1155.0	13.33	0.69	
1160.0	13.46	0.95	
1165.0	13.33	0.41	
1170.0	14.81	1.26	
1175.0	13.73	0.70	
1180.0	13.06	1.13	D=0.15
1185.0	12.25	1.28	(sonication at 20%
1190.0	11.64	0.67	duty cycle)
1195.0	10.90	0.54	
1200.0	10.57	0.58	
1205.0	9.69	0.25	
1210.0	8.88	0.28	
1215.0	8.62	2.58	
1220.0	8.68	0.33	
1225.0	8.68	0.21	
1230.0	8.62	0.35	
1235.0	8.28	0.39	
1240.0	8.28	0.67	

1245.0	12.72	0.20	D=0.15
1250.0	12.38	0.28	(no sonication)
1255.0	12.65	0.69	
1260.0	14.88	0.61	
1265.0	14.61	0.08	
1270.0	12.86	0.53	
1275.0	13.87	0.45	
1280.0	13.53	0.73	
1285.0	14.40	0.35	
1290.0	14.67	0.26	
1295.0	14.54	0.93	
1300.0	13.33	1.05	
1305.0	12.72	0.41	
1310.0	11.78	0.35	
1315.0	12.25	0.26	
1320.0	11.04	0.32	
1325.0	10.90	0.30	
1330.0	10.63	0.16	
1335.0	10.70	0.39	
1340.0	10.63	0.25	
1345.0	10.63	0.56	

b.5) Lactose concentration (g L^{-1}) at dilution rate of 0.2 h^{-1} for control (no sonication) and with sonication at 20% duty cycle (intensity at 11.8 W cm^{-2})

Fermentation time (h)	Average data	Standard deviation	Dilution rate (h^{-1})
1350.0	19.25	0.01	
1355.0	20.19	0.02	
1360.0	18.51	0.01	
1365.0	20.46	0.03	
1370.0	17.03	0.01	
1375.0	17.37	0.01	
1380.0	17.37	0.00	
1385.0	18.98	0.03	D=0.2
1390.0	18.51	0.05	(no sonication)
1395.0	22.48	0.02	
1400.0	23.36	0.01	
1405.0	22.14	0.01	
1410.0	22.62	0.03	
1415.0	22.41	0.02	
1420.0	20.80	0.09	
1425.0	21.07	0.01	
1430.0	19.05	0.05	

1435.0	17.30	0.05	
1440.0	16.83	0.02	
1445.0	16.89	0.01	
1450.0	16.83	0.01	
1455.0	16.89	0.01	
1460.0	28.94	0.02	D=0.2 (sonication at 20% duty cycle)
1465.0	24.57	0.01	
1470.0	24.23	0.01	
1475.0	30.56	0.09	
1480.0	34.53	0.05	
1485.0	24.57	0.01	
1490.0	27.13	0.01	
1495.0	26.18	0.01	
1500.0	24.57	0.00	
1505.0	29.21	0.03	
1510.0	25.31	0.01	
1515.0	27.87	0.03	
1520.0	34.06	0.07	
1525.0	21.07	0.03	
1530.0	21.61	0.01	
1535.0	28.34	0.01	
1540.0	22.48	0.01	
1545.0	15.14	0.02	
1550.0	15.08	0.02	
1555.0	15.14	0.03	
1560.0	15.14	0.03	

c.1) Ethanol concentration (g L^{-1}) at dilution rate of 0.05 h^{-1} for control (no sonication) and with sonication at 20% duty cycle (intensity at 11.8 W cm^{-2})

Fermentation time (h)	Average data	Standard deviation	Dilution rate (h^{-1})
0.0	0.00	0.00	Batch fermentation
2.0	0.00	0.00	
4.0	0.00	0.00	
6.0	0.00	0.00	
8.0	0.00	0.00	
10.0	0.82	0.04	
12.0	1.18	0.12	
14.0	1.19	0.05	
16.0	1.29	0.09	
20.0	4.44	0.09	D=0.05 (no sonication)
25.0	2.40	0.05	
30.0	0.62	0.04	

35.0	0.44	0.04	
40.0	1.48	0.18	
45.0	1.90	0.36	
50.0	3.45	0.05	
55.0	3.41	0.06	
60.0	3.41	0.45	
65.0	3.45	0.55	
70.0	3.33	0.01	D=0.05 (sonication at 20% duty cycle)
75.0	2.82	0.24	
80.0	2.96	0.01	
85.0	2.83	0.33	
90.0	3.45	0.10	
95.0	3.22	0.28	
100.0	3.91	0.42	
105.0	4.45	0.17	
110.0	4.45	0.11	
115.0	4.45	0.00	
120.0	4.45	0.00	
125.0	6.94	0.34	D=0.05 (no sonication)
130.0	7.46	0.59	
135.0	6.08	0.02	
140.0	4.31	0.03	
145.0	4.02	0.04	
150.0	3.87	0.04	
155.0	3.45	0.06	
160.0	3.45	0.06	
165.0	3.45	0.06	
170.0	3.46	0.10	

c.2) Ethanol concentration (g L^{-1}) at dilution rate of 0.075 h^{-1} for control (no sonication) and with sonication at 20% duty cycle (intensity at 11.8 W cm^{-2})

Fermentation time (h)	Average data	Standard deviation	Dilution rate (h^{-1})
175.0	0.51	0.24	D=0.075 (no sonication)
180.0	0.00	0.00	
185.0	0.65	0.04	
190.0	0.82	0.04	
195.0	1.27	0.10	
200.0	2.23	0.13	
205.0	2.83	0.16	
210.0	3.14	0.29	
215.0	4.65	0.16	
220.0	2.31	0.13	

225.0	2.35	0.06	
230.0	2.32	0.02	
235.0	2.35	0.07	
240.0	0.32	0.01	D=0.075 (sonication at 20% duty cycle)
245.0	1.07	0.01	
250.0	2.08	0.07	
255.0	2.14	0.02	
260.0	2.82	0.23	
265.0	2.68	0.07	
270.0	2.50	0.08	
275.0	2.57	0.04	
280.0	2.87	0.06	
285.0	2.86	0.08	
290.0	2.77	0.03	
295.0	2.96	0.07	
300.0	3.14	0.01	
305.0	3.58	0.06	
310.0	3.58	0.12	
315.0	3.58	0.10	
320.0	3.58	0.06	
325.0	0.51	0.24	D=0.075 (no sonication)
330.0	0.00	0.00	
335.0	0.65	0.04	
340.0	0.82	0.04	
345.0	1.27	0.10	
350.0	2.23	0.13	
355.0	2.83	0.16	
360.0	3.14	0.29	
365.0	4.65	0.16	
370.0	2.31	0.13	
375.0	2.35	0.06	
380.0	2.32	0.02	
385.0	2.35	0.07	

c.3) Ethanol concentration (g L^{-1}) at dilution rate of 0.1 h^{-1} for control (no sonication) and with sonication at 20% duty cycle (intensity at 11.8 W cm^{-2})

Fermentation time (h)	Average data	Standard deviation	Dilution rate (h^{-1})
390.0	3.04	0.66	D=0.1 (no sonication)
395.0	2.78	0.08	
400.0	2.72	0.09	
405.0	3.03	0.24	
410.0	2.54	0.12	

415.0	1.88	0.18	
420.0	1.75	0.09	
425.0	1.85	0.06	
430.0	1.82	0.21	
435.0	1.85	0.05	
440.0	1.82	0.10	
445.0	1.84	0.04	
450.0	1.82	0.24	D=0.1 (sonication at 20% duty cycle)
455.0	1.24	0.05	
460.0	1.16	0.00	
465.0	1.66	0.05	
470.0	1.89	0.07	
475.0	1.92	0.07	
480.0	2.12	0.20	
485.0	2.64	0.12	
490.0	2.64	0.05	
495.0	2.64	0.06	
500.0	2.64	0.01	
505.0	2.64	0.00	
510.0	3.04	0.66	D=0.1 (no sonication)
515.0	2.78	0.08	
520.0	2.72	0.09	
525.0	3.03	0.24	
530.0	2.54	0.12	
535.0	1.88	0.18	
540.0	1.75	0.09	
545.0	1.85	0.06	
550.0	1.82	0.21	
555.0	1.85	0.05	
560.0	1.82	0.10	
565.0	1.84	0.04	

c.4) Ethanol concentration (g L^{-1}) at dilution rate of 0.15 h^{-1} for control (no sonication) and with sonication at 20% duty cycle (intensity at 11.8 W cm^{-2})

Fermentation time (h)	Average data	Standard deviation	Dilution rate (h^{-1})
570.0	2.18	0.07	D=0.15 (no sonication)
575.0	2.50	0.09	
580.0	1.91	0.09	
585.0	1.43	0.23	
590.0	1.81	0.12	
595.0	1.92	0.01	
600.0	2.00	0.13	

605.0	2.02	0.10	
610.0	2.02	0.10	
615.0	1.62	0.08	
620.0	1.61	0.08	
625.0	1.18	0.07	
630.0	1.48	0.23	
635.0	1.14	0.10	
640.0	1.68	0.23	
645.0	1.31	0.12	
650.0	1.54	0.25	
655.0	1.00	0.03	
660.0	0.66	0.16	
665.0	1.05	0.06	
670.0	1.08	0.02	
675.0	1.06	0.03	
680.0	1.09	0.09	
685.0	1.05	0.00	
690.0	1.05	0.05	
695.0	1.58	0.12	D=0.15 (sonication at 20% duty cycle)
700.0	1.14	0.08	
705.0	0.53	0.08	
710.0	0.79	0.09	
715.0	0.40	0.12	
720.0	0.66	0.03	
725.0	0.74	0.07	
730.0	0.80	0.05	
735.0	0.44	0.04	
740.0	0.99	0.06	
745.0	1.02	0.01	
750.0	1.51	0.13	
755.0	2.15	0.08	
760.0	1.35	0.04	
765.0	0.68	0.07	
770.0	0.75	0.07	
775.0	0.51	0.06	
780.0	1.51	0.03	
785.0	1.28	0.06	
790.0	1.83	0.13	
795.0	1.81	0.04	
800.0	1.83	0.13	
805.0	1.82	0.07	
810.0	0.58	0.03	D=0.15 (no sonication)
815.0	0.52	0.05	
820.0	0.52	0.08	
825.0	0.32	0.02	
830.0	0.33	0.02	
835.0	0.32	0.05	
840.0	0.41	0.02	

845.0	0.55	0.02	
850.0	0.70	0.04	
855.0	0.70	0.02	
860.0	0.68	0.02	
865.0	0.60	0.02	
870.0	0.38	0.06	
875.0	0.39	0.04	
880.0	0.43	0.04	
885.0	0.30	0.02	
890.0	0.45	0.04	
895.0	0.69	0.04	
900.0	0.85	0.06	
905.0	0.88	0.08	
910.0	0.87	0.03	
915.0	0.87	0.05	
920.0	1.00	0.09	D=0.15 (sonication at 20% duty cycle)
925.0	1.11	0.12	
930.0	0.33	0.01	
935.0	0.59	0.06	
940.0	0.76	0.07	
945.0	0.84	0.06	
950.0	0.85	0.06	
955.0	0.83	0.08	
960.0	0.62	0.06	
965.0	0.75	0.06	
970.0	0.84	0.08	
975.0	0.91	0.04	
980.0	0.72	0.07	
985.0	0.90	0.01	
990.0	0.52	0.07	
995.0	0.64	0.07	
1000.0	1.18	0.11	
1005.0	1.16	0.07	
1010.0	1.57	0.11	
1015.0	1.57	0.14	
1020.0	1.58	0.13	
1025.0	1.59	0.09	
1030.0	0.69	0.11	D=0.15 (no sonication)
1035.0	0.65	0.03	
1040.0	0.58	0.02	
1045.0	0.53	0.03	
1050.0	0.44	0.01	
1055.0	0.43	0.01	
1060.0	0.58	0.05	
1065.0	0.57	0.02	
1070.0	0.55	0.05	
1075.0	0.45	0.06	
1080.0	0.49	0.07	

1085.0	0.56	0.01	
1090.0	0.57	0.02	
1095.0	0.61	0.02	
1100.0	0.67	0.06	
1105.0	0.52	0.01	
1110.0	0.75	0.06	
1115.0	0.78	0.06	
1120.0	0.86	0.05	
1125.0	0.86	0.02	
1130.0	0.87	0.01	
1135.0	0.86	0.02	
1140.0	0.87	0.03	
1145.0	0.88	0.13	D=0.15 (sonication at 20% duty cycle)
1150.0	0.79	0.06	
1155.0	0.81	0.17	
1160.0	0.79	0.05	
1165.0	0.56	0.05	
1170.0	0.83	0.07	
1175.0	0.93	0.07	
1180.0	1.30	0.03	
1185.0	1.31	0.05	
1190.0	1.35	0.11	
1195.0	1.36	0.10	
1200.0	1.37	0.03	
1205.0	1.30	0.02	
1210.0	1.47	0.05	
1215.0	1.57	0.05	
1220.0	1.59	0.06	
1225.0	1.59	0.03	
1230.0	1.59	0.02	
1235.0	0.86	0.08	D=0.15 (no sonication)
1240.0	0.73	0.05	
1245.0	1.23	0.04	
1250.0	1.25	0.15	
1255.0	1.20	0.13	
1260.0	0.61	0.06	
1265.0	0.82	0.07	
1270.0	1.15	0.00	
1275.0	0.97	0.07	
1280.0	0.83	0.13	
1285.0	1.09	0.05	
1290.0	1.32	0.15	
1295.0	1.23	0.05	
1300.0	1.11	0.08	
1305.0	1.17	0.07	
1310.0	1.14	0.02	
1315.0	0.90	0.14	
1320.0	0.91	0.05	

1325.0	0.89	0.12	
1330.0	0.89	0.09	
1335.0	0.89	0.16	
1340.0	0.89	0.04	
1345.0	0.89	0.05	

c.5) Ethanol concentration (g L^{-1}) at dilution rate of 0.2 h^{-1} for control (no sonication) and with sonication at 20% duty cycle (intensity at 11.8 W cm^{-2})

Fermentation time (h)	Average data	Standard deviation	Dilution rate (h^{-1})
1350.0	0.55	0.01	D=0.2 (no sonication)
1355.0	0.42	0.01	
1360.0	0.25	0.02	
1365.0	0.48	0.00	
1370.0	0.63	0.01	
1375.0	0.49	0.00	
1380.0	0.51	0.02	
1385.0	0.75	0.02	
1390.0	0.55	0.02	
1395.0	0.31	0.02	
1400.0	0.39	0.00	
1405.0	0.70	0.02	
1410.0	0.33	0.00	
1415.0	0.38	0.00	
1420.0	0.33	0.02	
1425.0	0.34	0.00	
1430.0	0.42	0.03	
1435.0	0.40	0.05	
1440.0	0.43	0.05	
1445.0	0.43	0.07	
1450.0	0.43	0.03	
1455.0	0.43	0.04	
1460.0	0.47	0.00	D=0.2 (sonication at 20% duty cycle)
1465.0	0.44	0.00	
1470.0	0.38	0.01	
1475.0	0.48	0.01	
1480.0	0.46	0.00	
1485.0	0.49	0.01	
1490.0	0.62	0.03	
1495.0	0.50	0.00	
1500.0	0.50	0.01	
1505.0	0.50	0.00	
1510.0	0.51	0.00	

1515.0	0.43	0.01	
1520.0	0.58	0.01	
1525.0	0.78	0.00	
1530.0	0.61	0.02	
1535.0	0.66	0.02	
1540.0	0.57	0.01	
1545.0	0.64	0.01	
1550.0	0.64	0.01	
1555.0	0.64	0.05	
1560.0	0.64	0.01	

A3.8 Steady state parameters for continuous culture of *K. marxianus* on lactose without sonication (control) and with sonication at 20 % duty cycle (Intensity = 11.8 W cm^{-2}) (Figure 4.11)

a) Biomass concentration (g L^{-1})

Dilution rate (h^{-1})	Control (no sonication)		Sonication at 20% duty cycle	
	Steady-state data	Standard deviation	Steady-state data	Standard deviation
0.05	10.48	0.09	14.79	0.01
0.075	9.95	0.04	13.17	0.01
0.1	8.85	0.09	11.25	0.01
0.15	7.59	0.04	9.85	0.01
0.2	6.16	0.00	7.01	0.00

b) Lactose concentration (g L^{-1})

Dilution rate (h^{-1})	Control (no sonication)		Sonication at 20% duty cycle	
	Steady-state data	Standard deviation	Steady-state data	Standard deviation
0.05	1.06	0.03	0.52	0.03
0.075	2.43	0.02	1.04	0.03
0.1	3.85	0.03	2.27	0.06
0.15	10.65	0.03	8.65	0.03
0.2	16.86	0.03	15.13	0.03

c) Ethanol concentration (g L^{-1})

Dilution rate (h^{-1})	Control (no sonication)		Sonication at 20% duty cycle	
	Steady-state data	Standard deviation	Steady-state data	Standard deviation
0.05	3.43	0.02	4.45	0.00
0.075	2.33	0.02	3.58	0.00
0.1	1.84	0.01	2.64	0.00
0.15	1.06	0.01	1.58	0.01
0.2	0.43	0.00	0.64	0.00

A3.8 Steady state ethanol productivity, P_E (g L^{-1} h^{-1}). The sonication intensity was 11.8 W cm^{-2} except for the nonsonicated control culture. (Figure 4.12)

Dilution rate (h^{-1})	P_E (no sonication)	P_E (sonication at 20% duty cycle)
0.05	0.172	0.223
0.075	0.175	0.269
0.1	0.184	0.264
0.15	0.159	0.238
0.2	0.085	0.127

APPENDIX 4

A4.1 Dissolved oxygen electrode response profile at 30 °C: a) air-water system; b) air-uninoculated sugar system

a) Air-water system (Figure 3.9)

Time (s)	% Air saturation, C_L
0.0	0.0
12.0	1.5
24.0	43.5
36.0	67.4
48.0	81.5
60.0	89.3
72.0	94.2
84.0	96.4
96.0	98.2
108.0	99.3
120.0	99.9
132.0	100.4
144.0	100.7
156.0	101.0
168.0	101.1
180.0	101.2
192.0	101.2
204.0	101.2
216.0	101.4
228.0	101.5
240.0	101.6
252.0	101.6

264.0	101.6
276.0	101.6
288.0	101.6
300.0	101.6
312.0	101.7
324.0	101.6
336.0	101.6
348.0	101.6
360.0	101.7
372.0	101.6

b) Air-uninoculated sugar system (Figure 3.10)

Time (s)	% Air saturation, C_L
0.0	0.0
12.0	1.0
24.0	20.1
36.0	42.3
48.0	58.3
60.0	65.7
72.0	76.2
84.0	81.7
96.0	84.4
108.0	87.4
120.0	89.7
132.0	91.4
144.0	92.7
156.0	93.6
168.0	94.5
180.0	95.3
192.0	95.9
204.0	96.2
216.0	96.4

228.0	96.8
240.0	97.1
252.0	97.2
264.0	97.6
276.0	97.7
288.0	97.7
300.0	97.9
312.0	97.9
324.0	98.3
336.0	98.1
348.0	98.2
360.0	98.2
372.0	98.5
384.0	98.5
396.0	98.7
408.0	98.8
420.0	98.7
432.0	98.8
444.0	98.8
456.0	99.0
468.0	99.1
480.0	99.2
492.0	99.2
504.0	99.2
516.0	99.0
528.0	99.4
540.0	99.4
552.0	99.4
564.0	99.3
576.0	100.1

A4.2 Goal seek function

Table A4.1 shows an example calculation of k_La_L value by using Equation (2.7) and the Goal Seek function of Microsoft Excel. The data are for an agitation rate of 700 rpm, aeration rate of 0 vvm (air-water system) and at 30 °C.

Table A4.1 Calculation method of k_La_L using Goal Seek function

t (s)	C_L (% air saturation)$_{(measured)}$ from experiment	C^*	C_p (measured) $C_p = (C^*-C_L)/C^*$	τ_p (s)	t_m(s) Calculated using Goal Seek function	C_p (calculated) Calculated using Equation (2.7)	t_m (s) (average)	$C_{p(calculated)}$ Calculated using Equation (2.7) & t_m average
0	0.085	100.99	0.999	21	70	1.000	82.517	1.000
12	1.42	100.99	0.985	21	196.525	0.985	82.517	0.967
24	6.702	100.99	0.933	21	136.531	0.933	82.517	0.893
36	15.08	100.99	0.850	21	111.787	0.850	82.517	0.805
48	25.305	100.99	0.749	21	96.687	0.749	82.517	0.715
60	35.103	100.99	0.652	21	89.874	0.651	82.517	0.628
72	41.749	100.99	0.586	21	92.865	0.585	82.517	0.549
84	53.138	100.99	0.473	21	81.392	0.473	82.517	0.478
96	59.897	100.99	0.406	21	80.328	0.406	82.517	0.415
108	64.924	100.99	0.357	21	81.758	0.357	82.517	0.360
120	70.974	100.99	0.297	21	78.997	0.296	82.517	0.312
132	75.177	100.99	0.255	21	78.983	0.255	82.517	0.270
144	78.812	100.99	0.219	21	78.951	0.219	82.517	0.233
156	82.107	100.99	0.186	21	78.506	0.186	82.517	0.202
168	85.004	100.99	0.158	21	77.7	0.157	82.517	0.175
180	87.049	100.99	0.138	21	78.584	0.138	82.517	0.151
192	89.008	100.99	0.118	21	78.633	0.118	82.517	0.130
204	90.968	100.99	0.099	21	77.7	0.099	82.517	0.113
216	92.047	100.99	0.088	21	79.077	0.088	82.517	0.097
228	93.212	100.99	0.077	21	79.491	0.077	82.517	0.084
240	94.262	100.99	0.066	21	79.697	0.066	82.517	0.073
252	95.257	100.99	0.056	21	79.434	0.056	82.517	0.063

264	96.137	100.99	0.048	21	79.009	0.048	82.517	0.054
276	96.705	100.99	0.042	21	79.781	0.042	82.517	0.047
288	97.358	100.99	0.035	21	79.407	0.036	82.517	0.040
300	97.813	100.99	0.031	21	79.877	0.031	82.517	0.035
312	98.21	100.99	0.027	21	80.334	0.027	82.517	0.030
324	98.579	100.99	0.023	21	80.546	0.024	82.517	0.026
336	98.977	100.99	0.019	21	79.829	0.020	82.517	0.022
348	99.233	100.99	0.017	21	80.192	0.017	82.517	0.019
360	99.46	100.99	0.015	21	80.488	0.015	82.517	0.017
372	99.687	100.99	0.012	21	80.271	0.013	82.517	0.014
384	99.801	100.99	0.011	21	81.614	0.012	82.517	0.012
396	100	100.99	0.009	21	80.874	0.010	82.517	0.011
408	100.11	100.99	0.008	21	81.593	0.009	82.517	0.009
420	100.22	100.99	0.007	21	81.958	0.007	82.517	0.008
432	100.36	100.99	0.006	21	77.7	0.005	82.517	0.007
444	100.48	100.99	0.005	21	77.7	0.004	82.517	0.006
456	100.53	100.99	0.004	21	77.7	0.003	82.517	0.005
468	100.59	100.99	0.003	21	77.7	0.003	82.517	0.004
480	100.68	100.99	0.003	21	77.7	0.002	82.517	0.003
492	100.73	100.99	0.002	21	77.7	0.002	82.517	0.003
504	100.71	100.99	0.002	21	77.7	0.002	82.517	0.002
516	100.79	100.99	0.001	21	77.7	0.001	82.517	0.002
528	100.88	100.99	0.001	21	70	0.000	82.517	0.002
540	100.85	100.99	0.001	21	70	0.000	82.517	0.001
552	100.88	100.99	0.001	21	70	0.000	82.517	0.001
564	100.93	100.99	0.000	21	70	0.000	82.517	0.001
576	100.96	100.99	0.000	21	70	0.000	82.517	0.001
588	100.96	100.99	0.000	21	70	0.000	82.517	0.001
600	100.99	100.99	0	21	70	0.000	82.517	0.000
612	100.99	100.99	0	21	70	0.000	82.517	0.000

t_m (s) (average)	**82.517**
$k_L a_L = 1/t_m$	**0.012**

A4.2.1 Using Goal Seek function

For a given formula, the Goal Seek function determines the value of an input parameter required to achieve the specified result. In this case, Goal Seek function was used to match the C_p calculated to the experimentally measured value of C_p measured, by changing the t_m value to achieve the fit. This gave different values for t_m at different measurement times. An average of t_m values was then used to calculate $k_L a_L$ as $1/t_m$ (average) (Table A4.1). A generally good agreement of the C_p values calculated using Equation (2.7) and the C_p measured by the dissolved oxygen probe is shown in Figure A4.1

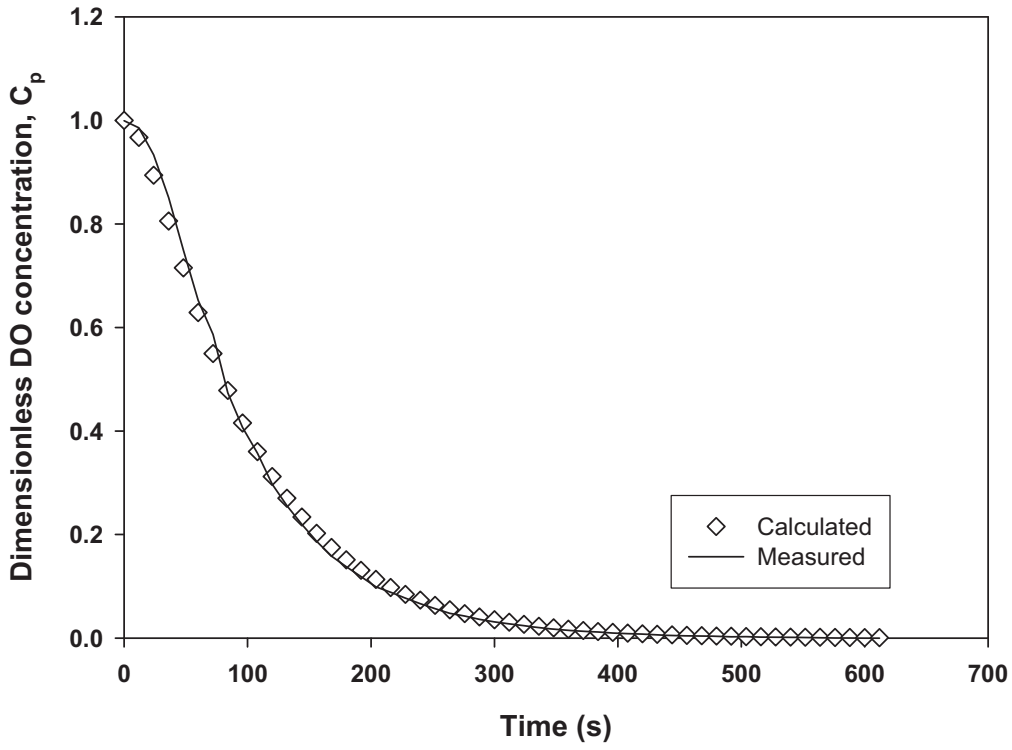

Figure A4.1 A comparison of C_p calculated and the C_p measured (solid line)

A4.3 Dependence of mass transfer coefficient on agitation rate and aeration rate in the absence of ultrasound in: a) air-water system; and b) air-uninoculated sugar system (30 °C). (Figure 4.14)

a) Air-water system (s^{-1})

Agitation (rpm)	Aeration rate		Aeration rate		Aeration rate		Aeration rate	
	0 vvm	Standard deviation	1 vvm	Standard deviation	2 vvm	Standard deviation	3 vvm	Standard deviation
200	4.667e-4	5.000e-6	7.918e-3	0	0.012	3.500e-4	0.012	5.000e-5
300	5.933e-4	1.000e-5	0.010	5.500e-4	0.014	7.000e-4	0.029	2.500e-4
400	1.332e-3	4.000e-5	0.011	7.500e-4	0.030	6.500e-4	0.040	3.500e-3
500	2.890e-3	6.500e-5	0.030	2.000e-3	0.075	1.400e-3	0.085	5.500e-4
600	7.145e-3	7.500e-5	0.041	3.050e-3	0.139	2.500e-4	0.142	3.500e-4
700	0.012	5.000e-4	0.069	1.950e-3	0.180	3.500e-4	0.200	3.000e-4
800	0.025	7.500e-4	0.131	8.500e-4	0.218	1.300e-3	0.250	5.000e-5

b) Air-uninoculated sugar system (s^{-1})

Agitation (rpm)	Aeration rate		Aeration rate		Aeration rate		Aeration rate	
	0 vvm	Standard deviation	1 vvm	Standard deviation	2 vvm	Standard deviation	3 vvm	Standard deviation
200	4.667e-4	2.333e-5	8.516e-3	4.258e-4	0.010	5.104e-4	0.023	1.193e-3
300	5.933e-4	2.966e-5	0.011	5.719e-4	0.024	1.216e-3	0.028	1.415e-3
400	2.044e-5	1.022e-6	0.019	9.870e-4	0.032	1.646e-3	0.053	2.677e-3
500	4.284e-5	2.142e-6	0.037	1.858e-3	0.051	2.586e-3	0.079	3.985e-3
600	1.056e-4	5.284e-6	0.069	3.496e-3	0.081	4.051e-3	0.125	6.250e-3
700	2.658e-4	1.329e-5	0.088	4.441e-3	0.093	4.665e-3	0.166	8.333e-3
800	1.213e-3	6.068e-5	0.114	5.722e-3	0.125	6.250e-3	0.250	0.012

A4.4 Dependence of mass transfer coefficient on agitation rate in the presence of ultrasound in: a) air-water system; and b) air-uninoculated sugar system. All data at 2 vvm aeration rate and 30 °C. (Figure 4.15)

a) Air-water system

Agitation rate (rpm)	Control (no sonication)		Sonication at 100% duty cycle at low intensity ultrasound (11.8 W cm^{-2})		Sonication at 100% duty cycle at high intensity ultrasound (50.3 W cm^{-2})	
	k_La_L (s^{-1})	Standard deviation	k_La_L (s^{-1})	Standard deviation	k_La_L (s^{-1})	Standard deviation
200	0.012	2.449e-4	0.015	4.109e-4	0.023	6.182e-4
300	0.014	5.715e-4	0.019	1.314e-3	0.032	7.930e-4
400	0.030	1.444e-3	0.034	1.065e-3	0.052	1.525e-3
500	0.075	1.586e-3	0.093	1.444e-3	0.117	9.741e-4
600	0.139	7.408e-4	0.200	9.843e-4	0.250	1.336e-3
700	0.180	1.496e-3	0.250	5.715e-4	0.333	9.977e-4
800	0.218	9.741e-4	0.333	8.498e-4	0.400	8.993e-4

b) Air-uninoculated sugar system

Agitation rate (rpm)	Control (no sonication)		Sonication at 100% duty cycle at low intensity ultrasound (11.8 W cm^{-2})		Sonication at 100% duty cycle at high intensity ultrasound (50.3 W cm^{-2})	
	k_La_L (s^{-1})	Standard deviation	k_La_L (s^{-1})	Standard deviation	k_La_L (s^{-1})	Standard deviation
200	0.010	5.104e-4	0.025	1.285e-3	0.023	1.168e-3
300	0.024	1.216e-3	0.035	1.769e-3	0.041	2.055e-3
400	0.032	1.646e-3	0.052	2.601e-3	0.076	3.846e-3
500	0.051	2.586e-3	0.124	6.229e-3	0.222	0.011
600	0.081	4.051e-3	0.213	0.010	0.370	0.018
700	0.093	4.665e-3	0.268	0.013	0.454	0.022
800	0.125	6.250e-3	0.333	0.016	0.526	0.026

APPENDIX 5

A5.1 Glucose production from lactose during nonsonicated enzymatic hydrolysis. Initial substrate concentrations $[S]_o$ = (5 – 60 g L^{-1}), initial enzyme concentration $[E]_o$ = 1.0 mL L^{-1}, T = 37 °C and pH = 6.5 (Figure 4.16).

Time (min)	Initial concentration of lactose (g L^{-1})							
	5		10		20		30	
	Glucose concentration (M)	Std Dev	Glucose concentration (M)	Std Dev	Glucose concentration (M)	Std Dev	Glucose concentration (M)	Std Dev
0	0.000	3.333e-5	0.000	1.388e-5	0.000	0.000	0.000	0.000
2	7.500e-4	9.212e-6	1.211e-3	3.928e-6	1.716e-3	1.210e-5	1.900e-3	5.555e-6
4	7.833e-4	6.804e-6	1.244e-3	3.928e-6	1.822e-3	2.500e-5	2.061e-3	5.931e-5
6	8.277e-4	9.107e-6	1.288e-3	3.716e-5	2.027e-3	1.012e-4	2.216e-3	9.622e-5
8	8.444e-4	6.054e-6	1.355e-3	1.388e-5	2.105e-3	1.101e-4	2.344e-3	1.355e-4
10	8.722e-4	9.918e-6	1.472e-3	2.873e-5	2.216e-3	1.502e-4	2.472e-3	1.541e-4
12	9.000e-4	6.054e-6	1.483e-3	2.605e-5	2.288e-3	6.530e-5	2.594e-3	1.989e-4
14	9.222e-4	4.606e-6	1.600e-3	6.976e-5	2.416e-3	3.611e-5	2.661e-3	1.595e-4
16	9.388e-4	3.154e-5	1.605e-3	5.377e-5	2.494e-3	3.017e-5	2.772e-3	1.781e-4
18	9.555e-4	9.918e-6	1.750e-3	8.983e-5	2.544e-3	9.918e-6	2.816e-3	1.427e-4
20	9.722e-4	1.619e-5	1.850e-3	1.252e-4	2.588e-3	1.145e-5	2.905e-3	7.871e-5
22	9.833e-4	1.381e-5	1.916e-3	1.190e-4	2.655e-3	1.540e-5	2.988e-3	9.945e-5
24	9.944e-4	4.811e-6	1.950e-3	1.112e-4	2.733e-3	3.796e-5	2.972e-3	7.781e-5
26	1.005e-3	6.804e-6	2.100e-3	1.355e-4	2.772e-3	4.035e-5	3.033e-3	5.137e-5
28	1.016e-3	9.107e-6	2.150e-3	1.287e-4	2.800e-3	3.935e-5	3.038e-3	2.777e-6
30	1.033e-3	9.107e-6	2.177e-3	1.020e-4	2.838e-3	4.321e-5	3.105e-3	2.777e-6

35	1.050e-3	9.622e-6	2.205e-3	9.029e-5	2.883e-3	5.305e-5	3.116e-3	0.000
40	1.066e-3	1.202e-5	2.227e-3	8.592e-5	2.894e-3	2.605e-5	3.161e-3	2.777e-6
45	1.100e-3	2.017e-5	2.272e-3	4.519e-5	2.916e-3	3.027e-5	3.172e-3	2.777e-6
50	1.105e-3	1.589e-5	2.305e-3	3.908e-5	2.938e-3	3.565e-5	3.227e-3	2.777e-6
55	1.111e-3	1.066e-5	2.361e-3	5.137e-5	2.950e-3	2.133e-5	3.233e-3	2.777e-6
60	1.116e-3	3.928e-6	2.366e-3	6.411e-5	2.944e-3	2.975e-5	3.238e-3	2.777e-6

Time (min)	**Initial concentration of lactose (g L^{-1})**					
	40		**50**		**60**	
	Glucose concentration (M)	Std Dev	Glucose concentration (M)	Std Dev	Glucose concentration (M)	Std Dev
0	0.000	1.388e-5	0.000	1.111e-5	0.000	8.333e-6
2	1.983e-3	2.777e-6	2.122e-3	5.555e-6	2.133e-3	1.302e-5
4	2.288e-3	3.213e-4	2.583e-3	1.000e-4	2.761e-3	2.336e-5
6	2.416e-3	1.999e-4	2.766e-3	9.722e-5	3.027e-3	2.735e-5
8	2.455e-3	1.399e-4	2.988e-3	5.833e-5	3.216e-3	2.605e-5
10	2.594e-3	3.521e-5	3.105e-3	5.833e-5	3.472e-3	1.066e-5
12	2.755e-3	6.001e-5	3.200e-3	9.722e-5	3.650e-3	1.571e-5
14	2.866e-3	5.061e-5	3.327e-3	1.500e-4	3.766e-3	3.055e-5
16	2.966e-3	3.215e-5	3.483e-3	2.777e-6	3.861e-3	1.778e-5
18	3.127e-3	4.070e-5	3.661e-3	0.000	3.961e-3	3.455e-5
20	3.150e-3	3.928e-6	3.766e-3	2.777e-6	4.027e-3	6.254e-5
22	3.272e-3	6.804e-6	3.872e-3	2.777e-6	4.161e-3	4.896e-5
24	3.300e-3	1.540e-5	4.033e-3	2.777e-6	4.311e-3	2.256e-5
26	3.483e-3	4.513e-5	4.138e-3	2.777e-6	4.494e-3	7.216e-5
28	3.433e-3	1.589e-5	4.155e-3	8.333e-6	4.644e-3	3.695e-5
30	3.472e-3	2.405e-6	4.177e-3	8.333e-6	4.750e-3	2.017e-5
35	3.611e-3	4.606e-6	4.233e-3	5.555e-6	4.827e-3	4.015e-5
40	3.661e-3	4.811e-6	4.283e-3	2.777e-6	4.861e-3	1.436e-5

45	3.727e-3	3.928e-6	4.327e-3	0.000	4.983e-3	5.137e-5
50	3.788e-3	3.535e-5	4.361e-3	2.777e-6	5.066e-3	8.179e-5
55	3.811e-3	2.405e-6	4.383e-3	1.111e-5	5.188e-3	9.406e-5
60	3.877e-3	4.606e-6	4.394e-3	5.555e-6	5.122e-3	2.965e-5

A5.2 Effects of ultrasonication on initial rate (V_i) at power intensities of: a) 2.4 W cm^{-2}; b) 4.7 W cm^{-2}; and c) 11.8 W cm^{-2} except for control (no sonication) (Figure 4.19)

a) Power intensity at 2.4 W cm^{-2}

Initial substrate concentration (g L^{-1})	Rate of product formation, V_i (M s^{-1})							
	Control (no sonication)		Sonication at 10% duty cycle		Sonication at 20% duty cycle		Sonication at 40% duty cycle	
	V_i (M s^{-1})	Standard deviation	V_i (M s^{-1})	Standard deviation	V_i (M s^{-1})	Standard deviation	V_i (M s^{-1})	Standard deviation
0	0.000	0.000	0.000	0.000	0.000	0.000	0.000	0.000
5	6.250e-6	3.240e-7	1.088e-5	8.265e-8	7.638e-6	1.241e-7	6.527e-6	1.202e-7
10	1.009e-5	1.388e-7	1.416e-5	2.080e-7	1.115e-5	2.860e-7	1.018e-5	6.952e-7
20	1.430e-5	4.629e-8	1.685e-5	9.820e-8	1.439e-5	1.616e-7	1.393e-5	1.403e-7
30	1.583e-5	4.629e-8	1.861e-5	6.847e-8	1.675e-5	6.944e-8	1.615e-5	2.346e-7
40	1.652e-5	9.259e-8	2.069e-5	9.820e-8	1.856e-5	1.653e-7	1.736e-5	1.807e-7
50	1.768e-5	4.629e-8	2.236e-5	8.890e-8	2.013e-5	7.677e-8	1.888e-5	2.394e-7
60	1.777e-5	9.259e-8	2.240e-5	8.661e-8	2.018e-5	1.919e-7	1.893e-5	1.426e-7

b) Power intensity at 4.7 W cm^{-2}

Initial substrate concentration (g L^{-1})	Rate of product formation, V_i (M s^{-1})							
	Control (no sonication)		Sonication at 10% duty cycle		Sonication at 20% duty cycle		Sonication at 40% duty cycle	
	V_i (M s^{-1})	Standard deviation	V_i (M s^{-1})	Standard deviation	V_i (M s^{-1})	Standard deviation	V_i (M s^{-1})	Standard deviation
0	0.000	0.000	0.000	0.000	0.000	0.000	0.000	0.000
5	6.250e-6	3.240e-7	1.175e-5	1.263e-6	9.120e-6	1.441e-7	7.129e-6	1.426e-7
10	1.009e-5	1.388e-7	1.611e-5	6.847e-8	1.236e-5	5.045e-8	1.060e-5	5.389e-7
20	1.430e-5	4.629e-8	1.842e-5	1.054e-7	1.500e-5	1.349e-7	1.393e-5	3.873e-7
30	1.583e-5	4.629e-8	2.032e-5	1.013e-6	1.842e-5	6.847e-8	1.671e-5	5.810e-7
40	1.652e-5	9.259e-8	2.199e-5	1.521e-6	2.060e-5	1.180e-7	1.856e-5	7.425e-7
50	1.768e-5	4.629e-8	2.324e-5	4.848e-7	2.263e-5	6.944e-8	2.041e-5	7.971e-7
60	1.777e-5	9.259e-8	2.328e-5	7.115e-7	2.254e-5	3.987e-7	2.060e-5	4.759e-7

c) Power intensity at 11.8 W cm^{-2}

Initial substrate concentration (g L^{-1})	Rate of product formation, V_i (M s^{-1})							
	Control (no sonication)		Sonication at 10% duty cycle		Sonication at 20% duty cycle		Sonication at 40% duty cycle	
	V_i (M s^{-1})	Standard deviation	V_i (M s^{-1})	Standard deviation	V_i (M s^{-1})	Standard deviation	V_i (M s^{-1})	Standard deviation
0	0.000	0.000	0.000	0.000	0.000	0.000	0.000	0.000
5	6.250e-6	3.240e-7	1.328e-5	8.052e-7	1.037e-5	9.544e-8	7.638e-6	1.464e-7
10	1.009e-5	1.388e-7	1.838e-5	9.974e-7	1.453e-5	1.009e-7	1.277e-5	1.408e-7
20	1.430e-5	4.629e-8	2.013e-5	1.308e-6	1.754e-5	1.104e-7	1.601e-5	1.548e-7
30	1.583e-5	4.629e-8	2.138e-5	1.562e-6	1.967e-5	1.866e-7	1.736e-5	1.552e-7
40	1.652e-5	9.259e-8	2.305e-5	2.020e-6	2.120e-5	2.543e-7	1.879e-5	8.890e-8
50	1.768e-5	4.629e-8	2.412e-5	2.148e-6	2.300e-5	2.860e-7	2.060e-5	1.060e-7

60	1.777e-5	9.259e-8	2.425e-5	2.125e-6	2.296e-5	6.847e-8	2.069e-5	9.427e-7

A5.3 Effects of ultrasonication at different levels of sonication power (0- 15 W) on: a) maximum reaction rate (V_{max}), b) Michaelis constant (K_m) at $[E]_o$ = 0.1 mL L^{-1} (Figure 4.20).

a) Maximum reaction rate, V_{max} (M s^{-1})

Power intensity (W cm^{-2})	Control (no sonication)		Sonication at 10% duty cycle		Sonication at 20% duty cycle		Sonication at 40% duty cycle	
	V_{max}	Standard deviation	V_{max}	Standard deviation	V_{max}	Standard deviation	V_{max}	Standard deviation
Control	2.241e-5	2.314e-7						
2.4			2.333e-5	2.178e-9	2.293e-5	1.930e-7	2.303e-5	6.513e-8
4.7			2.483e-5	2.627e-8	2.413e-5	6.018e-7	2.370e-5	1.175e-6
11.8			2.566e-5	3.307e-6	2.497e-5	1.371e-8	2.465e-5	3.279e-7

b) Michaelis-constant, K_m (g L^{-1})

Power intensity (W cm^{-2})	Control (no sonication)		Sonication at 10% duty cycle		Sonication at 20% duty cycle		Sonication at 40% duty cycle	
	K_m	Standard deviation	K_m	Standard deviation	K_m	Standard deviation	K_m	Standard deviation
Control	12.747	0.612						
2.4			5.938	0.048	5.593	1.393	4.578	1.569
4.7			10.173	0.282	8.595	0.220	7.126	0.045
11.8			12.651	0.325	11.842	0.745	10.824	0.513

A5.4 Residual enzyme activity (%) versus processing time at various sonication duty cycles including control (no sonication) at optimum power intensity 11.8 W cm^{-2}, pH = 6.5, T = 37 °C (Figure 4.21)

Time (min)	Control (no sonication)		Sonication at 10% duty cycle		Sonication at 20% duty cycle		Sonication at 40% duty cycle	
	Enzyme activity (%)	Standard deviation	Enzyme activity (%)	Standard deviation	Enzyme activity (%)	Standard deviation	Enzyme activity (%)	Standard deviation
0	100.00	0.00	100.00	0.00	100.00	0.00	100.00	0.00
2	99.82	1.08	93.38	0.32	88.79	0.92	83.09	0.31
4	99.82	0.78	90.44	0.46	84.74	1.45	73.16	4.97
6	99.63	0.86	89.89	0.68	84.01	1.05	72.43	4.83
8	99.63	0.55	89.34	0.70	83.46	0.28	71.69	4.79
10	99.82	0.74	88.79	0.65	82.72	1.34	70.96	4.93
12	99.82	0.76	88.24	0.69	81.99	1.38	70.22	4.88
14	99.82	0.97	87.68	0.75	81.25	1.59	69.49	5.06

16	99.63	0.87	87.13	0.73	80.51	2.23	68.75	4.92
18	99.63	0.95	86.58	0.67	79.78	3.51	68.01	4.88
20	99.45	0.90	85.85	0.59	79.04	3.08	67.28	4.88
22	99.63	1.14	85.29	0.58	78.31	3.34	66.54	5.06
24	99.82	1.22	84.74	0.64	77.57	3.59	65.81	4.97
26	99.82	1.28	84.19	0.87	76.84	4.02	65.07	5.24
28	99.63	1.18	83.27	0.43	76.10	9.36	64.34	4.37
30	99.63	1.42	82.72	0.35	75.37	9.76	63.60	4.46

APPENDIX 6

A.6.1 Time courses of the enzymatic hydrolysis of: a) carboxymethyl cellulose (CMC); b) Solka-Floc BH 300 (30 µm); c) Solka-Floc BH 40 (60µm); and d) Solka-Floc CH 10 (290µm) for nonsonicated enzymatic hydrolysis. Initial substrate concentrations $[S]_o$ = (5 – 40 g L^{-1}), initial enzyme concentration, $[E]_o$ = 0.1 g L^{-1}, T = 50 °C and pH = 4.8 (Figure 4.22)

a) CMC

Time (min)	Initial concentration of CMC (g L^{-1})											
	5		8		10		20		35		40	
	Glucose concentration (M)	Std Dev	Glucose concentration (M)	Std Dev	Glucose concentration (M)	Std Dev	Glucose concentration (M)	Std Dev	Glucose concentration (M)	Std Dev	Glucose concentration (M)	Std Dev
0	0.000	0.000	0.000	4.611e-5	0.000	4.243e-5	0.000	5.171e-5	0.000	3.186e-5	0.000	6.633e-5
2	4.222e-4	5.466e-5	4.055e-4	1.739e-5	7.388e-4	3.539e-5	8.666e-4	8.003e-5	9.388e-4	5.903e-5	9.444e-4	3.894e-5
4	5.055e-4	4.543e-5	5.000e-4	3.937e-5	8.722e-4	8.169e-5	1.005e-3	2.371e-5	9.944e-4	1.182e-4	1.033e-3	1.311e-4
6	5.055e-4	6.710e-5	5.722e-4	4.153e-5	9.111e-4	4.851e-5	1.138e-3	3.611e-5	1.127e-3	1.070e-4	1.072e-3	5.714e-5
8	5.833e-4	3.937e-5	6.388e-4	3.954e-5	9.500e-4	6.200e-5	1.177e-3	3.293e-5	1.200e-3	9.966e-5	1.183e-3	9.973e-5
10	6.111e-4	4.619e-5	7.166e-4	3.430e-5	1.027e-3	5.905e-5	1.266e-3	4.762e-5	1.227e-3	1.078e-4	1.244e-3	1.047e-4
12	6.444e-4	4.611e-5	7.611e-4	5.601e-5	1.088e-3	3.171e-5	1.294e-3	5.598e-5	1.294e-3	6.666e-5	1.300e-3	1.738e-4
14	6.722e-4	5.014e-5	8.388e-4	6.288e-5	1.188e-3	5.018e-5	1.305e-3	4.211e-5	1.305e-3	9.162e-5	1.477e-3	1.775e-4
16	7.111e-4	7.780e-5	8.777e-4	5.355e-5	1.205e-3	5.468e-5	1.361e-3	4.532e-5	1.394e-3	8.868e-5	1.544e-3	1.413e-4
18	7.444e-4	7.989e-5	9.277e-4	5.926e-5	1.277e-3	2.697e-5	1.433e-3	1.327e-4	1.544e-3	4.942e-5	1.600e-3	7.531e-5
20	7.944e-4	7.444e-5	9.722e-4	5.710e-5	1.305e-3	3.230e-5	1.488e-3	5.344e-5	1.650e-3	6.983e-5	1.705e-3	4.794e-5

b) Solka-Floc BH 300 (30 µm)

Time (min)	Initial concentration of Solka-Floc (g L^{-1})											
	5		8		10		20		35		40	
	Glucose concentration (M)	Std Dev	Glucose concentration (M)	Std Dev	Glucose concentration (M)	Std Dev	Glucose concentration (M)	Std Dev	Glucose concentration (M)	Std Dev	Glucose concentration (M)	Std Dev
0	0.000	0.000	0.000	0.000	0.000	0.000	0.000	0.000	0.000	0.000	0.000	0.000
2	1.222e-4	1.178e-5	2.111e-4	1.858e-5	2.944e-4	3.928e-6	4.833e-4	8.216e-6	6.500e-4	4.606e-6	6.555e-4	1.066e-5
4	1.611e-4	2.092e-5	2.277e-4	1.978e-5	3.166e-4	6.211e-6	5.111e-4	1.388e-5	6.777e-4	1.145e-5	6.944e-4	1.863e-5
6	1.944e-4	1.863e-5	2.666e-4	2.805e-5	3.388e-4	1.066e-5	5.444e-4	1.540e-5	7.111e-4	1.416e-5	7.277e-4	2.421e-5
8	2.111e-4	1.489e-5	2.888e-4	3.176e-5	3.777e-4	2.165e-5	5.722e-4	1.619e-5	7.444e-4	1.619e-5	7.722e-4	2.843e-5
10	2.333e-4	1.712e-5	3.166e-4	3.565e-5	4.055e-4	2.843e-5	6.000e-4	1.272e-5	7.666e-4	1.272e-5	8.222e-4	4.249e-5
12	2.611e-4	2.401e-5	3.444e-4	3.898e-5	4.333e-4	3.224e-5	6.333e-4	2.017e-5	8.000e-4	1.800e-5	8.611e-4	4.157e-5
14	2.888e-4	2.843e-5	3.666e-4	4.091e-5	4.666e-4	4.240e-5	6.611e-4	2.269e-5	8.277e-4	2.187e-5	9.111e-4	5.275e-5
16	3.111e-4	2.749e-5	4.055e-4	5.305e-5	4.833e-4	4.461e-5	6.833e-4	2.165e-5	8.500e-4	1.944e-5	9.555e-4	6.290e-5
18	3.444e-4	2.873e-5	4.277e-4	5.393e-5	5.055e-4	4.785e-5	7.055e-4	2.421e-5	8.777e-4	2.165e-5	9.888e-4	5.505e-5
20	4.055e-4	4.089e-5	4.388e-4	4.976e-5	5.166e-4	4.237e-5	7.500e-4	3.295e-5	9.166e-4	2.496e-5	1.016e-3	4.164e-5

c) Solka-Floc BH 40 (60µm)

Time (min)	Initial concentration of Solka-Floc (g L^{-1})											
	5		8		10		20		35		40	
	Glucose concentration (M)	Std Dev	Glucose concentration (M)	Std Dev	Glucose concentration (M)	Std Dev	Glucose concentration (M)	Std Dev	Glucose concentration (M)	Std Dev	Glucose concentration (M)	Std Dev
0	0.000	0.000	0.000	0.000	0.000	0.000	0.000	0.000	0.000	0.000	0.000	0.000

2	7.222e-5	3.928e-6	1.222e-4	9.918e-6	1.555e-4	4.606e-6	2.333e-4	3.027e-5	2.500e-4	8.216e-6	2.555e-4	8.216e-6
4	1.055e-4	1.265e-5	1.500e-4	1.637e-5	2.166e-4	2.616e-5	2.555e-4	2.952e-5	2.722e-4	2.022e-5	3.000e-4	9.918e-6
6	1.222e-4	1.388e-5	1.722e-4	2.003e-5	2.444e-4	1.816e-5	2.722e-4	2.620e-5	2.944e-4	1.324e-5	3.277e-4	2.545e-5
8	1.555e-4	1.899e-5	2.111e-4	2.760e-5	2.722e-4	5.726e-5	2.944e-4	2.760e-5	3.222e-4	1.521e-5	3.611e-4	3.272e-5
10	1.777e-4	2.200e-5	2.333e-4	2.791e-5	2.888e-4	3.001e-5	3.166e-4	2.896e-5	3.388e-4	1.863e-5	3.777e-4	3.621e-5
12	2.166e-4	3.001e-5	2.555e-4	2.896e-5	3.222e-4	3.869e-5	3.388e-4	2.256e-5	3.833e-4	2.545e-5	4.166e-4	3.876e-5
14	2.388e-4	3.342e-5	2.833e-4	3.203e-5	3.388e-4	5.506e-5	3.722e-4	2.389e-5	4.055e-4	2.165e-5	4.555e-4	3.796e-5
16	2.722e-4	4.833e-5	2.944e-4	2.896e-5	3.666e-4	3.955e-5	3.944e-4	2.500e-5	4.277e-4	2.290e-5	4.888e-4	3.876e-5
18	2.944e-4	4.536e-5	3.166e-4	3.215e-5	3.833e-4	6.423e-5	4.166e-4	4.185e-5	4.555e-4	2.115e-5	5.111e-4	3.955e-5
20	3.166e-4	4.623e-5	3.388e-4	2.859e-5	3.944e-4	3.896e-5	4.333e-4	4.237e-5	4.722e-4	1.360e-5	5.444e-4	3.200e-5

d) Solka-Floc CH 10 (290µm)

Time (min)	**Initial concentration of Solka-Floc (g L^{-1})**											
	5		**8**		**10**		**20**		**35**		**40**	
	Glucose concentration (M)	Std Dev	Glucose concentration (M)	Std Dev	Glucose concentration (M)	Std Dev	Glucose concentration (M)	Std Dev	Glucose concentration (M)	Std Dev	Glucose concentration (M)	Std Dev
0	0.000	0.000	0.000	0.000	0.000	0.000	0.000	0.000	0.000	0.000	0.000	0.000
2	4.444e-5	8.216e-6	7.777e-5	4.606e-6	1.055e-4	6.211e-6	2.166e-4	6.054e-6	2.388e-4	4.606e-6	2.444e-4	3.928e-6
4	5.555e-5	8.216e-6	8.888e-5	6.054e-6	1.166e-4	6.211e-6	2.333e-4	9.107e-6	2.500e-4	4.606e-6	2.611e-4	5.555e-6
6	6.666e-5	1.039e-5	1.000e-4	9.918e-6	1.277e-4	6.211e-6	2.444e-4	1.039e-5	2.666e-4	8.333e-6	2.833e-4	8.784e-6
8	7.777e-5	1.039e-5	1.111e-4	9.918e-6	1.500e-4	1.039e-5	2.555e-4	8.216e-6	2.833e-4	1.210e-5	3.055e-4	1.066e-5
10	8.888e-5	1.136e-5	1.222e-4	1.178e-5	1.611e-4	1.039e-5	2.722e-4	1.039e-5	3.000e-4	1.495e-5	3.333e-4	1.756e-5
12	1.000e-4	1.272e-5	1.333e-4	1.381e-5	1.833e-4	1.495e-5	2.888e-4	1.265e-5	3.166e-4	1.729e-5	3.611e-4	2.133e-5
14	1.111e-4	1.272e-5	1.444e-4	1.381e-5	1.944e-4	1.495e-5	3.055e-4	1.495e-5	3.333e-4	2.092e-5	3.888e-4	2.678e-5
16	1.333e-4	1.729e-5	1.555e-4	1.436e-5	2.055e-4	1.495e-5	3.222e-4	1.778e-5	3.500e-4	2.465e-5	3.944e-4	2.235e-5

18	1.388e-4	1.666e-5	1.666e-4	1.595e-5	2.166e-4	1.495e-5	3.333e-4	1.778e-5	3.666e-4	2.693e-5	4.222e-4	2.693e-5
20	1.500e-4	1.637e-5	1.777e-4	1.939e-5	2.277e-4	1.495e-5	3.500e-4	2.017e-5	3.833e-4	2.923e-5	4.500e-4	3.333e-5

A6.2 Effects of ultrasonication on reaction rate (V_i) of hydrolysis of CMC at different levels of sonication power intensity: (a) 11.8 W cm^{-2} (P_{ir} = 15 W) : (b) 4.7 W cm^{-2} (P_{ir} = 6 W) : (c) 2.4 W cm^{-2} (P_{ir} = 3 W), except for control (no sonication) of CMC. Data at 50 °C, pH = 4.8 (Figure 4.25)

a) Intensity 11.8 W cm^{-2} (P_{ir} = 15 W)

Time (min)	Rate of product formation, V_i (M s^{-1})							
	Control (no sonication)		Sonication at 10% duty cycle		Sonication at 20% duty cycle		Sonication at 40% duty cycle	
	V_i	Standard deviation	V_i	Standard deviation	V_i	Standard deviation	V_i	Standard deviation
0	0.000	0.000	0.000	0.000	0.000	0.000	0.000	0.000
5	2.592e-6	6.197e-7	8.287e-6	5.241e-7	7.592e-6	4.749e-7	6.018e-6	2.360e-7
8	3.703e-6	4.215e-7	1.125e-5	3.376e-7	8.935e-6	3.516e-7	7.500e-6	3.531e-7
10	4.398e-6	5.423e-7	1.213e-5	1.329e-7	9.444e-6	4.209e-7	8.101e-6	6.644e-7
20	7.222e-6	7.244e-7	1.370e-5	4.892e-7	1.101e-5	1.605e-6	9.166e-6	1.092e-6
35	7.824e-6	7.610e-7	1.453e-5	3.146e-7	1.148e-5	1.054e-6	9.814e-6	9.757e-7

40	7.870e-6	7.975e-7	1.444e-5	2.208e-7	1.157e-5	5.995e-7	9.814e-6	7.728e-7

b) Intensity 4.7 W cm^{-2} (P_{ir} = 6 W)

Time (min)	Rate of product formation, V_i (M s^{-1})							
	Control (no sonication)		Sonication at 10% duty cycle		Sonication at 20% duty cycle		Sonication at 40% duty cycle	
	V_i	Standard deviation	V_i	Standard deviation	V_i	Standard deviation	V_i	Standard deviation
0	0	0	0	0	0	0	0	0
5	2.59E-06	6.2E-07	6.3E-06	1.01E-07	5.69E-06	7.76E-07	4.07E-06	6.94E-08
8	3.7E-06	4.22E-07	8.06E-06	1.15E-07	7.13E-06	5.18E-07	5.19E-06	2.16E-07
10	4.4E-06	5.42E-07	8.47E-06	7.68E-08	7.82E-06	5.59E-07	5.74E-06	2.05E-07
20	7.22E-06	7.24E-07	9.95E-06	4.11E-07	9.44E-06	3.12E-07	7.78E-06	1.15E-07
35	7.82E-06	7.61E-07	1.24E-05	2.08E-07	9.91E-06	5.12E-07	8.29E-06	2.77E-07
40	7.87E-06	7.98E-07	1.25E-05	6.94E-08	0.000	2.87E-07	8.24E-06	3.62E-07

c) Intensity 2.4 W cm^{-2} (P_{ir} = 3 W)

Time (min)	Rate of product formation, V_i (M s^{-1})							
	Control (no sonication)		Sonication at 10% duty cycle		Sonication at 20% duty cycle		Sonication at 40% duty cycle	
	V_i	Standard deviation	V_i	Standard deviation	V_i	Standard deviation	V_i	Standard deviation
0	0.000	0.000	0.000	0.000	0.000	0.000	0.000	0.000
5	2.592e-6	6.197e-7	4.907e-6	6.563e-7	4.259e-6	2.606e-7	3.750e-6	2.928e-7
8	3.703e-6	4.215e-7	6.388e-6	1.180e-7	5.787e-6	2.372e-7	4.861e-6	3.007e-7
10	4.398e-6	5.423e-7	7.037e-6	1.513e-7	6.527e-6	6.202e-7	5.463e-6	2.196e-7
20	7.222e-6	7.244e-7	8.333e-6	2.916e-7	7.685e-6	6.258e-7	7.731e-6	3.182e-7
35	7.824e-6	7.610e-7	1.027e-5	2.360e-7	8.657e-6	7.241e-7	8.240e-6	7.777e-7
40	7.870e-6	7.975e-7	1.032e-5	4.926e-7	8.703e-6	4.310e-7	8.287e-6	7.411e-7

A6.3 Effect of sonication on: (a) maximum reaction rate V_{max} and (b) Michaelis-constant K_m of CMC. The control was not sonicated. (I is sonication intensity, P_{ir} is sonication power.) (Figure 4.26). Data at 50 °C, pH = 4.8

a) Maximum reaction rate, V_{max} (M s^{-1})

Power intensity (W cm^{-2})	Control (no sonication)		Sonication at 10% duty cycle		Sonication at 20% duty cycle		Sonication at 40% duty cycle	
	V_{max}	Standard deviation	V_{max}	Standard deviation	V_{max}	Standard deviation	V_{max}	Standard deviation
Control	9.200e-6	2.500e-8						
2.4			1.200e-5	4.000e-7	1.060e-5	2.000e-7	1.051e-5	2.000e-7
4.7			1.390e-5	1.500e-7	1.150e-5	1.500e-7	1.010e-5	2.500e-7
11.8			1.700e-5	2.500e-7	1.260e-5	1.000e-7	1.100e-5	2.500e-7

b) Michaelis constant, K_m (g CMC L^{-1})

Power intensity (W cm^{-2})	Control (no sonication)		Sonication at 10% duty cycle		Sonication at 20% duty cycle		Sonication at 40% duty cycle	
	K_m	Standard deviation	K_m	Standard deviation	K_m	Standard deviation	K_m	Standard deviation
Control	10.220	0.210						
2.4			7.200	0.150	7.100	0.350	9.070	0.215
4.7			6.120	0.140	5.010	0.095	7.430	0.085
11.8			4.819	0.140	3.310	0.095	3.990	0.110

A6.4 Glucose production from sonicated and nonsonicated hydrolysis (50 °C, pH 4.8) of insoluble cellulose at different particle size: (a) 30 µm, (b) 60 µm, and (c) 290 µm. Sonication at 10% duty cycle and power intensity 11.8 W cm^{-2} (Figure 4.27)

a) Solka floc of particle size of 30 µm (sonication at 10% duty cycle and power intensity 11.8 W cm^{-2})

Time (min)	Initial concentration of Solka-Floc (g L^{-1})											
	5		8		10		20		35		40	
	Glucose concentration (M)	Std Dev	Glucose concentration (M)	Std Dev	Glucose concentration (M)	Std Dev	Glucose concentration (M)	Std Dev	Glucose concentration (M)	Std Dev	Glucose concentration (M)	Std Dev
0	0.000	0.000	0.000	0.000	0.000	0.000	0.000	0.000	0.000	0.000	0.000	0.000
2	2.388e-4	3.928e-6	3.722e-4	4.606e-6	4.722e-4	8.216e-6	6.388e-4	4.606e-6	7.111e-4	1.066e-5	7.166e-4	6.211e-6
4	4.000e-4	4.212e-5	5.333e-4	2.949e-5	6.388e-4	4.502e-5	8.055e-4	2.389e-5	1.022e-3	2.587e-5	1.144e-3	3.263e-5
6	5.444e-4	5.505e-5	6.444e-4	4.849e-5	7.777e-4	4.564e-5	9.666e-4	5.372e-5	1.127e-3	4.015e-5	1.244e-3	3.524e-5
8	6.055e-4	7.216e-5	7.555e-4	4.110e-5	9.000e-4	6.228e-5	1.133e-3	2.187e-5	1.244e-3	3.272e-5	1.350e-3	6.815e-5
10	6.555e-4	4.581e-5	8.111e-4	5.434e-5	9.611e-4	4.738e-5	1.188e-3	3.105e-5	1.327e-3	4.722e-5	1.427e-3	3.632e-5
12	7.055e-4	5.429e-5	8.666e-4	4.110e-5	1.033e-3	4.381e-5	1.250e-3	4.164e-5	1.394e-3	4.381e-5	1.544e-3	6.092e-5
14	7.555e-4	3.653e-5	9.277e-4	5.574e-5	1.094e-3	3.768e-5	1.311e-3	3.402e-5	1.455e-3	6.277e-5	1.566e-3	5.520e-5
16	7.944e-4	4.470e-5	9.833e-4	3.955e-5	1.122e-3	4.157e-5	1.361e-3	4.201e-5	1.522e-3	5.334e-5	1.661e-3	7.216e-5
18	8.333e-4	3.151e-5	1.027e-3	4.519e-5	1.183e-3	3.768e-5	1.416e-3	3.390e-5	1.588e-3	7.130e-5	1.716e-3	6.014e-5
20	8.611e-4	3.458e-5	1.088e-3	4.327e-5	1.238e-3	4.536e-5	1.483e-3	4.803e-5	1.655e-3	6.098e-5	1.738e-3	6.166e-5

b) Solka floc of particle size of 60 µm (sonication at 10% duty cycle and power intensity 11.8 W cm^{-2})

Time (min)	Initial concentration of Solka-Floc (g L^{-1})											
	5		8		10		20		35		40	
	Glucose concentration (M)	Std Dev	Glucose concentration (M)	Std Dev	Glucose concentration (M)	Std Dev	Glucose concentration (M)	Std Dev	Glucose concentration (M)	Std Dev	Glucose concentration (M)	Std Dev
0	0.000	0.000	0.000	0.000	0.000	0.000	0.000	0.000	0.000	0.000	0.000	0.000
2	1.611e-4	8.216e-6	2.111e-4	6.211e-6	2.388e-4	9.212e-6	3.222e-4	1.436e-5	3.666e-4	7.856e-6	3.777e-4	8.216e-6
4	2.166e-4	1.589e-5	3.277e-4	1.145e-5	3.611e-4	1.202e-5	4.166e-4	7.856e-6	4.944e-4	1.778e-5	5.111e-4	2.777e-6
6	2.777e-4	3.608e-5	3.611e-4	1.242e-5	4.055e-4	9.918e-6	5.055e-4	1.637e-5	6.000e-4	1.800e-5	6.277e-4	1.729e-5
8	3.388e-4	4.803e-5	4.500e-4	1.863e-5	4.944e-4	2.843e-5	5.944e-4	1.265e-5	6.777e-4	1.489e-5	7.500e-4	8.333e-6
10	4.055e-4	4.400e-5	5.333e-4	1.884e-5	5.833e-4	6.054e-6	6.777e-4	1.778e-5	7.833e-4	1.816e-5	8.722e-4	1.884e-5
12	4.666e-4	3.818e-5	5.666e-4	2.169e-5	6.777e-4	1.816e-5	7.666e-4	2.003e-5	9.055e-4	1.039e-5	9.888e-4	2.675e-5
14	5.222e-4	4.164e-5	6.500e-4	2.815e-5	7.611e-4	1.863e-5	8.833e-4	2.991e-5	1.011e-3	2.055e-5	1.105e-3	3.077e-5
16	5.833e-4	4.051e-5	7.333e-4	3.224e-5	8.500e-4	1.643e-5	9.888e-4	3.004e-5	1.133e-3	2.092e-5	1.211e-3	3.004e-5
18	6.444e-4	4.598e-5	8.166e-4	1.210e-5	9.333e-4	2.465e-5	1.094e-3	2.949e-5	1.244e-3	1.178e-5	1.327e-3	2.763e-5
20	7.055e-4	3.611e-5	9.000e-4	2.923e-5	1.044e-3	2.055e-5	1.205e-3	3.986e-5	1.350e-3	4.129e-5	1.433e-3	2.239e-5

c) Solka floc of particle size of 290 µm (sonication at 10% duty cycle and power intensity 11.8 W cm^{-2})

Time (min)	Initial concentration of Solka-Floc (g L^{-1})											
	5		8		10		20		35		40	
	Glucose concentration (M)	Std Dev	Glucose concentration (M)	Std Dev	Glucose concentration (M)	Std Dev	Glucose concentration (M)	Std Dev	Glucose concentration (M)	Std Dev	Glucose concentration (M)	Std Dev
0	0.000	0.000	0.000	0.000	0.000	0.000	0.000	0.000	0.000	0.000	0.000	0.000
2	9.444e-5	4.606e-6	1.388e-4	6.211e-6	1.666e-4	1.272e-5	2.722e-4	7.856e-6	3.000e-4	6.211e-6	3.055e-4	7.856e-6
4	1.222e-4	1.066e-5	1.722e-4	7.856e-6	2.000e-4	8.216e-6	3.055e-4	8.784e-6	3.333e-4	1.489e-5	3.555e-4	1.202e-5
6	1.611e-4	1.388e-5	2.111e-4	1.589e-5	2.444e-4	6.054e-6	3.388e-4	7.216e-6	3.666e-4	1.039e-5	4.055e-4	2.303e-5
8	1.944e-4	9.107e-6	2.444e-4	5.555e-6	2.833e-4	1.324e-5	3.722e-4	1.145e-5	4.055e-4	1.637e-5	4.388e-4	1.683e-5
10	2.277e-4	1.666e-5	2.833e-4	8.333e-6	3.166e-4	1.265e-5	4.055e-4	2.777e-6	4.388e-4	1.521e-5	4.777e-4	1.683e-5
12	2.611e-4	8.216e-6	3.166e-4	1.039e-5	3.500e-4	1.066e-5	4.388e-4	1.521e-5	4.611e-4	8.216e-6	5.166e-4	1.039e-5
14	3.000e-4	6.804e-6	3.555e-4	6.211e-6	4.000e-4	1.066e-5	4.777e-4	9.212e-6	5.000e-4	2.129e-5	5.500e-4	1.416e-5
16	3.333e-4	6.211e-6	3.944e-4	8.216e-6	4.222e-4	1.039e-5	5.111e-4	6.054e-6	5.333e-4	1.884e-5	5.833e-4	2.843e-5
18	3.666e-4	1.001e-5	4.222e-4	9.918e-6	4.611e-4	9.918e-6	5.444e-4	9.918e-6	5.666e-4	1.712e-5	6.166e-4	2.405e-5
20	4.000e-4	6.804e-6	4.555e-4	8.333e-6	5.111e-4	2.239e-5	5.833e-4	6.211e-6	6.000e-4	3.118e-5	6.555e-4	2.923e-5

A6.5 Effects of ultrasound on the residual cellulase activity (%) in the absence of substrates at different duty cycles and power intensities. All at $[E]_o$ = 1.0 g L^{-1}, 50 °C and pH 4.8 (Figure 4.29)

a) Power intensity at 2.4 W cm^{-2} (P = 3 W)

Time (min)	Control (no sonication)		Sonication at 10% duty cycle		Sonication at 20% duty cycle		Sonication at 40% duty cycle	
	Enzyme activity (%)	Standard deviation	Enzyme activity (%)	Standard deviation	Enzyme activity (%)	Standard deviation	Enzyme activity (%)	Standard deviation
0	100.0	0.0	100.0	0.0	100.0	0.0	100.0	0.0
2	99.8	2.2	95.8	0.9	94.4	1.2	95.0	1.4
4	99.6	0.9	95.4	0.9	94.0	0.7	94.8	0.5
6	99.2	2.1	95.0	1.0	93.8	0.6	94.6	0.5
8	98.8	1.6	94.6	1.1	93.5	0.7	94.4	0.4
10	98.7	1.6	93.8	1.2	93.3	0.6	94.2	0.3
12	98.5	1.1	93.4	1.5	93.1	0.6	94.0	0.2
14	98.3	1.7	93.1	1.6	92.9	0.6	93.8	0.3
16	98.1	0.6	92.7	1.7	92.5	0.7	93.6	0.3
18	97.9	1.2	92.3	1.9	92.3	0.6	93.4	0.3
20	97.7	1.2	91.1	2.0	92.1	0.7	93.3	0.3

b) Power intensity at 4.7 W cm^{-2} (P = 6 W)

Time (min)	Control (no sonication)		Sonication at 10% duty cycle		Sonication at 20% duty cycle		Sonication at 40% duty cycle	
	Enzyme activity (%)	Standard deviation	Enzyme activity (%)	Standard deviation	Enzyme activity (%)	Standard deviation	Enzyme activity (%)	Standard deviation
0	100.0	0.0	100.0	0.0	100.0	0.0	100.0	0.0
2	99.8	2.2	93.8	0.7	90.6	0.3	87.3	0.8
4	99.6	0.9	93.6	0.7	90.2	0.3	86.9	0.8
6	99.2	2.1	93.3	0.5	89.8	0.6	86.5	0.8
8	98.8	1.6	92.9	0.5	89.4	0.5	86.1	0.8
10	98.7	1.6	92.5	0.6	89.0	0.6	85.7	0.8
12	98.5	1.1	92.3	0.5	88.7	0.6	85.4	0.8
14	98.3	1.7	91.9	0.4	88.3	0.6	85.0	0.9
16	98.1	0.6	91.5	0.3	87.9	0.6	84.6	0.9
18	97.9	1.2	91.7	0.4	87.5	0.6	84.2	1.0
20	97.7	1.2	91.3	0.4	87.1	0.6	83.8	1.0

c) Power intensity at 11.8 W cm^{-2} (P = 15 W)

Time (min)	Control (no sonication)		Sonication at 10% duty cycle		Sonication at 20% duty cycle		Sonication at 40% duty cycle	
	Enzyme activity (%)	Standard deviation	Enzyme activity (%)	Standard deviation	Enzyme activity (%)	Standard deviation	Enzyme activity (%)	Standard deviation
0	100.0	0.0	100.0	0.0	100.0	0.0	100.0	0.0
2	99.8	2.2	84.2	3.6	79.0	2.1	77.6	3.1
4	99.6	0.9	83.8	3.7	78.7	2.3	77.3	3.1
6	99.2	2.1	83.4	3.6	78.3	2.5	76.9	3.2
8	98.8	1.6	83.0	3.5	77.9	2.5	76.5	3.2
10	98.7	1.6	82.7	3.5	77.5	2.5	76.1	3.2
12	98.5	1.1	82.3	3.4	77.1	2.5	75.7	3.2
14	98.3	1.7	81.7	3.4	76.7	2.5	75.3	3.2
16	98.1	0.6	81.3	3.3	76.3	2.5	75.0	3.2
18	97.9	1.2	80.9	3.0	76.0	3.0	74.6	3.2
20	97.7	1.2	80.7	3.4	75.6	3.0	74.2	3.2